Sediment Dispersal in the Southern Beaufort Sea

B.R. PELLETIER

Technical Report No. 25a

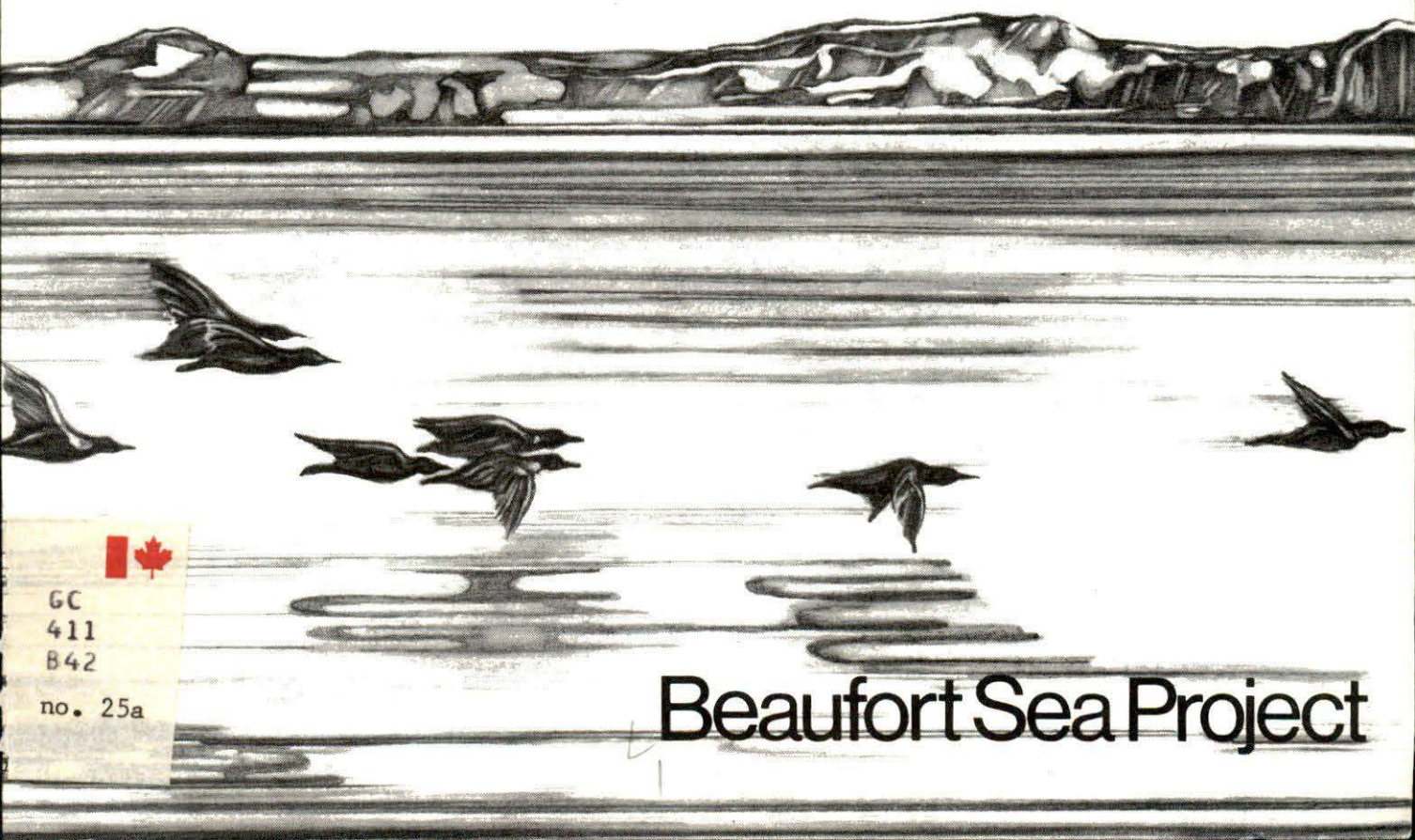

Beaufort Sea Project

SEDIMENT DISPERSAL IN THE SOUTHERN BEAUFORT SEA

B.R. Pelletier

Geological Survey of Canada
601 Booth Street
Ottawa, Ontario
K1A 0E8

Beaufort Sea Technical Report #25a

Beaufort Sea Project
Dept. of the Environment
512 Federal Building
1230 Government St.
Victoria, B.C. V8W 1Y4

December, 1975

TABLE OF CONTENTS

1. SUMMARY

Beaufort Sea sediments have been obtained by means of bottom grabbers and cores from ship-borne and helicopter-supported operations since 1970. A total of 1200 samples has been collected and texturally analyzed. This report is based on the description and interpretation of 244 representative samples obtained from the following cruises: CSS HUDSON - 1970; CSS RICHARDSON 1970: CSS BAFFIN - 1970; CSS PARIZEAU - 1970, 1971, 1972; and charter Helicopters (Polar Continental Shelf Project) - 1970, 1971, 1972 and 1975. Inferences on the texture, distribution and origin of these bottom samples are given.

Both bathymetry and geography have been considered, but lacking is a fuller knowledge and appreciation of ocean dynamics. As these studies progress on other companion projects, the data so obtained may be utilized for the sedimentary and coastal studies. What is known however, provides a reasonable framework for the sedimentary model in the Beaufort Sea as follows. Sediment discharged from the Mackenzie River, as seen in the satellite photographs, is transported seaward to the north and east, the latter direction in particular because the flow of currents is influenced by the Coriolis force. Some of the sediment plume moves westerly along the coast and toward Herschel Island where it is deflected to the deeper areas of the Mackenzie Canyon and the adjacent shelf to the east. This leaves an area north and west of Herschel Island somewhat deficient in sediments derived from the Mackenzie River and western coastal areas.

Coarse sediments are present on the western and most easterly portions of the shelf; in the western part, deposition from ice-rafting appears to be most significant whereas in the eastern part erosion exposing relict deposits of fluvial and coastal sediments is suggested. Generally though, most of the relict sediments are being buried by sediments being discharged from the Mackenzie River. Other areas along the coast, particularly those associated with islands, offshore bars and spits, are commonly the sites of vigorous sedimentary processes, and may be providing considerable material to the sedimentary system. This is apparent from studies of satellite photographs, in which the sediment plume and the direction of its movements are clearly visible. Sediments appear to move easterly toward the Archipelago in the inshore regions, and this movement is confirmed by summer-time current observations. Locally though along the coast, a westerly movement is apparent, and this is also confirmed by current-meter readings, surface drifters and the direction of growth of numerous sand spits.

Offshore however, a distinct trend is noted in the sedimentary maps for the possible westerly movement of fine sediments from the eastern part of the shelf. This suggests that ocean currents, perhaps in winter, move westerly in this part of the Beaufort Sea. As a result, fine sediments are accumulating in the central area of the shelf and the Mackenzie Canyon, and are being augmented by direct sedimentary increments from the Mackenzie River.

.../2

The plot of silt/clay ratios indicates the occurrences of a hydrodynamic energy gradient that is consistent with the direction of sediment transport. This gradient is based on a plot of the calculation of energy volume, derived from the size of the sediment and the associated depositional velocities of the currents. From these considerations three major hydrodynamic environments were determined. The first is in the coastal and deltaic area, as well as portions of the eastern shelf, and is characterized by intermediate energy. The second environment lies in the inshore area paralleling the coast generally, but transecting the shelf in both eastern and western portions. This region is one of low hydrodynamic vigour. Finally the third major environment occurs seaward of the second one. It extends from the 10-m isobath in the southerly regions, and over the Mackenzie Canyon and adjacent continental shelf to east and west. This is an area of very low vigour, and is the ultimate repository for fine sediments exclusive of those which may move down the continental slope due to mass movement such as slumping or turbidity flows.

Studies on clay mineralogy have been completed for 244 representative samples of the deltaic, coastal and offshore regions. Generally the distributions of illite, chlorite and kaolinite are fairly uniform. This suggests a common provenance in the terrigenous source area, and thorough mixing in the marine environment. It also partly corroborates the routes of sediment transport in that sediments move easterly, predominately, over the inner shelf and westerly over the outer shelf. Montmorillonite is unique in that its absence in the eastern channel of the Mackenzie Delta, and in an area directly seaward (in the coastal zone and somewhat in the Mackenzie Canyon), suggests the absence of this mineral in the sub-soil of the eastern portion of the delta.

Carbonate content and organic carbon were determined for 50 widely-spaced representative samples of the shelf and delta. Both constituents are in greater amounts in the deltaic and coastal areas than in the offshore. This may be a combined effect of grain size, the proximity of the Mackenzie River discharge, and the ice cover which persists for the greater part of the year. Considerable amounts of organic debris from land, and shelly material in the inshore zones would probably occur in the textural classes coarser than the clays already examined. Therefore this would help to explain relatively low contents of $CaCO_3$ and organic carbon, particularly in areas receiving coarser sediments than the remote offshore.

2. INTRODUCTION

This is a study of sediment dispersal based on textural examination of the bottom sediments. It involves the nature, distribution and origin of these sediments as they occur on the sea bottom. With reference to the offshore exploratory drilling, the nature of the sea bottom is important for the following reasons: (1) to determine foundation strength of material, (2) to deduce the fate of sediment particles in connection with deposition and erosion, and (3) to establish a data baseline in the event of an oil spill. All data are recorded in Appendices A to D, and displayed in illustrations in Appendix E.

At present there is no comprehensive report on sediment dispersal in the southern Beaufort Sea, exclusive of the work of Carsola (1952) and that carried out by CSS HUDSON in 1970 (Pelletier, 1974). Suspended sediments were recently

.../3

studied by Bornhold (1975). Other related subjects deal with sea-floor scouring by ice keels (Pelletier and Shearer, 1972, and Lewis, 1976), the nature and distribution of submarine pingos (Shearer et al, 1971), reports on molluscs (Wagner, 1972), and foraminifera (Vilks, 1973).

3. STUDY AREA

The study area is restricted to the southern Beaufort Sea between the Alaskan boundary on the west and Cape Bathurst on the east (Fig. 1). Lying between longitudes 127°:00' and 141°:00', and latitudes 69°:30' and 72°:00'; it extends a distance of 150 km offshore to a depth of 1000 m. Generally though, the seaward limit does not reach beyond the upper continental slope. As shown in Figure 1, the floor of the Beaufort Sea is characterized by three main physiographic feature: (1) the continental shelf which grades gently toward the 100-m isobath; (2) the continental slope which falls fairly steeply from the shelf edge, and whose isobaths in the upper portion conform to both those of the continental shelf and Mackenzie Canyon; and (3) the Mackenzie Canyon which transects the continental shelf and upper slope in a pronounced V-shaped pattern, with the headward portion immediately adjacent to the submarine portion of the Mackenzie River delta. From this point it extends a distance of approximately 120 kms along a northwest axis to a depth of some 500 m and thence to the upper slopes of the Canada Basin. The bathymetric map also shows possible routes of old drainage systems, particularly off Kugmallit Bay and regions to the east. One submarine feature lying at the edge of the continental shelf directly northeast of Mackenzie Bay may represent ancient mass wastage of the sub-soil.

Other morphological features not shown are submarine hills which resemble the pingos occurring on the Tuktoyaktuk Peninsula. The so-called submarine pingos (Shearer et al 1971) represent a threat to shipping in the area, particularly to deep-draught vessels, as the summits of some pingos lie within 11 m of sea level. These pingos are ice-cored conical mounds up to 300 m in diameter at their base, but rising 20 to 50 m to form narrow peaks which are commonly breached by expansive forces within the pingo. Finally grooves or furrows, produced by ice-scouring as keels of drifting ice dragged the bottom, occur in profusion on the sea floor. Some occur on pingos as well, as observed from side scan sonargraphs. These features are described by Pelletier and Shearer (1972), and are the subject of a special report by Lewis (1976).

Along the low-lying coast of the mainland, spits and bars associated with numerous headlands and offshore islands are present, and are extending their growth generally in an easterly direction. This latter phenomenon may be a response to longshore current action being influenced somewhat by the Coriolis force which, at this latitude, is directed to the east. However, some growth of these spits and bars is to the west. Further aspects of the deltas and coasts involving geography, erosion, aggradation and sedimentary processes are given by Lewis and Forbes (1976).

4. METHODS AND SOURCES OF DATA

For the purpose of this report, only part of the work carried out from ship-borne and helicopter-supported operations is reported. This involves

the analyses of 244 representative samples selected at approximately 20-km intervals over the continental shelf, and some at closer intervals in the Mackenzie delta (Fig. 2). These locations are recorded in Appendix A.

4.1 Field Techniques

The Van Veen grabber was used to obtain all samples during ship-board operations, and the Dietz-La Fonde grabber was used to sample through open leads on holes drilled through the ice during the helicopter-supported work. All locations are shown in Figure 2. These samples were stored aboard ship, or at Polar Base (Polar Continental Shelf Project) and transferred to laboratories at the Bedford Institute of Oceanography in Dartmouth, Nova Scotia.

4.2 Experimental Techniques

In the laboratory, all 244 samples were texturally analyzed by means of sieves and pipettes. The clay fraction (<.004 mm) was further examined for the identification of the major clay groups by means of X-ray diffraction (Appendix-F). Fifty representative samples from different parts of the shelf and inshore areas were selected for additional geochemical determination of the amount of carbonate ($Ca\ CO_3$) and organic carbon in the clay-size portion of the sample.

4.3 Data Analysis

Statistical operations using standard moment measures were applied in order to describe the textural data (Appendix B) and to provide some aid in the genetic interpretation of the sediments. Values of relative entropy were calculated and plotted in order to determine and portray the sorting index of the sediments, and to show its relationship to the various textural distributions. Clastic ratios, in which the major fractions such as gravel, sand, and mud, were plotted on ternary diagrams for use as descriptive and interpretative devices. The silt/clay ratio was examined separately, and used in conjunction with mean grain size and associated current velocities in order to determine the various zones of hydrodynamic vigour that are characteristic of given sedimentary environments. Calculations of energy volume were made from these data.

Data from the analyses on clay minerals, (Appendix C) was plotted directly onto maps, and summarized in graphs in order to present baseline information and the quantitative relationships of these minerals.

The results of the geochemical studies on the determination of carbonate ($CaCO_3$) was reached by calculations on the analytically derived CO_2 content in the sediment. Organic carbon was determined by burning after an acid digest first removed the inorganic carbonate. All geochemical results (Appendix D) were plotted on maps, as representations of baseline data.

4.4 Phasing of the Work.

All the shelf has been sampled for bottom sediments, except for an area in the northeast which represents about 10 percent of that required for uniform coverage. This sampling will have to be carried out on an opportunity basis with DOE*when its vessels carry out programs in that area, and when suitable navigational aids are in use.

* Dept. of the Environment

.../5

The mechanical analysis of all samples collected to date is complete, but the data will not be analyzed and plotted for perhaps another two years.

Mineralogical studies on the clay minerals and the analyses of 50 samples for the determination of carbonate ($CaCO_3$) content and organic carbon are complete, and the data are plotted. An additional 150 samples are also being similarily analyzed for CO_2 and organic C but this work will not be completed and plotted for several months.

5. RESULTS

All results of the various studies on sediment dispersal in the southern Beaufort Sea are shown in the sedimentological maps and graphs given in appendix E of this report.

5.1 Sediment Types

The first approach to the study of sediments in a given area is to show the distribution of the main textural classes such as gravel (>2 mm), sand (.062 to 2 mm), silt (.004 to .062 mm) and clay (<.004 mm). In a bar diagram (Fig. 3) distribution of these textural classes is compared with the number of stations with those classes.

Distribution of the gravel content of each sample is shown in Figure 4. The highest concentration is 41 %, and occurs northwest of Herschel Island. This area is thought to receive a considerable amount of ice-rafted sediments which originated in offshore and coastal areas. Ice commonly resides north and west of Herschel Island, the latter of which forms a barrier for ice moving easterly and southeasterly into Mackenzie Bay and the inshore area to the east. Only 9 % of all samples contain more than 1 % of gravel, and in 35 % of the samples gravel is absent altogether (Fig. 3). With a preponderance of samples showing an absence of gravel between Herschel Island on the west and Baillie Island on the east, it is unlikely that ice-rafting would have by-passed the intervening area. On the eastern part of the shelf, the gravel present may be relict, particularly as bottom currents are fairly active in this area and submerged beaches and river channels are also thought to be present.

Sand (Fig. 5) is more widespread than gravel but is absent almost entirely in Mackenzie Canyon and on the adjacent continental shelf to the east. Although some samples contain nearly 100 % sand (and all samples contain some) only 20% of all samples contain more than 20% sand, and only 14% of all samples contain more than 30% sand (Fig. 3). In the area off western Herschel Island the high concentrations are thought to be ice-rafted in origin, but along the coast and eastern shelf it is erosional. Some of the sand along the coast, particularly near the islands, spits and bars is in transport. To the east, particularly over the continental shelf, it is thought to be relict (possibly fluvial or beach) and has been exposed by the scouring action of bottom currents. In some areas sand, retrieved by the bottom samples, may have lain just beneath a veneer of finer sediments and recovered when the sampler penetrated both fine and coarse sediment successively. This is thought to be the case in the hydrodynamically quiet areas of Kugmallit and Liverpool Bays.

Distribution of the silt content is shown in Figure 6. Only 18% of all samples have less than 20% silt, and no sample is without it (Fig. 3). The heaviest concentration is in Mackenzie Bay and the coastal areas to the east.

.../6

However, a major concentration occurs over the easternmost continental shelf, extending off Liverpool Bay and the eastern end of the Tuktoyaktuk Peninsula. The least concentration is in the area over the middle and outer parts of the Mackenzie Canyon, and the adjacent shelf areas to the east and west. Satellite photographs (Fig. 7 and 8) show a major sediment plume containing silt being discharged from the Mackenzie River and moving easterly about 30 to 40 kms offshore at the mouth of Mackenzie Bay. The area north of Herschel Island is uninfluenced by this plume and consequently is somewhat deficient in those sediments.

Clay is perhaps the most widespread sediment over the shelf. It is present in all samples, although in 25% of the samples it comprises less than 30% of the sediment and in 9% of the samples, less than 10% (Fig. 3). Distribution of the clay content over the Beaufort Sea shelf is shown in Figure 9. It appears to have the same general pattern as that of sand and silt except for the extreme ends of the shelf, but in reciprocal amounts. For example, the least content of clay per sample (< 20% occurs in Mackenzie Bay, the coastal areas and the eastern portion of the shelf; but these are characteristically areas of high silt content (40 to 100%) and of various content of sand (up to 40% in the delta, and up to 98% along the coast). Conversely the highest amounts of clay (80 to 100%) are found in the Mackenzie Canyon and the adjacent continental shelf to the east. In this vicinity, the lowest contents of sand (<20%) and silt (<40%) are found. Clay deposition is by-passed in the coastal areas where currents are sufficiently strong to transport fine sediments offshore and deposit them in areas of less vigorous hydrodynamic conditions. In the eastern part of the shelf the textural gradient, showing increasing clay content from east to west, suggests scouring in the east with sediment transport taking place toward the central part of the shelf and Mackenzie Canyon. These localities thus become the sites of major clay deposition.

5.2 Clay Composition

Although not part of the mechanical study on sediment dispersal in the Beaufort Sea, mineralogical and chemical studies were carried out on the clay portion of the sample in order to provide baseline data in the event of an accidental spill from a well blowout or a collision at sea.

Mineralogy. Montmorillonite, illite, chlorite and kaolinite were determined and their contents for each sample are given in Appendix C. These data were plotted in a bar diagram (Fig. 10) showing the composite range of each constituent according to percentage frequency and the number of stations with that range of occurrence. Illite is the most common in terms of occurrence and content; its percentage content ranges between 20 and 70%, with 96% of the samples containing between 40 and 65% (Fig. 10). Chlorite is next in widespread occurrence but is less abundant in the sample. Its range in percentage content of the sample is from 10 to 35%, with 95% of all samples containing between 10 and 25% (Fig. 10). Kaolinite is common everywhere but in moderate amounts varying to 40%, although 96% of all samples contain 10 to 35% of this mineral (Fig. 10). Montmorillonite is the least common and least widespread of the four clay minerals determined. Its range in terms of percentage content of the sample is 0 to 50%, but for 95% of all samples, this range is 0 to 20% (Fig. 10).

Data on the percentage composition of the clay-mineral assemblages were plotted on a series of maps (Figs. 11 to 14) in order to relate the frequency

.../7

of occurrence with geographic distribution. All maps show that this assemblage appears to be characterized by thorough mixing of the constituents, and in no preferred area of the shelf. Montmorillonite is exceptional in that it is absent in many areas, particularly in the eastern channels of the Mackenzie Delta and the adjacent offshore area. It is possible that Montmorillonite is absent in these channels and therefore, can not be contributed to the offshore from this local provenance.

Geochemistry. The carbonate content was determined for 50 representative bottom samples, and calculated as though all carbonate were derived from calcium carbonate ($CaCO_3$). This may not be entirely true as manganese, magnesium and iron also form carbonate compounds. However, no analyses were carried out for the determination of the major metallic elements so that the basic assumption of utilizing $CaCO_3$ in the calculation must stand for the present. Results of CO_3 analysis are recorded in Appendix D, and plotted on the regional map (Fig. 15). The highest values are found in Mackenzie Bay and easterly in the inshore area half way along the Tuktoyaktuk Peninsula. Progressively decreasing values occur offshore in a seaward direction. Most values in the inshore area are low, probably because only material of clay sizes (.004 mm) and less were analyzed. Generally coarser sediments (to 2 mm) when analyzed give higher (CO_3) values.

Organic carbon is also reported for the same 50 samples utilized for the CO_3 analyses and similarly only material less than .004 in diameter was analyzed. The analytical results are given in Appendix D, and plotted on the regional map (Fig. 16). The highest content occurs in Mackenzie Bay and some coastal areas, and in the northeastern portion of the continental shelf. This latter occurrence may be due to upwelling in the area, or a westerly drift of suspended material originating from the mainland. Generally though, values are low, except for the offshore where fine sediments are deposited and the analytical results conform more to those for finer sediments.

5.3 Textural Parameters

For purposes of presentation, comparison of data from station to station, and as an aid to interpretation, statistical studies were carried out in which the first three moments were calculated, tabulated and plotted. In order to obtain a regional distributional map of sediment types, the mean grain diameter on the phi scale was determined. This determination was complemented with an analysis of the phi modal classes. To obtain some measure of the sorting process, standard deviations for each sample were determined and were augmented by a study of the relative entropy for the respective sediment. To aid in distinguishing the effects of erosional and depositional energies on the sediment texture, the property of skewness was examined.

In succeeding sections of this report, these concepts of mean grain size, sorting and skewness are related to textural ratios, energy volume and the phenomena of erosion, sediment transport and deposition. Gross textural relationships are initially discussed by means of ternary diagrams. These devices give a qualitative portrayal of the various depositional environments and the sedimentary processes acting within them. Later the textural data are refined, as demonstrated in the silt/clay ratios, and are combined with an examination of the mean grain size in order to present a quantitative assessment of the various environments in terms of hydrodynamic vigour.

.../8

The classification of sediment sizes (diameters) is based on the convention shown in Table 1.

Table 1.- Classification of Sediment Sizes

Sediment Type	Diameter (mm)	Phi Diameters (Ø)
Gravels	>2.00	> - 1.00
Sands	2.00 - 1.00	-1.00 - 0.00
	1.00 - 0.50	0.00 - +1.00
	0.50 - 0.25	+1.00 - +2.00
	0.25 - 0.125	+2.00 - +3.00
	0.125 - 0.062	+3.00 - +4.00
Silts	0.062 - 0.031	+4.00 - +5.00
	0.031 - 0.016	+5.00 - +6.00
	0.016 - 0.008	+6.00 - +7.00
	0.008 - 0.004	+7.00 - +8.00
Clays	<0.004	>+8.00

Mean grain diameters. From a plot of the mean grain diameter on the phi scale a distribution map of the main sediment type was constructed (Fig. 17). This map shows the presence of sand in the coastal areas lying both east and west of the Mackenzie Delta, in bars and spits around the periphery of nearshore islands, in a large area lying immediately adjacent to the western and northern coasts of Herschel Island, and in small isolated areas on the eastern portion of the continental shelf. Silt is the major textural component occurring offshore, and it occupies almost all of the continental shelf exclusive of the central portion. Clay is found predominately in the Mackenzie Canyon and the central portion of the continental shelf immediately adjacent to the east. It generally occurs seaward of the silt distribution.

Despite this rather simple presentation of the main sediment types, the gravel occurrences failed to appear on the map (Fig. 17). This is due to poor sorting in the sediments, and the fact that the first moment (arithmetic mean) is not representative of such sediments. Because of this limitation, a map based on the chief modal class (Fig. 18) was drawn. This map clearly shows the locations of those samples containing gravel as its chief constituent. One such occurrence lies northwest of Hershel Island, a zone characterized by the deposition of ice-rafted sediments, particularly because of its occurrence with clay so remote from shore. Another area of gravel occurrences lies on the extreme eastern end of the shelf, a zone suggestive of current action particularly as the gravels are associated with sands and silt predominately.

The main areas of sand are also delineated on this sediment map (Fig. 18), which further demonstrates the relationship of sand to the presumed ice-rafted gravels northwest of Herschel Island. The moderate occurrences of sand in the inshore areas and on the eastern part of the shelf are also shown. Silt distri-

.../9

bution in Figure 18 does not appear to be as widespread as shown in Figure 17, but the general distribution is similar. Its absence over much of the continental shelf is due to the masking effect produced by the deposition of clay, the latter being supplied primarily as a discharge from the Mackenzie River in the southern part of the area, and secondarily from the eastern shelf to the northern and central part of the shelf.

Sorting. A plot of the second moment (standard deviation) (Fig. 19) was made in order to distinguish areas characterized by different amounts of re-working. This application of the standard deviation is based on the assumption that re-working of sediments will tend to eliminate the finer textural classes and thus improve the sorting. Phi values are used and, on this scale, the smaller values are associated with the better sorting. Generally the results are consistent with the type of sediment, for example, poor sorting (>2.3) for the ice-rafted sediments, but good sorting (<1.3) for coastal sediments undergoing erosion. However the central area, occupied by well-sorted (<1.3) sediments, is anomalous in that the full range of textural classes for the fine sediments has been compressed artificially into a few classes. Consequently the sorting will appear to be good, as only two clay classes (all the clay) and the 4 silt classes (all the silt) are considered. Therefore the limitations on using sorting values here must be considered with the number of textural classes of the sediment type analyzed.

To obtain an idea of sorting based on class proportionality, and to give a more comparative measure of sorting with such easily visualized sediments as tills, dune sands etc, calculations of relative entropy were made for each sample and recorded in Appendix B. Relative entropy (Hr) as defined by Pelto (1954) was used as a measure of sorting because it is independent of the arithmetic mean size of the sediment. It is calculated as follows:

$$Hr = \frac{-100 \sum p \ln p}{\ln N}$$

where p is the percentage frequency and N is the total number of textural classes chosen to represent the size distribution of the sediments. Here 18 classes have been arbitrarily selected, ranging from a coarse gravel (256 mm) to a coarse clay (.001 mm), using the grade scale based on $-\log_2$. Because the finer sediments of the Beaufort Sea have been arbitrarily grouped into only a few classes, the same limitations on interpretations must be applied as in the case of standard deviation. Generally high values of relative entropy (>50%, as seen in Figure 20) correspond to poor sorting and low values (<50%) to good sorting. Sediments of low entropy are found in coastal or highly dynamic areas; those with high entropy are found in areas of mixed sedimentation such as that northwest of Herschel Island. Areas of low hydrodynamic vigour are also characterized by high entropy; however, the central area of the shelf is anomalously low because the sub-silt sizes (<.004 mm) are grouped into two classes only. The low entropy (<50%) in this area reflects the arbitrary cut-off in textural classes finer than 10 phi, rather than mechanical re-working by current activity.

A ternary diagram (Fig. 21) was constructed to show the relationship of texture and relative entropy. This plot utilizes the three-fold classification of gravel (>2 mm), sand (0.062 to 2.0 mm) and mud (<0.062 mm). Thus the apices represent 100% gravel, 100% sand and 100% mud respectively. All samples were located on the ternary diagram according to their textural composition, and the corresponding values of relative entropy were assigned to these sample points. Isopleths denoting very high relative entropy (>70%), high (50% to 70%) and low (<50%) were drawn. Because relative entropy includes all textural components,

.../10

the ternary diagram must be constructed on the gravel, sand and mud apices.

Theoretically each apex should have a relative value of 0%, and the mid-point along any textural border should be 50% because it is a mixture of two major textural classes. The centre of the diagram should have the highest value of relative entropy (100%) because it represents the greatest mixture of all textural classes. However, the mud apex actually consists of the combined silt and clay classes, and the value of relative entropy here would be higher than that for the sand and gravel apices. The values though would still tend to approach 0% as progressively more clay appeared in the sample or alternately, progressively more silt appeared.

In this entropy plot (Fig. 21), the isopleths are restricted to the lower part of the diagram and mainly to the right. Values of relative entropy shown in the lower right of the diagram are mostly high (50 to 80%). This is due to the presence of samples containing varying amounts of silt and clay, with minor amounts of sand or gravel, or both. With increasing amounts of either silt or clay in the sample (as explained above), the value of relative entropy approaches the lower amounts. Some low values (30 to 50%) are plotted in the lower left portion of the diagram near the sand apex. Because some of these samples have sediments restricted to a few classes in the combined sand/silt range, a low degree of relative entropy results.

On a high-energy sea bottom such as Minas Basin (Pelletier 1974) isopleths of relative entropy depicted in a ternary textural diagram such as Figure 21, lie close to the gravel/sand and sand/mud border, because the sediment is in dynamic equilibrium with the minimal available hydrodynamic energy in the environment. In the textural/entropy plot for the sediments of the Beaufort Sea, the disequilibria is apparent for the coarser sediments because many sample points lie within the diagram and the relative entropy is high. A great number of sample points lie along the sand/mud border, showing that much of the finer sediments are in dynamic equilibrium with the minimal energy available, that is, with the depositional velocities in their respective environments.

This overall pattern demonstrates the relationships between relative entropy and those textural elements in sediments that are deposited in a low-energy sea. Thus it serves as a model for sedimentation in the Beaufort Sea and may be applied as an additional interpretation tool in a sedimentological analysis.

Skewness. In this report the skewness sign (whether it is positive or negative) is used interpretatively rather than the magnitude. Positive phi skewness suggests erosional activity particularly as fine sediments when removed leave a coarser fraction as a lag deposit. In such a case the size/frequency curve would be skewed to the coarser sizes. Negative phi skewness suggests deposition from waning currents as the fine sediments would tend to accumulate after the coarser ones had been deposited elsewhere. In this case the size/frequency curve would be skewed toward the finer sizes. This hypothesis may be tested by examining (Figs. 22 and 23) the ternary diagrams of skewness and texture and the map showing the distribution of phi skewness for each sample (Fig. 24).

Ternary diagrams were used to demonstrate the relationships of skewness and sedimentary texture. The first approach involves an examination of the skewness sign in relation to the grosser textural classes such as gravel, sand and mud (Fig. 22). This diagram clearly shows the overlap of positively and negatively

.../11

skewed samples. However despite this overlap, the field of negatively skewed sediments is immediately apparent in the vicinity of the mud apex. To obtain a refinement of this representation, another ternary diagram (Fig. 23) was drawn in which the gravel component was excluded and the sand, silt and clay components were re-calculated to 100% and selected as the apices. Because the mud component has been separated into its silt and clay fractions, the different fields of skewness are more easily seen. Negative phi skewness is naturally associated with the finer sediments because of their high clay content, and because of their depositional origin. On the other hand, positive phi skewness is seen for the more arenaceous sediments which, in part, represent a lag type of deposit. The overlapping area of positive and negative skewness in the interior part of the diagram is a reflection of a mixture of normal marine and non-current deposition.

Skewness of the sediments according to its positive and negative qualities, was also plotted on a map of the southern Beaufort Sea (Fig. 24). These sample points were derived from the data in Appendix B, and may be compared with the ternary textural/skewness diagrams (Figs. 22 and 23). The areas of positive skewness occur in the Mackenzie Delta and Bay, along the coast to the east and over the far eastern and western parts of the continental shelf. These areas contain sediments that are undergoing erosion and transportation by marine currents. On the eastern part of the continental shelf a positive skewness is suggestive of scouring in this area. However, the western portion of the shelf north of Herschel Island shows that some sediments have a positively skewed, textural distribution. This latter area though, is thought to be receiving a considerable amount of coarse ice-rafted debris; but also, it is an area somewhat deficient in fine sediments as the sediment plume from the Mackenzie Delta does not reach this area and consequently is unable to supply fine sediments to it. This phenomenon would tend to bias the distribution toward the coarser fraction and thus produce a positive phi skewness.

Most of the offshore areas, particularly the central portion including Mackenzie Canyon and the adjacent shelf to the east, are characterized by the presence of negatively skewed sediments and, as such, are areas of fairly quiet sedimentation. This central area is the major site receiving fine sediments which suggests the occurrence of waning currents. Other areas occupied by negatively skewed sediments lie in coastal regions, particularly in wave-protected waters. Such locations are refuges of fine sediments which generally deposit under quiet hydrodynamic conditions. These occurrences of both positive and negative phi skewness of the bottom sediments are consistent with present opinions in this report concerning the phenomena of erosion and sedimentation.

5.4 Silt/Clay Ratios and Hydrodynamic Vigour

Silt/Clay ratios were selected because they offered additional information, to that previously discussed, in interpreting the hydrodynamic conditions on the floor of the Beaufort Sea. From earlier analyses on sediments from the Bay of Fundy (Pelletier, 1974), from Baffin Bay (Pelletier, 1975) and other areas (Pelletier 1973), it was determined that the higher silt/clay ratios reflected conditions of considerable hydrodynamic vigour, and the lower ratios indicated quieter conditions. In the Beaufort Sea, the highest ratios (>5.0) occur in Mackenzie Bay and adjacent coastal areas (Fig. 25). Less than 10 kms from shore the silt/clay ratio decreases markedly (<1.0), and in the central area over Mackenzie Canyon and the continental shelf, they are lowest (<0.25). The ratio of 0.40 was contoured separately, and generally outlines the area of least values of the silt/clay ratio. This suggests that the area enclosed by the .40 silt/clay boundary is the site of least vigorous sedimentation; the 0.40 ratio also suggests that sediments as well as discharging from the Mackenzie River and moving easterly,

may also move westerly from the eastern end of the continental shelf toward the area of quiet deposition immediately to the west and over the Mackenzie Canyon. It is interesting to note that the isopleths of the silt/clay ratios parallel the coastline and isobaths generally, except in the eastern part of the Beaufort Sea where they transect the isobaths over the continental shelf.

In order to obtain a relatively quantitative idea of the depositional energy characteristic of different areas of the shelf, the curves adapted by Hjulstrom (1935) were used to obtain the depositional velocity of the mean grain size of sample. This value was substituted in the following energy/volume equation:

$$\text{Energy volume} = \text{density} \times \frac{\text{velocity}^2}{2}$$

assuming the density of water (in CGS units) to be unity approximately, then the calculated value of energy/volume is a direct function of the square of the velocity. Because the form of the equation is similar to K.E. = $\frac{1}{2}$ mv^2 in which K.E. is kinetic energy in ergs, the unit of energy/volume is ergs/cm^3. Hjulstrom values tend to be too high because the velocities were measured up to 1 m above the bottom. However, the energies so calculated represent minimal energies available in the environment, and neglect the higher energies required to initiate scour and sediment transport. To determine this latter quantity, a full range of sediment sizes would be needed in situ in order to record the smallest remaining sediment as this would represent the limit below which sediments were deposited.

In Figure 26, a plot of the silt/clay ratios versus the phi mean diameter shows the relationship of these two textural parameters to the degree of hydrodynamic energy. No samples occurred in the high energy zone similar to those reported for the high energy zones of the Bay of Fundy and Minas Basin (Pelletier 1973, 1974) and the Scotian Shelf (Pelletier 1973). The upper limit of this zone is not shown but its minimal designation would be equivalent to an energy volume of approximately 5400 ergs/cm^3, based on average current velocity of 2 kts or 104 cm/s; its lower limit would be about 113 to 613 ergs/cm^3, based on a current velocity of 15 to 35 cm/s. It is interesting to note that the ratio occurrences northwest of Herschel Island are actually in a lower energy zone rather than the higher one characterized by high-velocity currents and deposits of gravel and sand exclusively. This dynamic aspect, together with the poor sorting, suggests ice-rafting as the responsible agent of deposition. On the other hand, the gravels on the eastern part of the shelf are also in an environment of lower energy but this situation is consistent with nature of the sediment admixture present, and the scouring action presumed to be taking place.

The zone of intermediate energy is distinct from the high energy zone because it occurs in an area where the velocities of the bottom currents are less than those of the higher zones. Consequently the sea floor is occupied by sediments of sand and sub-sand size, such as silt, predominately. The energy volume associated with the lower limit of this zone is 0.0017 to 0.0256 ergs/cm^3, based on depositional current velocities ranging between 0.058 and 0.226 cm/s.

In a parallel manner, the zone of low energy is also distinct. Its lower limit is designated at the energy-volume level of 0.0013 to 0.0015 ergs/cm^3, based on depositional velocities ranging between 0.051 and 0.055 cm/s. The mechanical composition of the bottom sediment is at least 65% silt with almost all of the remainder consisting of clay.

A zone of very low energy was selected to represent those areas influenced by only very low current velocities. The energy volume is correspondingly low and is generally less than 0.0015 ergs/cm^3, based on depositional velocities below 0.055 cm/s. Sediments in this zone consist predominately of clay with generally less than 35% silt in the remainder. Some few percent of fine sand may be present, but in amounts 1% or less.

On the plot silt/clay versus phi mean diameters (Fig. 26), the energy gradient is shown passing orthogonally through the energy zones. This is consequent upon the premise that decreasing energy corresponds both to decreasing silt/clay ratios, and decreasing grain size. The gradient approaches zero along the abscissa because the silt/clay ratio is zero along that axis. However on the ordinate, the gradient extends asymptotically because the silt/clay ratios tend toward infinity as their greatest magnitude. Practically however, an upper limit is drawn at some threshold value of the silt/clay ratio (in this case 10), because the ratio can not be plotted at infinity. If coarser sediments are more abundant in the sample then a different clastic ratio must be used, and a correspondingly different plot of clastic ratio versus phi mean diameter is produced.

Another aspect of this plot (Fig. 26) is noteworthy. This is the widely spaced spread between two distinctly different fields of samples in the intermediate zone chiefly. One field lies near the abscissa in the lower part of the diagram, and the other extends across the diagram in subparallel orientation with the energy gradient. The first field contains samples presumed to be ice-rafted, and others that may represent sediments in mechanical disequilibrium with their environment in that the sedimentary processes may not have gone to completion. In the second field, the samples contain sediments that appear to be in equilibrium with their respective environments and that mechanical processes acting upon them appear to have gone to completion.

Finally it is worthwhile to consider skewness in relation to a plot of the silt/clay ratio versus phi mean diameter (Fig. 27). Generally the positively skewed sediments occur in the coarser sizes and the negatively skewed ones in the fines. This too is consistent with previous interpretations in this report that positive skewness suggests scour and transportation, and that negative skewness indicates quiet deposition from waning currents. An overlapping area of positive and negative skewness occurs on the graph (Fig. 27) which generally corresponds to within 10% of a similar area of overlap on the skewness/textural ternary diagram (Fig. 23).

5.5 Hydrodynamic Environments

Based on the graph of the silt/clay ratios versus phi mean diameters (Fig. 26), all samples for each arbitrarily chosen environment were plotted on a regional map of the Beaufort Sea (Fig. 28), and the various environments were delineated. It is felt that several areas of the coast are characterized by considerable hydrodynamic vigour but, as yet, analysis and interpretation of samples from these areas are incomplete. In such a high-energy environment, the lower limit of the energy volume ranges from 113 to 613 ergs/cm^3. The upper limit of energy volume (not shown) would be approximately 5400 ergs/cm^3. Above this value, the energy volume would be associated with a zone of very high hydrodynamic vigour.

Generally the sediments reported here fall within three major hydrodynamic environments: (1) the intermediate energy zone, (2) the low energy zone and (3) the very low energy zone. As a rule, these zones decrease in vigour seaward from the Mackenzie Delta and most coasts bordering the Beaufort Sea.

.../14

The intermediate zone, or hydrodynamic environment, lies within the Mackenzie Delta, Mackenzie and Kugmallit Bays, the adjacent coastal areas, and the eastern portion of the continental shelf. In terms of energy volume, the full range to be expected as acting on these sediments in terms of minimal depositional energy would be 0.0056 to 613.0 ergs/cm^3. These amounts overlap with the low and high-energy zones respectively.

The second environment is one of low energy and lies seaward of the intermediate environment. It extends to the shelf/slope break west of Mackenzie Canyon, easterly along the 25-m isobath (approximately) west of Mackenzie Bay to a point half way along the Tuktoyaktuk Peninsula, and then northerly across the shelf to the upper part of the continental slope. The energy volume in this zone ranges between 0.0017 and 113 ergs/cm^3. This is considered to be a low-energy environment.

Finally a zone of very low energy occurs seaward beyond the boundaries of the low-energy environment. It extends from almost the head of Mackenzie Bay over Mackenzie Canyon, and across the immediately adjacent shelf to the east. The energy volume, derived from depositional velocities acting on the sediments, is less than 0.0017 ergs/cm^3. Thus almost the entire central area of the southern Beaufort Sea can be characterized as a zone of very low hydrodynamic vigour.

5.6 Texture and Hydrodynamic Environments

A ternary diagram (Fig. 29) is used to demonstrate the relationships between sediment texture, and depositional mode within the framework of various hydrodynamic environments. Normally in the case of sediments depositing from waning currents, the gravels, sands and muds (silts plus clays) deposit in that order. This order is also the progression of decreasing depositional and tractional energy. The border between gravel and mud represents a mixture of sediments deposited from suspension, such as ice-rafting, and the intermediate areas of the diagram may represent contributions of sediments from current and non-current deposition. In the present study, the gravels are excluded so that a closer examination of the finer sediments can be made. Therefore, the sand/silt and silt/clay boundaries in this case represent deposition from waning currents, and the sand/clay boundary represents non-current deposition.

Based on the energy zones determined from the plot of the silt/clay ratios versus the phi mean diameter (Fig. 26), all sample points were plotted according to textural content. As gravel was excluded the content of sand, silt and clay were re-calculated to 100% (Fig. 29). The major hydrodynamic environments were delineated according to the interpretation of Figure 28, so that three main fields of sedimentation are presented. The intermediate energy zone lies in the left part of the ternary diagram (Fig. 29), which is expected as the coarser sediments are plotted there and deposition from tractional and waning currents are characteristic of those sediments. The low energy zone lies in the central part of the diagram where finer sediments deposited from waning currents, together with those deposited from non-current suspension, are plotted, and the very low energy zone is in the lower right corner of the diagram where the finest sediments are plotted, and which represent chiefly sediments deposited almost entirely from waning currents. Some overlap of these sedimentational fields is present on the diagram and this is to be expected because dynamic conditions are not always uniform.

.../15

An additional refinement of this textural/energy plot is shown in a simplified ternary diagram (Fig. 30). Here the mean diameters of each sample (not shown) have been contoured and isopleths of phi values drawn. These values have been related to the depositional energy available, and an energy gradient has been drawn orthogonally to the respective isopleths. The corresponding relationship of decreasing energy with progressively decreasing sediment texture is demonstrated within the textural fields of the sediments. For textural sizes of 2 Ø (0.25 mm), the minimal depositional energy is 1.62 ergs/cm^3. This energy volume decrease is a power function of the decrease in size of the depositing sedimentary particle. For particles that are 8 Ø (.004 mm) in diameter the energy volume is approximately 1/1200 that for particles 2 Ø (0.25 mm) in diameter. This amount, although small, is sufficient to act as a threshold above which sediments 8 Ø in diameter may be maintained in a state of transport.

5.7 Sediment Transport

Based on the textural analyses and interpretation of the results of the clastic ratios and presumed hydrodynamic environments, as shown in Figure 28, a model of sediment transport has been drawn to show the movement of sediments in the southern Beaufort Sea (Fig. 31). Longshore drift takes place in both easterly and westerly directions along the coast, as shown by the direction of growth of bars and spits adjacent to headlands and islands. The major contribution of sediments however is from the Mackenzie River, from which a plume of sediments (observable on satellite photographs) originates and moves a distance of 55 to 70 kms seaward along the axis of the Mackenzie Canyon. This plume veers easterly as it is influenced by the Coriolis force, and forms a distinctive band about 30 to 40 kms wide where it dissipates off the eastern part of Kugmallit Bay. A similar sediment plume emerges from the eastern channel of the Mackenzie Delta and merges with the plume from the western Mackenzie River in the western part of Kugmallit Bay. Some sediment also moves directly seaward along the Tuktoyaktuk Peninsula particularly in the eastern part where it appears to deposit to the edge of the continental shelf.

It is important to note that flocculation of the clay particles occurs within and on the periphery, of the sediment plume. However such particles remain fairly small (clay and fine silt, as seen in filtered suspended material), and are carried seaward and deposited with organic mats. These organic mats appear to bind the sediments and organic particles and deposit them in quieter waters. These organic/inorganic suspensions are shown in photomicrographs (Bornhold, 1976) of suspended sediments obtained in the water column at different depths across the continental shelf.

During the winter the Arctic gyre migrates southward (R. Herlinveaux, personal communication) so that a westerly current is then available to scour and transport fine material (silt and clay) to the west. A possible "race-track" model for sediment transport can be envisioned in which sediments continually move easterly and veer northerly off Liverpool Bay and continued to veer to the left so that the direction of movement is westerly. However this model is unlikely to be true as certain shear forces associated with the movement of the Arctic gyre south would tend to produce discontinuities along the boundary separating easterly and westerly moving sediments. Upwelling observed along the western continental shelf/slope break (see Bornhold, 1976) may introduce sediments to the outer shelf, and this may occur east of Mackenzie Canyon as well.

.../16

An ice-rafted deposit occurs north of Herschel Island, and this is distinct from most other occurrences of gravel on other parts of the shelf. This origin is suggested by the presence of poor sorting, a low content of fine sediment and the fact that sediments occur in a low energy environment.

This model of sediment transport (Fig. 31) is in accordance with the observed movement of sediments from environments of higher hydrodynamic energy to those of lower vigour. Concomitant with this movement, the sediments decrease in size in the direction of sediment transport.

6. Conclusions

6.1 Except for the area northwest of Herschel Island, which is thought to be receiving ice-rafted deposits, sediments of the floor of the Beaufort Sea are mainly fine-grained and consist predominately of clay and silt in the western and central areas, and somewhat coarser types in the eastern part. In the delta area and its immediate offshore, this dispersal pattern is partly a result of the fine-grained sediment discharge from the Mackenzie River. Over the eastern portion of the shelf, the dispersal pattern is partly due to sedimentation of fine particles over a relict surficial sand and partly to the possibility that this sand is presumably intermittently eroded by westward-moving bottom currents. Thus the eastern shelf appears to serve alternately as a depositional and erosional site.

Based on the sediment distribution and the relationship of various textural parameters to hydrodynamic vigour, the model of sediment transport appears to be satisfactory.

The nature and distribution of the clay minerals analyzed can provide baseline data in the event of contamination from oil spills or other anthropogenic sources; similarily, the carbonate and organic carbon can provide such a measure. Although these data are not safeguards in themselves, they will yield some clues on the transport and fate of oil-contaminated particles, so that safeguards to protect the environment can be initiated. Sediment texture is commonly an indicator of bearing stress, so that some idea of such stress can be determined from an examination of the sediment maps, and the proper engineering practises applied. Deposits of coarse sediments suitable for the construction of islands as drilling platforms may be located from a study of the sediment maps, although fuller exploration and development of such deposits would involve the undertaking of ancillary sonic and seismic surveys. This is particularly true in the coastal areas which extend perhaps to the 20 or 30-m isobath.

7. Implications and Recommendations

7.1 Scientifically the Beaufort Sea represents a sedimentary model of relic sediments being obscured by encroaching sedimentation from the discharge of a major fluvial system. The role of sea level has not been discussed but a preliminary support study of the cores indicates that recent submergence has been a dominant factor in creating a site of quiet deposition near the delta front. Additional textural relationships regarding submarine physiography, hydrodynamic vigour, currents, ice and remoteness from shore and other sedimentary source areas must be established. The sub-bottom studies of the unconsolidated material by means of sonic and seismic investigations must be made in order to determine sediment thickness and its origin. Further geochemical studies are needed in order to establish sufficient baseline data that will provide information on the transport and fate of oil-contaminated particles in suspension as well as in the bottom

.../17

sediment load.

7.2 Sediment thickness and geotechnical properties are a major concern in resources development of the sub-sea bed, mainly in developing an engineering background for the emplacement of installations of the sea floor, as they may provide information on the routes of sedimentary transport as well as on the fate of the sediments upon entry into the Beaufort Sea environment. Locating suitable sediments (sand and gravel) for the construction of drill sites is important in view of costs and environmental damage.

7.3 A critical engineering factor is strength of material with reference to loads placed on the sea floor. Because of the widespread nature of sea-floor scouring by keels of drifting ice, shear-stress readings may vary considerably in a local area. Ice tends to compact as well as plough the sediments so that coring and testing to a safe stratigraphic depth is required. Geochemical studies on suspended matter are very dependent on oceanic circulation with regards to the application of such studies on the transport of spilt oil, or oil-contaminated particles. With regard to the removal of sediment for construction purposes certain factors must be kept in mind. If the removal is in a high energy zone, erosion of natural features as distant as several kilometres could be affected. Safeguards can only be established from a detailed study of the oceanographic factors in the prospective exploitable area together with an overview on the natural system of erosion and sedimentation, geography and meteorology.

8. Needs for Further Study

8.1 Identification of existing gaps in knowledge. The following studies are urgently needed: 1) sediment thickness; 2) core analyses of the sub-bottom; 3) sonic and seismic studies to establish the post-Tertiary stratigraphy; 4) completion of the bottom-sampling survey; 5) completion of the mineralogic and geochemical analyses; 6) oceanographic information particularly that dealing with the dynamic aspects such as air-sea interface, tides, waves and currents, (the latter two being most significant when considering sediment erosion and transportation); 7) flow studies on the Mackenzie River, particularly to determine the amount and kind of sedimentary material entering the Beaufort Sea; 8) additional coastal studies particularly those related to the sediment budget; 9) detailed bathymetric studies on ice-scour features and their relationship to sedimentation; 10) shallow drilling to bedrock in order to obtain information on the unconsolidated sediments; and 11) many other related studies which are likely to emerge from other related Beaufort Sea Projects.

8.2 Proposals for Additional Studies

Many proposals are implied in 9.1 above. However for a continuation of this study, the main proposal involves additional sampling by means of ship-supported or helicopter-supported operations, and to observe the sea bottom from direct observations in submersibles. The use of the submersible should be an important arm of Arctic marine research, and should be employed whenever possible in order to develop sufficient skill and knowledge in such operations.

Much of the present scientific information on the Beaufort Sea is to be published in the format of an Atlas. As an additional proposal the writer would be most grateful if he could receive such material from other workers involved in

.../18

the Beaufort Sea Project. Although the Atlas is not part of the project, it will serve as an excellent medium to disseminate knowledge on the various phenomena of the region, in a succinct, interesting and useful format for the educator and the engineer, and for those interested in environmental aspects of this part of the Canadian Arctic, particularly those involved in the development of our natural resources.

Acknowledgements. The writer is most grateful to the following for their participation and assistance involving the technical aspects of this study: the Polar Continental Shelf Project (EMR) for providing logistical support on helicopter and ship operations; the Marine Sciences Directorate (DOE) for providing research platforms such as CSS RICHARDSON, CSS PARIZEAU, CSS BAFFIN, CSS HUDSON, M/V THETA, M/V PANDORA II and the submersible PISCES IV; my associates Gustaves Vilks, Michael Gorveatt, the late David Clark, Donald Clattenburg, David Frobel, Kevin Robertson, Michael Lewis and Lyall Brown for carrying out much of the bottom sampling from the ships as well as the ice surface; Donald Clatterburg who performed the mechanical analyses on the sediments; Robert Delabio for carrying out the X-ray diffraction analyses on the clay minerals, Nicole Bertrand for carrying out the geochemical determination for carbonate and organic carbon; the draughting unit of the Bedford Institute of Oceanography for some of the illustrative work; and Suzanne Costaschuk who plotted the data, assisted on the calculations, prepared the final copy of the illustrations, and provided many suggestions for the final report. The Geological Survey of Canada also provided draughting services, photography, and analytical services in the geochemical, X-ray and sedimentological laboratories.

9. REFERENCES

Bornhold, B.D.

1976 Suspended matter in the southern Beaufort Sea. Beaufort Sea Project Technical Report #25b. Dept. of the Environment, Victoria, B.C. (In Press).

Carsola, A.J.

1952: Marine Geology of the Arctic Ocean and Adjacent Seas off Alaska and Northwestern Canada: Ph.D. dissertation, Univ. of California, Los Angeles, 221 p.

Hjulstrom, F.

1935: The morphological activity of rivers as illustrated by Rivers Fyris, Bull. Geol. Inst. Uppsala, Vol. 25, chap.III.

Lewis, C.P., and Forbes, D.L.

1976: Beaufort Sea coast sediments and sedimentary processes. Beaufort Sea Project Technical Report #24. Dept. of the Environment, Victoria, B.C. (In Press).

Lewis, C.F.M.

1976: Bottom scour by sea ice in Southern Beaufort Sea. Beaufort Sea Project Technical Report #23. Dept. of the Environment, Victoria, B.C. (In Press).

Pelletier, B.R.

1973: A re-examination of the use of the silt/clay ratios as indicators of sedimentary environments. A study for students; Maritime Sediments, v. 9, no. 1, p. 1-12.

1974: Sedimentary textures and relative entropy and their relationship to the hydrodynamic Bay of Fundy system: Offshore Geology of Eastern Canada, Vol. 1, Ed B.R. Pelletier, Geol. Surv. Can., Paper 74-30, p 77-95, 24 pp.

Pelletier, B.R., Ross, D.I., Keen, C.E. and Keen, M.J.

1975: Geology and Geophysics of Baffin Bay; in offshore Geology of Eastern Canada. Vol. 2. Ed. W. van der Linden and J. Wade, Geol. Surv. Can. Paper 74-30, p 247-258.

Pelletier, B.R. and Shearer, J.M.

1972: Sea bottom scouring in the Beaufort Sea of the Arctic Ocean; in Proceedings of 24th International Geological Congress, Montreal, 1972, Section 8, p. 251-261.

Pelto, C.R.

1954: Mapping of multicomponent systems; J. Geol., v. 62, no. 5, p. 501-511.

Shearer, J.M. and Blasco, S.

1975: Further observations on the scouring phenomena in the Beaufort Sea; Report of Activities, Geol. Surv. Can; paper 75-1, Part A, p 483-493.

Shearer, J.M., Macnab, R.F., Pelletier, B.R. and Smith, T.B.

1971: Submarine pingos in the Beaufort Sea; Science, v. 174, P. 816-818.

Vilks, G.

1973: A study of *Globorotalia pachyderma* (Ehrenberg) = *Globigerina pachyderma* (Ehrenberg) in the Canadian Arctic; Unpubl. Ph.D. thesis, Dalhousie University, Halifax, Nova Scotia, 256 p.

Wagner, F.J.E.

1972: Molluscan fauna as indicators of Late Pleistocene history southeastern Beaufort Sea; in 245h International Geological Congress, Montreal, 1972, Section 8, p. 142-153.

APPENDIX A - STATION LOCATIONS AND CRUISES

STATION	CRUISE	YEAR	LATITUDE	LONGITUDE
1	Hudson	1970	60:43.00	140:37.00
2	Hudson	1970	60:59.28	140:15.74
3	Helicopter	1972	69:45.10	140:15.00
4	Helicopter	1972	69:55.00	140:00.00
5	Hudson	1970	69:12.00	139:42.10
6	Helicopter	1970	69:50.00	139:15.00
7	Hudson	1970	69:53.20	139:05.00
8	Hudson	1970	69:54.20	139:28.10
9	Helicopter	1970	70:06.10	139:49.00
10	Hudson	1970	70:10.30	139:52.60
11	Hudson	1970	70:08.40	139:15.90
12	Hudson	1970	70:15.50	139:12.30
13	Hudson	1970	70:22.00	139:05.50
14	Hudson	1970	70:22.00	139.42.00
15	Hudson	1970	70:37.00	139:29.00
16	Hudson	1970	70:27.50	138:57.00
17	Hudson	1970	70:30.50	138:19.59
18	Hudson	1970	70:19.00	138:47.50
19	Hudson	1970	70:19.80	138:11.00
20	Hudson	1970	70:12.50	138:40.00
21	Hudson	1970	70:06.50	138:31.00
22	Parizeau	1970	70:00.00	138:55.00
23	Hudson	1970	69:57.50	138:27.00
24	Hudson	1970	60:56.00	138:54.80
25	Hudson	1970	69:50.00	138:18.00
26	Hudson	1970	69:45.00	138:34.00
27	Hudson	1970	69:40.00	138:14.00
28	Hudson	1970	69:38.00	138:45.00

STATION	CRUISE	YEAR	LATITUDE	LONGITUDE
29	Parizeau	1970	69:34.30	138:55.90
30	Hudson	1970	69:36.00	138:24.00
31	Hudson	1970	69:33.00	138:11.80
32	Hudson	1970	69:28.00	138:48.00
33	Parizeau	1970	69:26.00	138:31.00
34	Hudson	1970	69:22.10	138:04.80
35	Parizeau	1970	69:16.00	138:17.00
36	Hudson	1970	69:11.00	137:57.00
37	Parizeau	1970	69:06.00	137:50.00
38	Helicopter	1971	69:00.83	137:07.33
39	Helicopter	1971	69:09.75	137:30.00
40	Parizeau	1970	69:16.00	137:35.00
41	Helicopter	1971	69:17.33	137:05.00
42	Parizeau	1970	69:20.00	137:35.00
43	Helicopter	1971	69:23.00	137:40.00
44	Parizeau	1970	69:30.00	137:50.00
45	Hudson	1970	69:27.00	137:10.00
46	Helicopter	1971	69:31.50	137:03.50
47	Hudson	1970	69:36.00	137:20.00
48	Parizeau	1970	69:40.00	137:50.00
49	Parizeau	1970	69:46.00	137:06.00
50	Hudson	1970	69:47.00	137:32.00
51	Parizeau	1970	69:55.00	137:49.00
52	Parizeau	1970	70:00.00	137:20.00
53	Hudson	1970	70:01.00	137:50.00
54	Parizeau	1970	70:05.00	137:33.00
55	Hudson	1970	70:08.20	137:15.80
56	Hudson	1970	70:10.50	137:59.50
57	Hudson	1970	70:21.50	137:33.00
58	Parizeau	1971	70:24.20	137:08.20

STATION	CRUISE	YEAR	LATITUDE	LONGITUDE
59	Hudson	1970	70:29.80	137:49.00
60	Hudson	1970	70:45.70	137:04.00
61	Hudson	1970	70:50.85	136:17.92
62	Hudson	1970	70:32:00	136:40.00
63	Parizeau	1971	70:30.20	136:03.00
64	Parizeau	1971	70:19.00	136:51.80
65	Hudson	1970	70:18.00	136:15.00
66	Parizeau	1971	70:08.80	136:35.40
67	Parizeau	1970	70:00.00	135:23.00
68	Hudson	1971	69:58.00	137.00.00
69	Hudson	1970	69:51.00	136:48.00
70	Parizeau	1970	69:50.00	136:10.00
71	Hudson	1970	69:44.70	136:37.30
72	Helicopter	1971	69:42.50	136:07.50
73	Parizeau	1970	69:35.00	136:39.00
74	Helicopter	1971	69:04.50	136:08.00
75	Helicopter	1971	69:26.50	136.31.00
76	Helicopter	1971	69:21.41	136:50.00
77	Helicopter	1971	69:21.41	136:50.00
78	Helicopter	1971	69:14.33	136:20.60
79	Helicopter	1971	69:08.00	136:44.13
80	Helicopter	1971	68:56.66	136.44.50
81	Helicopter	1971	68:54.33	136:20.00
82	Helicopter	1971	68:56.00	136:16.00
83	Helicopter	1971	68:53.50	136:02.00
84	Helicopter	1971	68:49.50	135:46.00
85	Helicopter	1971	68:44.16	135:29.50
86	Helicopter	1970	68:53.50	135:03.30
87	Helicopter	1970	68:54.00	135:22.00
88	Helicopter	1971	69:37.00	135:52.00

STATION	CRUISE	YEAR	LATITUDE	LONGITUDE
89	Helicopter	1971	69:35.06	135:10.75
90	Richardson	1970	69:41.47	135:11.46
91	Helicopter	1971	69:44.50	135:24.00
92	Hudson	1970	69:51.00	135:20.00
93	Hudson	1970	70:00.60	135:39.10
94	Parizeau	1971	70:03.40	135:15.60
95	Hudson	1970	70:10.60	135:54.50
96	Parizeau	1971	70:14.30	135:31.80
97	Hudson	1970	70:10.60	135:54.50
98	Parizeau	1971	70:19.40	135:47.80
99	Hudson	1970	70:26.00	135:27.00
100	Hudson	1970	70:37.60	135:49.40
101	Hudson	1970	70:42.50	135:52.00
102	Parizeau	1971	70:41.10	135:16.30
103	Hudson	1970	70:57.40	135:03.40
104	Hudson	1970	71:12.00	134.22.50
105	Hudson	1970	71:01.00	134:07.00
106	Hudson	1970	40:52.35	134:57.00
107	Parizeau	1971	70:51.70	134:27.20
108	Hudson	1970	70:46.50	134:50.00
109	Hudson	1970	70:41.30	134:41.50
110	Parizeau	1971	70:41.10	134:11.10
111	Parizeau	1971	70:30.40	134:59.90
112	Parizeau	1971	70:24.90	134:44.00
113	Hudson	1970	70:26.50	134:17.50
114	Parizeau	1971	70:14.10	134:28.30
115	Hudson	1970	70:08.00	134:54.00
116	Parizeau	1971	70:98.90	134:11.90
117	Parizeau	1971	69:57.00	134:12.80
118	Hudson	1970	69:56.50	134:33.00

STATION	CRUISE	YEAR	LATITUDE	LONGITUDE
119	Parizeau	1971	69:58.00	134:59.60
120	Helicopter	1971	69:50.00	134:30.00
121	Helicopter	1971	69:46.50	134:54.00
122	Helicopter	1970	69:46.50	134:22.00
123	Richardson	1970	69:47.40	134.09.96
124	Helicopter	1971	69:40.50	134.04.00
125	Helicopter	1970	69:42.50	134:21.00
126	Helicopter	1970	69:33.50	134:31.00
127	Helicopter	1971	69:11.50	134:13.00
128	Helicopter	1971	69:09.58	134:24.00
129	Helicopter	1970	68:58.30	134.39.00
130	Helicopter	1970	68:53.30	134.54.30
131	Helicopter	1970	68:51.30	134:29.30
132	Helicopter	1970	68:45.00	134:22.00
133	Helicopter	1970	68:40.00	134:21.00
134	Helicopter	1970	68:29.50	134:12.00
135	Helicopter	1970	69:23.50	133:55.00
136	Helicopter	1970	69:22.00	133.45.50
137	Richardson	1970	69:30.18	133:22.86
138	Richardson	1970	69:30.18	133:22.86
139	Richardson	1970	69:34.66	133:02.76
140	Richardson	1970	69:38.63	133:06.93
141	Richardson	1970	69:37.94	133:99.86
142	Richardson	1970	69:45.33	133:34.91
143	Hudson	1970	69:52.00	133:19.50
144	Parizeau	1971	70:02.80	133:09.60
145	Hudson	1970	70:02.00	133:45.80
146	Parizeau	1971	70:08.60	133:25.60
147	Hudson	1970	70:17.00	134:00.00
148	Parizeau	1971	70:19.30	133:23.80

STATION	CRUISE	YEAR	LATITUDE	LONGITUDE
149	Hudson	1970	70:24.00	133:09.00
150	Parizeau	1971	70:24.70	133:33.90
151	Parizeau	1971	70:30.20	133:55.40
152	Hudson	1970	70:38.00	133:29.00
153	Parizeau	1971	70:40.30	133:06.50
154	Hudson	1970	70:47.00	133:47.00
155	Parizeau	1971	70:50.70	133:19.80
156	Hudson	1970	70:56.00	133:59.00
157	Baffin	1970	71:01.67	133:29.28
158	Hudson	1970	71:09.50	133:07.00
159	Hudson	1970	71:18.50	133:23.50
160	Hudson	1970	71:25.70	132.06.00
161	Baffin	1970	71:07.48	132:32.94
162	Hudson	1970	71:02.80	132:59.50
163	Baffin	1970	71:00.07	132:21.45
164	Hudson	1970	70:56.20	132:47.00
165	Baffin	1970	70:50.85	132:19.01
166	Hudson	1970	70:45.20	132:27.60
167	Hudson	1970	70:31.80	132:10.00
168	Parizeau	1971	70:29.60	132:51.30
169	Parizeau	1971	70:18.90	132:36.30
170	Hudson	1970	70:14.50	132:06.10
171	Helicopter	1971	69:41.00	132:52.50
172	Parizeau	1971	70:07.80	132:21.90
173	Hudson	1970	70:08.50	132.47.90
174	Hudson	1970	70:00.00	132:32.00
175	Helicopter	1971	69:59.00	132:03.00
176	Helicopter	1971	69:52.50	132.03.00
177	Richardson	1970	69:51.74	132:36.01
178	Helicopter	1971	69:54.33	132:49.00

STATION	CRUISE	YEAR	LATITUDE	LONGITUDE
179	Helicopter	1971	69:46.50	132:50.50
180	Richardson	1970	69:45.94	132:42.15
181	Helicopter	1971	69:46.83	132:04.00
182	Richardson	1970	69:52.25	131:44.03
183	Richardson	1970	69:56.50	131:45.16
184	Richardson	1970	69:57.40	131:19.00
185	Helicopter	1971	70:04 .41	131:12.50
186	Hudson	1970	70:07.00	131:35.00
187	Helicopter	1971	70:12.25	131:13.00
188	Parizeau	1971	70:17.50	131:33.50
189	Parizeau	1972	70:28.40	131:16.90
190	Baffin	1970	70:33.82	131:42.84
191	Parizeau	1972	70:39.10	131:18.00
192	Baffin	1970	70:42.17	131:48.53
193	Parizeau	1972	70:49.70	131:35.50
194	Parizeau	1972	70:50.00	131:03.00
195	Hudson	1970	70:56.50	131:24.70
196	Parizeau	1972	70:00.80	131:03.90
197	Hudson	1970	71:03.50	131:42.70
198	Parizeau	1972	71:11.60	131:05.10
199	Hudson	1970	71:14.14	131:54.76
200	Hudson	1970	71:26.75	130:53.87
201	Hudson	1970	71:16.60	130:37.60
202	Hudson	1970	71:07.00	130:17.80
203	Hudson	1970	70:56.80	130:03.60
204	Parizeau	1972	70:55.70	130:30.40
205	Parizeau	1972	70:45.00	130:29.70
206	Hudson	1970	70:41.30	130:52.10
207	Parizeau	1972	70:39.70	130:13.30
208	Hudson	1970	70:31.80	130:41.60

STATION	CRUISE	YEAR	LATITUDE	LONGITUDE
209	Helicopter	1971	70:30.00	130:11.00
210	Helicopter	1971	70:24.50	130:07.50
211	Hudson	1970	70:22.40	130:31.00
212	Parizeau	1972	70:17.70	130:59.20
213	Helicopter	1971	70:15.25	130:05.00
214	Helicopter	1971	70:08.50	130:03.00
215	Helicopter	1971	69:39.50	130:34.00
216	Helicopter	1971	69:46.00	130:10.00
217	Helicopter	1971	69:51.25	129:46.00
218	Parizeau	1971	69:52.90	129:51.10
219	Helicopter	1970	69:58.00	129:39.00
220	Helicopter	1970	69:42.00	129:06.00
221	Helicopter	1971	69:57.50	129:16.00
222	Parizeau	1971	70:06.00	129:14.00
223	Parizeau	1972	70:18.50	128:59.60
224	Parizeau	1972	70:23.80	129:59.10
225	Hudson	1970	70:29.80	129:22.80
226	Hudson	1970	70:38.70	129:39.40
227	Parizeau	1972	70:45.40	129:08.20
228	Hudson	1970	70:50.00	129:52.00
229	Parizeau	1972	70:56.10	129.24.70
230	Parizeau	1972	71:01.50	129:41.40
231	Hudson	1970	71:25.20	129:27.30
232	Hudson	1970	71:25.20	129:27.30
233	Hudson	1970	71:17.50	129:10.60
234	Hudson	1970	71:07.90	128:59.10
235	Hudson	1970	71:01.00	128:49.50
236	Parizeau	1972	70:56.20	128:18.60
237	Hudson	1970	70:52.00	128:23.00
238	Hudson	1970	70:41.00	128:19.00

STATION	CRUISE	YEAR	LATITUDE	LONGITUDE
239	Parizeau	1972	70:34.70	128:51.60
240	Helicopter	1971	70:24.50	128:47.50
241	Helicopter	1971	70:13.00	128:21.50
242	Parizeau	1971	70:03.00	128:55.05
243	Parizeau	1971	70:09.80	128:46.50
244	Helicopter	1970	69:47.00	128:19.00

APPENDIX B - TABLE OF TEXTURAL DATA (ANALYSES BY DONALD CHATTENBERG)

STATION NUMBER (Fig.1)	WATER DEPTH (m)	SEDIMENT TYPE				MOMENT MEASURES			RELATIVE ENTROPY (Hr %)
		GRAVEL %	SAND %	SILT %	CLAY %	MEAN DIAM (ø)	STANDARD DEVIATION (ø)	SKEWNESS (ø)	
1	26	6.64	18.83	37.95	36.57	5.94	3.51	-0.45	72.53
2	51	9.23	55.89	12.67	22.22	3.64	3.76	+0.14	78.50
3	32	0.33	3.56	38.04	58.07	7.93	1.96	-0.66	57.16
4	42	3.30	20.15	36.55	40.00	6.32	3.15	-0.41	72.73
5	25	3.89	34.03	33.37	28.71	5.15	3.45	-0.13	82.12
6	45	40.45	13.99	16.90	28.66	2.58	5.49	+0.06	81.52
7	60	38.30	31.67	10.73	19.30	1.46	5.05	+0.17	88.29
8	44	28.25	32.64	15.95	23.15	2.76	4.63	+0.11	87.42
9	62	38.12	25.81	9.72	26.36	1.86	5.78	+0.03	81.90
10	62	19.60	35.37	12.38	32.65	3.69	4.97	-0.14	85.68
11	211	0.27	3.54	25.35	70.84	8.35	1.83	-0.95	49.83
12	451	0.00	0.27	25.33	74.40	8.65	1.29	-0.73	43.59
13	610	0.00	0.23	26.19	73.58	8.61	1.30	-0.67	44.11
14	537	0.18	0.30	26.12	73.41	8.58	1.39	-1.14	45.29
15	1455	0.01	0.26	23.78	75.95	8.69	1.20	-0.78	42.82
16	740	0.00	0.22	25.14	74.64	8.66	1.22	-0.72	43.70
17	801	0.31	4.60	18.92	76.16	8.51	1.80	-1.26	46.29
18	549	0.00	0.27	26.06	73.67	8.61	1.28	-0.73	45.02
19	421	0.07	0.19	30.80	68.94	8.46	1.38	-0.69	47.98
20	390	0.24	0.33	25.18	74.26	8.63	1.38	-1.13	42.91
21	295	0.05	0.18	22.67	77.10	8.72	1.24	-0.88	41.91
22	300	0.36	0.65	20.40	78.59	8.69	1.48	-1.52	41.89
23	250	0.15	0.16	22.65	77.04	8.75	1.19	-1.07	48.58
24	200	0.01	1.17	28.89	69.94	8.44	1.51	-0.70	48.68
25	198	0.22	0.35	26.72	72.71	8.54	1.45	-0.94	45.62
26	177	0.06	1.07	26.70	72.18	8.50	1.43	-0.83	47.99
27	139	0.10	1.81	39.83	58.26	7.91	1.87	-0.43	56.51
28	66	1.19	2.30	28.78	67.73	8.17	2.14	-0.20	53.01
29	9	0.01	3.56	47.35	49.08	7.48	2.06	-0.25	60.35
30	131	0.20	9.08	41.94	48.77	7.38	2.18	-0.32	62.57
31	100	0.02	0.96	45.96	53.06	7.84	1.73	-0.28	56.79
32	49	0.00	1.09	40.41	58.50	8.01	1.75	-0.41	54.45
33	22	0.00	25.57	31.05	43.38	6.63	2.71	-0.12	65.84
34	42	0.21	0.74	33.56	65.49	8.28	1.61	-0.83	51.68
35	13	0.00	7.23	66.55	26.22	6.29	2.07	+0.21	61.70
36	33	0.02	0.11	28.93	70.94	8.52	1.31	-0.66	47.13
37	15	0.00	1.06	35.64	63.30	8.16	1.73	-0.54	52.85
38	4	0.00	0.03	83.92	16.05	6.08	1.56	+0.60	50.54
39	17	0.03	0.02	60.26	39.69	7.56	1.52	-0.02	55.92
40	34	0.00	0.23	31.70	68.07	8.54	1.23	-0.56	45.51

STATION NUMBER (Fig.1)	WATER DEPTH (m)	SEDIMENT TYPE				MOMENT MEASURES			RELATIVE ENTROPY (Hr %)
		GRAVEL %	SAND %	SILT %	CLAY %	MEAN DIAM (ø)	STANDARD DEVIATION (ø)	SKEWNESS (ø)	
41	3	0.01	0.03	58.84	41.12	7.70	1.43	-0.04	55.41
42	33	0.00	0.49	40.85	58.66	8.08	1.45	-0.37	54.85
43	26	0.05	0.21	24.92	74.82	8.65	1.28	-0.88	44.15
44	63	0.00	0.93	26.48	72.59	8.52	1.52	-0.80	46.38
45	24	0.00	0.09	29.35	70.56	8.59	1.17	-0.54	45.20
46	8	0.02	0.05	33.60	66.33	8.48	1.22	-0.48	46.88
47	44	0.02	0.10	38.22	61.66	8.37	1.22	-0.35	49.92
48	73	0.00	0.96	28.80	70.23	8.54	1.55	-0.77	42.43
49	43	0.00	0.03	35.35	64.62	8.44	1.22	-0.39	47.40
50	60	0.03	0.08	37.22	62.66	8.40	1.21	-0.42	47.63
51	113	1.38	1.62	23.55	73.55	8.39	2.10	-1.55	47.29
52	66	0.00	0.33	20.13	79.54	8.81	1.15	-0.98	39.72
53	98	0.10	0.83	22.50	76.86	8.65	1.42	-1.02	43.20
54	66	0.00	1.39	17.58	81.03	8.79	1.34	-1.31	39.88
55	47	0.04	0.31	18.54	81.11	8.85	1.13	-1.13	38.77
56	240	29.44	2.81	15.71	52.03	4.39	6.49	-0.38	58.07
57	322	0.02	2.91	35.55	61.54	8.04	1.83	-0.51	55.16
58	539	0.06	0.76	34.14	65.05	8.26	1.60	-0.58	51.72
59	846	0.02	0.47	23.51	76.00	8.69	1.28	-0.87	42.79
60	1390	0.00	0.22	27.26	72.52	8.59	1.28	-0.66	44.95
61	864	4.31	2.13	17.23	76.33	8.21	2.88	-1.55	47.07
62	700	0.00	0.09	29.53	70.38	8.49	1.39	-0.58	46.91
63	67	0.04	0.37	22.44	77.14	8.70	1.29	-0.96	42.63
64	64	0.79	1.76	30.27	67.18	8.41	1.90	-1.27	43.81
65	57	0.05	0.23	19.57	80.16	8.82	1.18	-1.10	39.19
66	43	0.08	0.93	21.14	77.85	8.74	1.30	-1.27	41.44
67	34	0.00	0.32	31.15	68.53	8.50	1.29	-0.63	46.80
68	38	0.06	0.18	23.41	76.36	8.74	1.15	-0.99	41.38
69	27	0.00	0.03	25.55	74.42	8.70	1.09	-0.60	42.53
70	18	0.09	0.17	47.27	52.46	7.99	1.51	-0.36	53.74
71	18	0.01	0.04	31.99	67.97	8.49	1.26	-0.49	46.53
72	20	0.01	0.48	49.09	50.43	7.97	1.46	-0.23	27.79
73	17	0.00	0.20	37.39	62.41	8.34	1.33	-0.41	49.21
74	4	0.00	0.03	57.12	42.85	7.85	1.35	-0.03	52.91
75	6	0.00	0.02	56.36	43.62	7.85	1.33	-0.03	53.02
76	2	0.02	0.06	54.52	45.40	7.88	1.36	-0.13	53.61
77	2	0.00	56.56	37.38	6.06	4.40	1.55	+1.03	45.35
78	2	0.00	6.01	71.36	22.63	6.49	1.80	+0.17	64.42
79	2	0.00	2.96	92.26	4.78	4.81	1.14	+1.63	23.46
80	2	0.00	2.21	87.59	10.20	5.58	1.49	+0.77	50.09

STATION NUMBER (Fig.1)	WATER DEPTH (m)	SEDIMENT TYPE				MOMENT MEASURES			RELATIVE ENTROPY (Hr %)
		GRAVEL %	SAND %	SILT %	CLAY %	MEAN DIAM (ø)	STANDARD DEVIATION (ø)	SKEWNESS (ø)	
81	2	0.00	1.37	83.36	15.27	6.17	1.56	+0.49	55.99
82	2	0.00	0.07	82.43	17.51	6.38	1.52	+0.48	53.91
83	5	0.00	17.72	70.20	12.08	5.55	1.76	+0.51	59.34
84	1	0.00	22.28	71.62	6.09	4.86	1.41	+0.99	48.74
85	2	0.01	1.32	85.47	13.20	6.03	1.63	+0.42	55.92
86	1	0.00	0.72	87.98	11.30	5.65	1.55	+0.68	50.09
87	1	0.00	0.85	92.65	6.50	5.12	1.29	+1.11	36.87
88	3	0.60	0.35	70.37	28.68	7.08	1.71	-0.35	57.38
89	3	0.00	0.46	71.00	28.54	6.86	1.70	+0.18	59.99
90	6	0.00	0.58	77.32	22.09	6.60	1.66	+0.26	59.90
91	6	0.01	0.30	64.21	35.47	7.29	1.70	+0.05	57.70
92	16	0.04	0.14	47.00	52.82	8.06	1.42	-0.28	52.84
93	28	0.00	0.03	32.67	67.30	8.52	1.21	-0.44	45.95
94	42	0.00	0.03	34.21	65.76	8.43	1.17	-0.35	47.67
95	46	0.00	0.07	23.06	76.87	8.77	1.17	-0.77	40.30
96	55	0.00	0.28	19.60	80.12	8.83	1.11	-0.92	39.27
97	55	0.04	0.91	17.35	81.71	8.84	1.18	-1.27	29.05
98	62	0.00	0.13	19.22	80.64	8.82	1.09	-0.85	39.81
99	62	0.00	0.15	19.17	80.67	8.84	1.05	-0.84	32.80
100	87	0.17	1.98	25.95	71.89	8.43	1.64	-0.90	48.79
101	495	0.08	0.14	31.45	68.32	8.42	1.46	-0.66	48.96
102	71	0.17	1.40	22.83	75.60	8.58	1.53	-1.07	45.26
103	457	0.00	0.06	28.68	71.27	8.54	1.33	-0.57	45.56
104	850	0.00	0.16	27.33	72.51	8.57	1.31	-0.65	45.52
105	277	0.07	0.37	29.98	69.58	8.43	1.52	-0.68	48.23
106	146	0.18	8.37	27.66	63.79	7.90	2.26	-0.74	57.70
107	78	0.00	0.19	20.58	79.23	8.77	1.24	-0.93	40.31
108	73	0.01	0.15	22.51	77.33	8.71	1.21	-0.82	51.06
109	58	1.59	13.09	14.53	70.53	7.90	2.70	-0.99	52.24
110	64	0.00	2.37	20.88	76.75	8.60	1.56	-1.09	44.67
111	60	0.07	0.92	19.18	79.83	8.76	1.29	-1.18	41.10
112	54	0.09	41.57	10.41	47.93	6.20	3.31	-0.12	57.84
113	62	0.02	0.39	16.74	82.85	8.87	1.11	-1.13	38.24
114	42	0.00	1.99	25.28	72.72	8.53	1.46	-1.00	58.15
115	37	0.01	0.92	22.82	76.25	8.70	1.24	-0.97	42.60
116	33	0.00	15.24	21.05	63.41	7.70	2.56	-0.65	55.11
117	12	0.00	10.86	48.02	41.11	7.19	2.19	-0.39	62.60
118	16	0.10	1.15	37.41	61.34	9.26	1.50	-0.71	51.04
119	23	0.00	0.06	41.27	58.67	8.23	1.35	-0.30	50.98
120	4	0.00	0.03	54.78	45.20	7.85	1.39	-0.06	52.38

STATION NUMBER (Fig.1)	WATER DEPTH (m)	SEDIMENT TYPE				MOMENT MEASURES			RELATIVE ENTROPY (Hr %)
		GRAVEL %	SAND %	SILT %	CLAY %	MEAN DIAM (ø)	STANDARD DEVIATION (ø)	SKEWNESS (ø)	
121	4	0.00	0.09	90.31	9.60	5.86	1.40	+0.76	47.16
122	1	0.00	97.86	0.93	1.21	2.69	0.87	+3.02	20.21
123	5	0.03	3.83	60.70	35.44	7.21	1.81	-0.17	63.58
124	32	0.00	0.09	40.64	59.27	8.29	1.27	-0.29	48.45
125	1	0.00	97.17	0.80	2.03	2.84	1.07	+2.49	23.70
126	1	0.00	7.53	86.67	5.80	5.01	1.27	+1.21	40.96
127	1	0.46	42.37	39.15	18.02	5..09	2.57	+0.20	71.21
128	1	0.00	6.05	64.65	29.30	6.59	2.04	+0.13	63.44
129	1	0.04	19.96	74.88	5.12	4.87	1.37	+0.93	47.51
130	1	0.00	0.76	85.04	14.19	6.05	1.59	+0.45	56.99
131	1	0.17	24.62	68.73	6.48	4.81	1.56	+0.74	50.51
132	1	0.00	5.16	85.52	12.32	5.72	1.64	+0.58	56.13
133	1	0.00	9.25	70.38	20.37	6.16	2.01	+0.04	68.42
134	1	0.00	0.53	73.92	25.55	6.88	1.65	+0.09	61.48
135	1	0.00	3.96	76.05	19.99	6.35	1.77	+0.25	62.53
136	1	0.00	83.36	14.83	1.81	3.74	0.93	+2.28	22.46
137	4	0.00	0.03	77.00	22.97	6.67	1.62	+0.29	58.10
138	3	2.07	96.78	0.69	0.46	1.55	1.12	-0.25	22.18
139	3	0.13	98.87	0.32	0.68	1.95	0.88	+2.02	25.96
140	5	0.00	0.15	59.09	40.76	7.66	1.45	-0.05	55.69
141	4	0.00	1.87	78.10	20.03	6.27	1.79	+0.29	60.18
142	8	0.00	0.36	53.98	45.66	7.74	1.54	-0.10	56.08
143	16	0.02	0.06	43.48	56.44	8.16	1.37	-0.28	51.32
144	22	0.08	39.04	19.02	41.86	6.00	3.34	-0.13	62.86
145	30	0.00	0.05	32.88	67.07	8.50	1.23	-0.46	46.61
146	42	0.06	1.75	21.99	76.20	8.66	1.77	-1.21	43.04
147	45	0.05	10.74	16.64	72.57	8.24	2.08	-0.88	48.86
148	40	0.04	1.79	21.43	76.74	8.66	1.43	-1.27	43.48
149	42	0.13	23.33	19.30	57.24	7.15	2.93	-0.46	61.16
150	69	0.44	11.89	21.54	66.13	7.88	2.39	-0.76	55.75
151	67	0.00	14.91	21.57	63.82	7.73	2.40	-0.52	66.92
152	62	0.06	0.35	22.02	77.56	8.69	1.30	-0.98	43.03
153	49	0.02	30.03	19.66	50.29	6.64	3.09	-0.24	55.64
154	70	0.04	2.14	28.58	69.24	8.28	1.79	-0.70	50.62
155	66	0.04	17.21	22.11	60.64	7.39	2.86	-0.55	58.33
156	85	0.01	0.53	31.14	58.32	8.30	1.66	-0.63	50.11
157	110	0.04	2.08	26.49	71.39	8.31	1.72	-0.69	50.51
158	346	0.00	0.05	55.80	44.14	7.05	2.18	-0.04	56.67
159	699	0.01	0.15	33.28	66.55	8.41	1.38	-0.52	47.87
160	580	0.02	0.29	30.02	69.67	8.50	1.36	-0.66	47.14

STATION NUMBER (Fig.1)	WATER DEPTH (m)	SEDIMENT TYPE				MOMENT MEASURES			RELATIVE ENTROPY (Hr %)
		GRAVEL %	SAND %	SILT %	CLAY %	MEAN DIAM (ø)	STANDARD DEVIATION (ø)	SKEWNESS (ø)	
161	90	0.02	4.21	36.51	59.26	7.26	2.02	-0.48	57.78
162	80	0.20	23.89	34.73	41.18	6.40	2.80	-0.11	66.26
163	71	0.08	12.73	29.40	57.79	7.63	2.38	-0.61	47.40
164	50	0.21	20.55	21.77	57.46	7.26	2.78	-0.45	60.20
165	50	0.04	32.82	49.46	17.68	5.20	2.35	.30	70.26
166	32	0.15	27.39	35.88	36.59	6.15	2.77	-0.07	69.09
167	63	0.04	6.18	28.00	65.78	8.07	2.04	-0.79	54.33
168	46	0.14	17.45	21.14	61.27	7.54	2.67	-0.60	58.42
169	35	0.09	14.93	20.46	64.51	7.61	2.48	-0.72	58.51
170	31	0.58	64.70	8.79	25.93	4.07	3.49	+0.33	53.69
171	2	0.00	98.84	0.56	0.59	2.52	0.68	+3.53	17.95
172	24	0.01	0.29	32.91	66.80	8.50	1.24	-0.51	45.72
173	25	0.02	9.96	20.77	69.25	8.15	2.10	-0.85	51.84
174	19	0.15	16.11	27.54	56.20	7.47	2.61	-0.61	58.53
175	11	0.19	0.17	46.75	52.89	8.01	1.52	-0.45	53.49
176	6	0.03	0.23	64.43	35.31	7.46	1.48	+0.02	56.60
177	11	0.00	2.19	57.68	40.14	7.49	1.70	-0.27	58.81
178	10	0.05	1.09	66.89	31.96	7.11	1.70	+0.01	58.17
179	8	0.00	0.44	69.74	29.82	7.09	1.61	+0.14	57.49
180	7	0.00	0.18	54.51	45.31	7.78	1.79	-0.14	55.91
181	4	0.14	1.29	39.92	58.65	8.21	1.51	-0.95	44.81
182	10	0.00	41.53	33.41	25.06	5.57	2.90	+0.04	65.42
183	12	0.00	0.42	58.71	40.87	7.65	1.51	-0.11	56.31
184	4	0.03	3.67	45.46	50.83	7.67	1.95	-0.51	61.13
185	12	0.03	5.78	58.56	35.63	7.14	1.90	-0.21	63.39
186	17	0.10	1.48	47.44	50.98	7.90	1.64	-0.53	56.58
187	24	0.00	0.11	44.95	54.94	8.10	1.43	-0.26	52.92
188	35	0.01	0.09	35.10	64.79	8.42	1.24	-0.46	47.79
189	34	0.18	28.62	23.55	47.65	6.74	2.87	-0.24	45.84
190	21	0.00	0.62	49.40	49.98	7.85	1.60	-0.26	56.93
191	31	0.00	42.56	21.27	36.17	5.62	3.24	+0.03	66.44
192	48	0.07	28.29	30.50	41.14	6.37	2.87	-0.13	69.83
193	53	0.11	23.32	24.72	51.85	6.99	2.90	-0.37	62.88
194	50	0.10	12.75	35.84	51.31	7.38	2.36	-0.45	65.12
195	54	2.76	14.06	30.57	52.61	7.12	3.01	-0.66	66.69
196	56	0.35	14.73	26.02	58.90	7.46	1.99	-0.27	61.96
197	62	0.35	14.73	26.02	58.90	7.49	2.59	-0.58	61.13
198	63	0.04	82.76	4.63	12.58	3.28	2.52	+0.90	43.31
199	97	0.23	44.51	19.51	35.75	5.63	3.14	+0.04	65.20
200	300	0.00	0.20	33.93	65.87	8.33	1.48	-0.50	49.97

STATION NUMBER (Fig.1)	WATER DEPTH (m)	SEDIMENT TYPE				MOMENT MEASURES			RELATIVE ENTROPY (Hr %)
		GRAVEL %	SAND %	SILT %	CLAY %	MEAN DIAM (ø)	STANDARD DEVIATION (ø)	SKEWNESS (ø)	
201	62	6.20	32.27	26.75	34.78	5.37	3.72	-0.37	73.47
202	44	0.17	1.68	50.54	47.60	7.50	1.97	-0.30	60.42
203	32	0.29	2.36	55.11	42.23	7.26	2.04	-0.25	62.27
204	43	0.04	12.88	35.76	51.33	7.35	2.49	-0.47	63.12
205	35	0.08	1.99	40.83	57.09	7.96	1.80	-0.65	57.17
206	32	0.05	43.96	20.99	35.00	5.72	3.12	.01	60.67
207	27	0.07	2.44	44.50	53.00	7.75	1.94	-0.48	59.58
208	25	0.30	22.06	27.51	50.12	7.13	2.66	-0.42	64.45
209	20	0.09	12.22	34.93	52.76	7.54	2.29	-0.54	61.64
210	7	0.08	89.45	4.74	5.73	3.49	1.69	1.23	41.55
211	18	0.36	11.63	40.23	47.78	7.83	2.31	-0.49	64.02
212	18	0.00	1.65	40.62	57.73	8.05	1.67	-0.55	55.42
213	8	0.11	88.05	6.27	5.58	3.38	1.76	1.77	46.41
214	1	0.00	92.80	3.99	3.21	2.87	1.37	1.89	33.14
215	8	0.25	13.64	27.21	58.90	7.44	2.66	-0.49	59.68
216	10	0.50	2.01	29.13	68.37	8.35	1.78	-1.08	49.88
217	10	0.09	97.33	0.39	2.19	2.19	1.23	2.16	29.83
218	9	0.07	69.28	14.60	16.05	3.94	2.76	.56	57.85
219	1	7.21	91.64	0.40	0.75	1.81	1.79	-0.81	41.40
220	1	0.19	2.90	68.65	28.26	6.15	2.05	-0.06	63.67
221	14	0.02	0.99	30.65	68.35	8.49	1.38	-0.75	46.97
222	11	0.09	2.81	28.90	58.20	8.07	1.75	-0.66	54.79
223	11	0.00	8.13	61.25	30.62	6.58	2.09	.12	63.85
224	11	0.00	55.52	34.35	10.13	4.68	1.91	.82	49.92
225	16	0.09	2.61	68.46	28.83	6.46	2.03	.11	61.84
226	22	1.04	3.03	47.27	48.66	7.54	2.13	-0.70	61.88
227	25	0.59	4.37	54.62	40.42	7.31	2.19	-0.45	60.58
228	29	0.43	2.10	60.48	36.99	6.86	2.20	-0.18	70.89
229	32	0.63	15.36	52.56	31.45	6.34	2.32	-0.12	70.10
230	38	0.10	7.28	54.47	38.14	6.89	2.22	-0.10	65.42
231	225	0.04	0.14	32.21	67.61	8.44	1.37	-0.57	47.82
232	69	0.79	2.78	42.70	53.73	7.63	2.39	-0.72	60.61
233	475	0.93	11.61	58.31	29.15	6.20	2.40	-0.03	63.67
234	45	0.25	39.14	32.83	27.78	5.63	2.70	.12	69.97
235	40	10.07	7.21	41.64	41.08	6.31	3.83	-0.71	72.84
236	49	36.18	29.15	16.15	18.52	1.79	4.93	.15	87.72
237	36	1.35	31.80	36.17	30.68	5.73	3.13	-0.19	72.84
238	29	0.84	74.49	14.75	9.92	3.59	2.33	.70	54.86
239	15	0.15	21.59	40.55	37.71	6.49	2.61	-0.10	68.61
240	13	0.00	42.25	34.43	23.32	5.60	2.41	.28	63.15

STATION NUMBER (Fig.1)	WATER DEPTH (m)	SEDIMENT TYPE				MOMENT MEASURES			RELATIVE ENTROPY (Hr %)
		GRAVEL %	SAND %	SILT %	CLAY %	MEAN DIAM (ø)	STANDARD DEVIATION (ø)	SKEWNESS (ø)	
241	12	0.04	1.62	65.57	32.76	6.95	1.89	+0.04	61.99
242	11	0.00	0.90	25.27	73.83	8.64	1.32	-0.87	44.02
243	14	0.06	1.00	31.83	67.10	8.41	1.49	-0.70	48.91
244	1	0.07	13.61	64.94	21.39	5.77	2.90	+0.04	63.50

APPENDIX C - CLAY MINERALS (Analysis by R.N. Delabio)

STATION No. (Fig.2)	COMPOSITION (%) ILLITE	KAOLINITE	CHLORITE	MONTMORILLONITE
1	50	25	15	10
2	50	19	18	13
3	46	27	15	12
4	46	30	13	11
5	51	25	14	10
6	50	30	11	9
7	53	27	12	8
8	52	27	13	8
9	50	17	21	12
10	55	18	18	9
11	49	27	15	9
12	67	13	20	-
13	48	22	20	10
14	49	24	17	10
15	49	12	25	14
16	49	22	19	10
17	62	10	28	-
18	50	25	18	7
19	51	25	16	8
20	52	12	24	12
21	48	18	20	14
22	17	18	21	14
23	61	17	22	-
24	52	22	16	10
25	52	13	21	14
26	46	16	19	19
27	46	18	18	18
28	45	31	16	8

STATION No. (Fig.2)	COMPOSITION (%) ILLITE	KAOLINITE	CHLORITE	MONTMORILLONITE
29	52	25	16	7
30	47	16	18	19
31	47	11	20	22
32	48	27	14	11
33	50	25	18	7
34	46	22	20	12
35	51	18	19	12
36	53	21	18	8
37	51	22	18	9
38	50	24	18	8
39	47	24	19	10
40	49	24	19	8
41	50	32	14	4
42	57	15	28	-
43	48	30	15	7
44	49	36	12	3
45	59	19	22	-
46	54	26	16	4
47	48	35	12	5
48	57	16	27	-
49	49	28	16	7
50	51	26	14	10
51	47	29	18	6
52	47	26	18	9
53	47	31	14	8
54	51	22	17	10
55	46	26	16	12
56	49	21	18	12

STATION No. (Fig. 2)	COMPOSITION (%) ILLITE	KAOLINITE	CHLORITE	MONTMORILLONITE
57	49	21	18	12
58	46	24	18	12
59	49	22	17	12
60	51	21	17	9
61	45	28	18	9
62	51	19	20	10
63	46	22	21	11
64	48	35	13	4
65	51	31	12	6
66	45	35	13	7
67	45	32	16	8
68	49	23	19	9
69	47	34	12	7
70	51	19	21	9
71	49	27	16	8
72	44	32	15	9
73	47	30	19	4
74	51	24	18	7
75	46	33	13	8
76	47	30	16	7
77	44	36	15	5
78	43	33	13	5
79	52	24	17	7
80	47	28	17	8
81	58	19	23	-
82	60	15	25	-
83	54	21	20	5
84	49	24	18	9

STATION No. (Fig. 2)	COMPOSITION (%) ILLITE	KAOLINITE	CHLORITE	MONTMORILLONITE
85	49	26	16	9
86	56	22	22	-
87	48	29	16	7
88	49	27	17	7
89	50	29	14	7
90	45	26	19	10
91	44	25	18	13
92	42	24	19	16
93	46	24	18	12
94	48	23	20	9
95	42	29	18	11
96	46	27	18	9
97	44	31	19	6
98	48	27	19	6
99	47	20	19	14
100	44	27	17	12
101	51	20	17	12
102	47	23	17	13
103	49	20	18	13
104	50	17	21	12
105	48	17	20	15
106	49	16	20	15
107	47	20	20	13
108	52	8	25	15
109	45	14	22	19
110	47	15	23	15
111	47	23	18	12
112	48	21	20	11

STATION No. (Fig. 2)	COMPOSITION (%) ILLITE	KAOLINITE	CHLORITE	MONTMORILLONITE
113	48	13	24	15
114	51	18	21	10
115	50	18	22	10
116	47	23	18	12
117	60	19	21	-
118	58	21	21	-
119	60	21	19	-
120	62	22	16	-
121	60	20	20	-
122	61	16	23	-
123	61	21	18	-
124	64	20	16	-
125	60	13	27	-
126	64	17	19	-
127	42	38	15	5
128	62	15	23	-
129	60	18	22	-
130	50	26	24	-
131	59	19	22	-
132	60	20	20	-
133	64	17	19	-
134	64	19	17	-
135	60	12	28	-
136	46	29	17	8
137	46	31	17	6
138	51	20	20	9
139	49	23	21	7
140	58	20	22	-

STATION No. (Fig. 2)	COMPOSITION (%) ILLITE	KAOLINITE	CHLORITE	MONTMORILLONITE
141	46	33	16	5
142	48	35	13	4
143	60	18	22	-
144	44	29	17	10
145	45	25	17	13
146	47	18	21	14
147	48	21	18	13
148	46	17	22	15
149	55	18	18	9
150	50	27	18	5
151	46	24	19	11
152	47	18	20	15
153	49	21	18	12
154	45	12	24	19
155	49	15	26	10
156	41	22	19	8
157	47	25	19	9
158	50	20	21	9
159	51	23	15	11
160	49	23	18	10
161	47	18	18	17
162	43	26	19	12
163	46	31	11	12
164	52	14	20	14
165	47	16	17	20
166	47	13	19	21
167	54	19	16	11
168	51	19	17	13

STATION No. (Fig. 2)	COMPOSITION (%) ILLITE	KAOLINITE	CHLORITE	MONTMORILLONITE
169	46	26	16	12
170	51	15	20	14
171	52	21	21	6
172	49	36	11	4
173	50	26	14	10
174	61	16	23	-
175	59	22	19	-
176	58	15	20	7
177	46	29	17	8
178	58	24	18	-
179	59	19	22	-
180	47	28	16	9
181	47	30	16	7
182	46	29	17	8
183	39	37	16	8
184	48	34	13	5
185	45	29	17	9
186	48	23	17	12
187	49	29	16	6
188	46	27	15	12
189	46	26	19	9
190	44	39	11	6
191	43	25	19	13
192	47	28	14	11
193	44	25	17	14
194	41	30	16	13
195	50	18	20	12
196	43	31	14	12

STATION No. (Fig. 2)	COMPOSITION (%) ILLITE	KAOLINITE	CHLORITE	MONTMORILLONITE
197	50	10	23	17
198	46	23	15	16
199	49	15	17	19
200	49	15	18	18
201	46	8	20	26
202	44	10	22	24
203	48	22	11	19
204	44	18	18	20
205	46	17	21	16
206	52	9	21	18
207	49	20	17	14
208	47	24	16	13
209	48	15	21	16
210	49	21	18	12
211	46	23	18	13
212	48	18	21	13
213	42	23	19	16
214	63	6	31	-
215	37	25	17	21
216	41	23	18	18
217	47	29	16	8
218	41	26	20	13
219	49	8	27	16
220	23	16	12	49
221	49	5	27	19
222	47	22	18	13
223	44	37	12	7
224	48	31	13	8

STATION No. (Fig. 2)	COMPOSITION (%) ILLITE	KAOLINITE	CHLORITE	MONTMORILLONITE
225	42	14	28	16
226	39	24	22	15
227	41	26	19	14
228	29	24	20	17
229	44	31	14	11
230	46	23	17	14
231	48	10	23	19
232	46	9	24	21
233	45	15	20	20
234	49	9	22	20
235	47	24	15	14
236	42	28	15	15
237	39	23	17	21
238	47	23	16	14
239	45	29	15	11
240	47	21	21	11
241	45	23	17	15
242	41	30	13	16
243	42	25	20	13
244	30	13	15	42

APPENDIX D - GEOCHEMICAL DATA ON CO_2, $CaCO_3$ and ORGANIC CARBON (C).
(Analysis by Nicole Bertrand, GSC)

STATION No. (Fig. 2)	COMPOSITION (%)			STATION No. (Fig. 2)	COMPOSITION (%)		
	CO_2	$CaCO_3$	C		CO_2	$CaCO_3$	C
1	1.06	2.40	1.6	167	0.57	1.29	1.7
4	1.23	2.80	1.5	170	0.78	1.77	1.6
10	0.83	1.89	1.4	172	1.19	2.70	1.5
15	0.26	0.59	1.4	175	1.19	2.70	1.6
46	1.50	3.41	1.6	176	1.73	3.93	1.5
49	1.72	3.97	1.7	181	1.49	3.38	1.4
55	0.97	2.20	1.6	200	0.48	1.09	1.6
58	1.00	2.27	1.5	201	0.51	1.16	2.1
60	0.35	0.79	1.4	022	0.62	1.41	1.5
74	1.55	3.52	1.8	206	0.81	1.84	1.6
76	1.52	3.45	1.7	215	0.08	0.18	1.5
80	2.12	4.81	1.9	220	0.08	0.18	2.5
102	0.80	1.82	1.3	221	0.57	1.29	1.5
103	0.78	1.77	1.3	222	0.72	1.63	1.4
111	0.78	1.77	1.5	223	1.13	2.57	1.4
112	0.80	1.82	1.5	225	0.92	2.09	1.4
115	1.09	2.47	1.5	226	0.84	1.91	1.5
119	1.40	3.18	1.4	228	0.84	1.91	1.5
121	1.08	2.45	1.5	230	1.01	2.29	1.4
124	1.47	3.34	1.5	231	0.48	1.09	1.9
127	0.29	0.66	1.9	234	0.75	1.70	1.7
159	0.27	0.61	1.1	236	0.90	2.04	1.6
162	0.63	1.43	1.6	237	0.71	1.61	1.5
164	0.50	1.34	1.7	239	1.04	2.36	1.4
166	0.63	1.43	1.6	241	1.10	2.50	1.4

APPENDIX E - LIST OF ILLUSTRATIONS

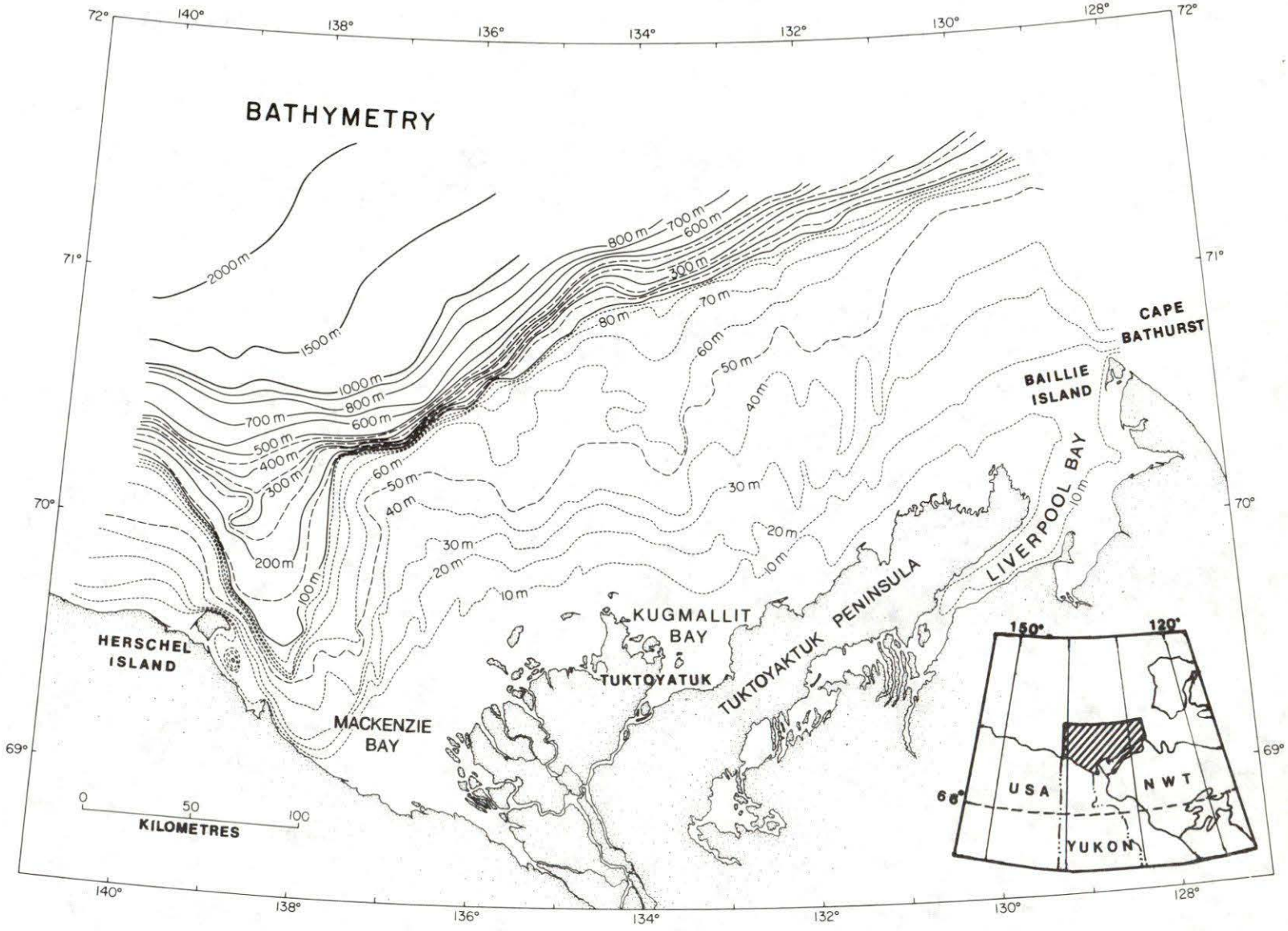

Figure 1. Bathymetric map showing continental shelf and slope, and the Mackenzie Canyon.

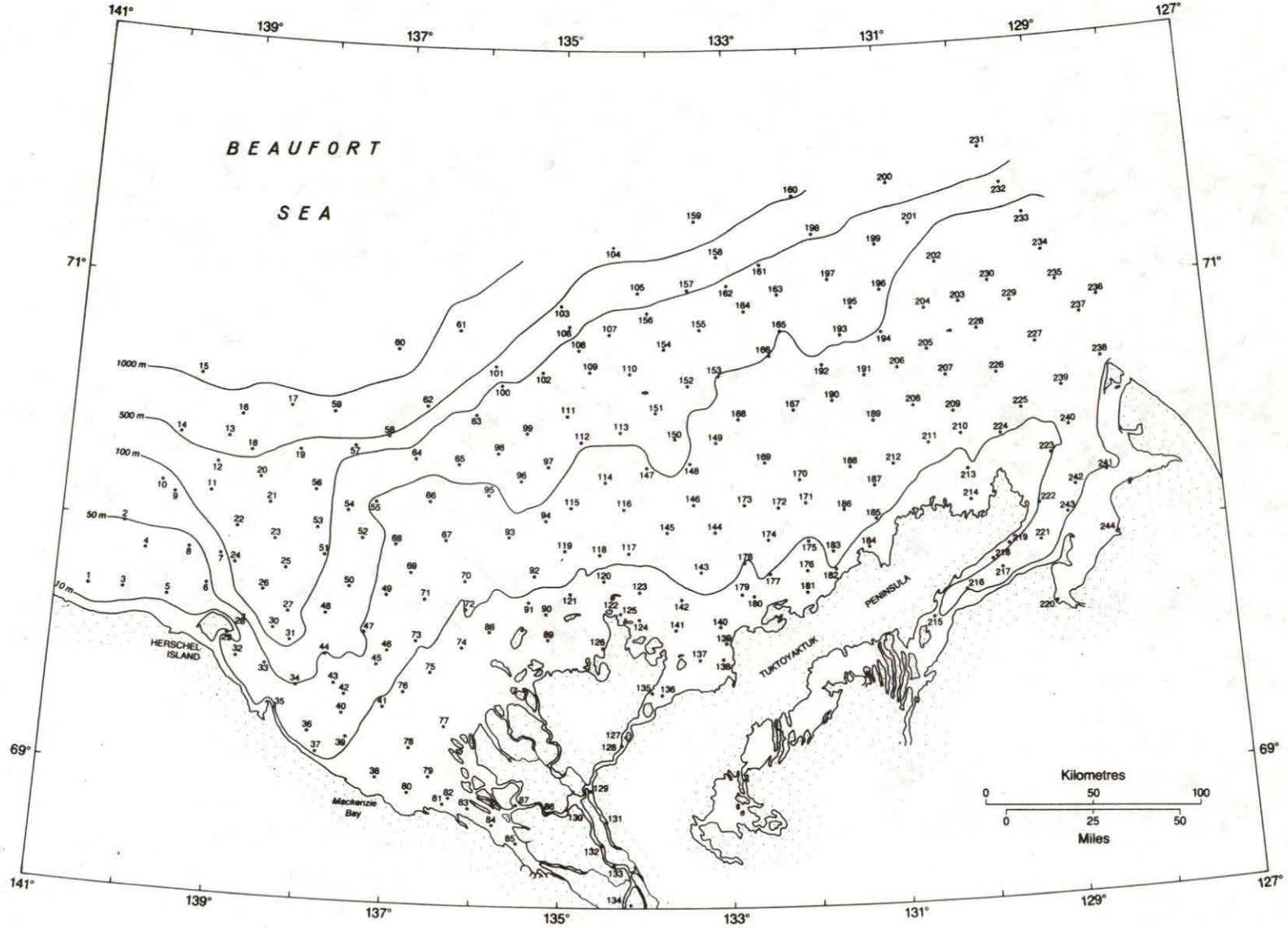

Figure 2. Location of bottom-sampling stations.

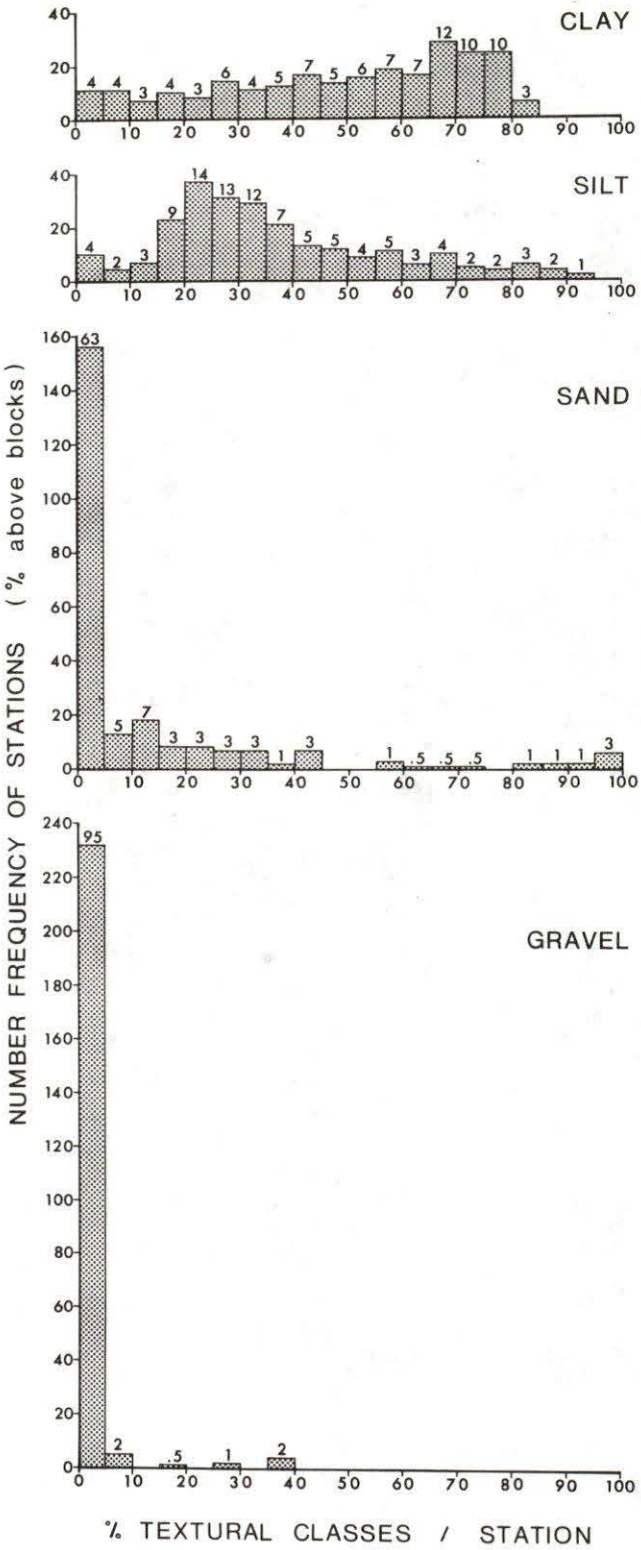

Figure 3. Bar diagram showing the frequency of stations and the textural classes for those stations.

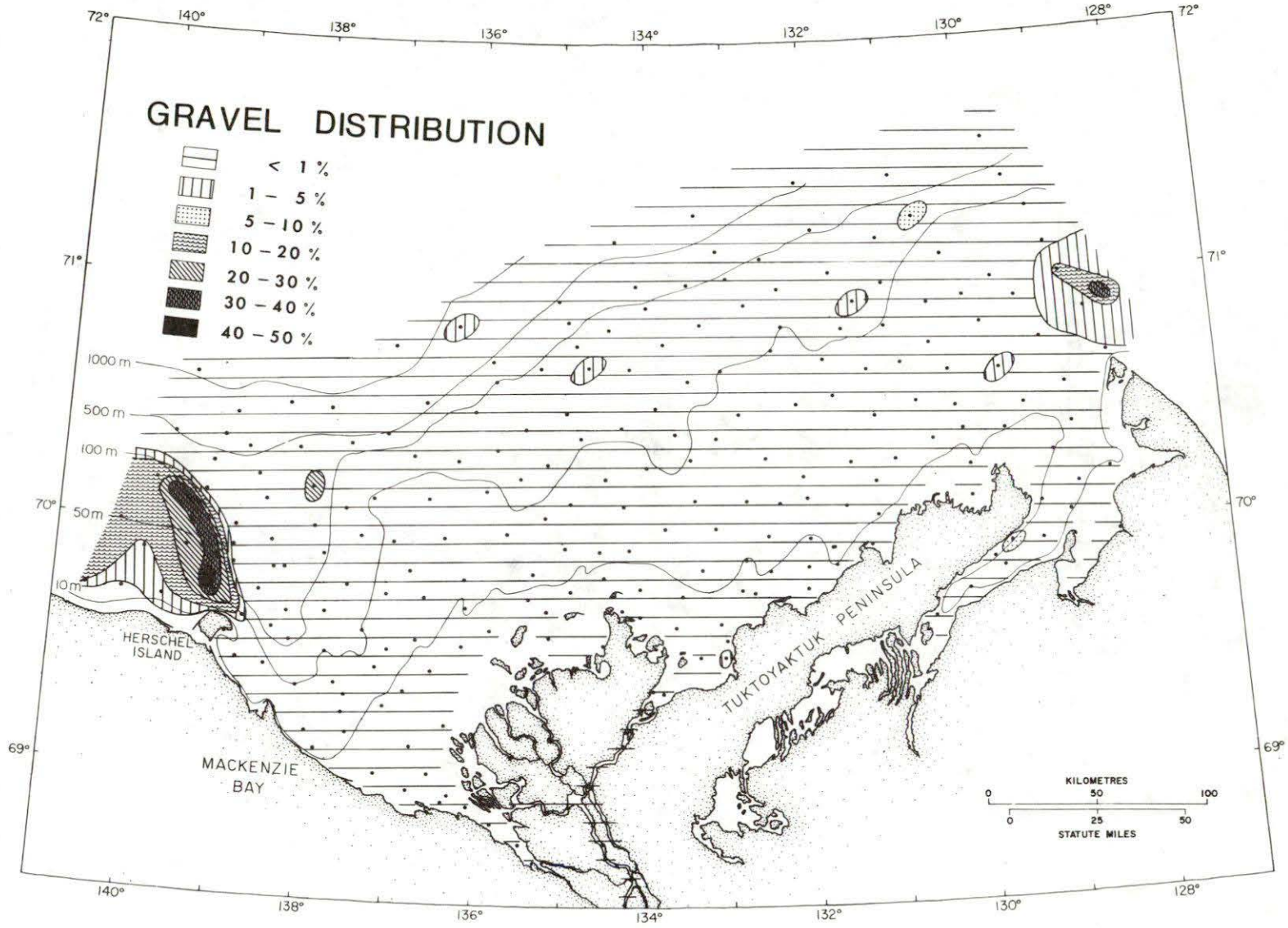

Figure 4. Distribution of gravel per sample shows virtual absence of gravel in nearby areas except west of Herschel Island, and extreme eastern part of shelf.

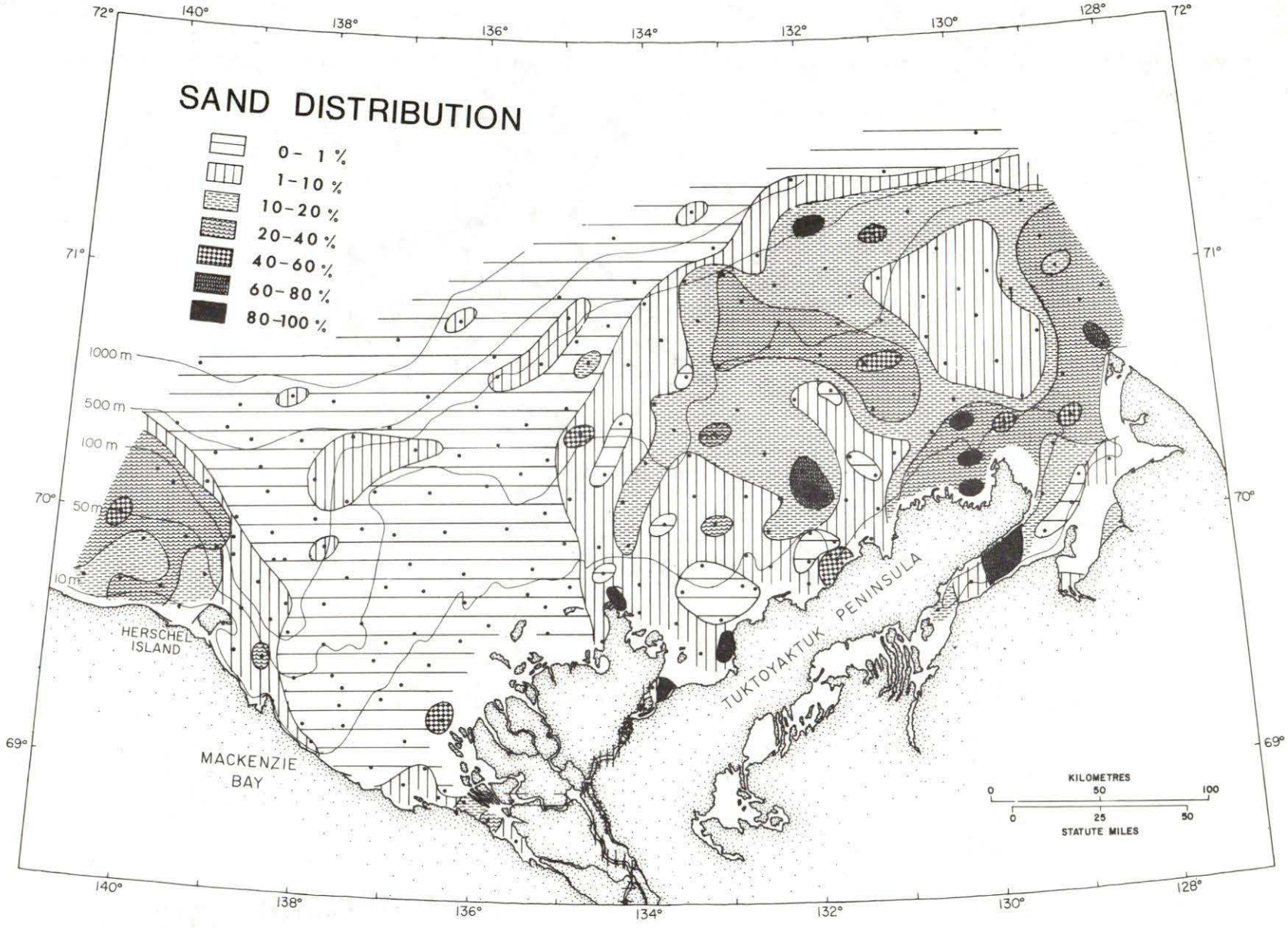

Figure 5. Distribution of sand increasing importance of sand in coastal areas, eastern part of shelf and area west of Herschel Island.

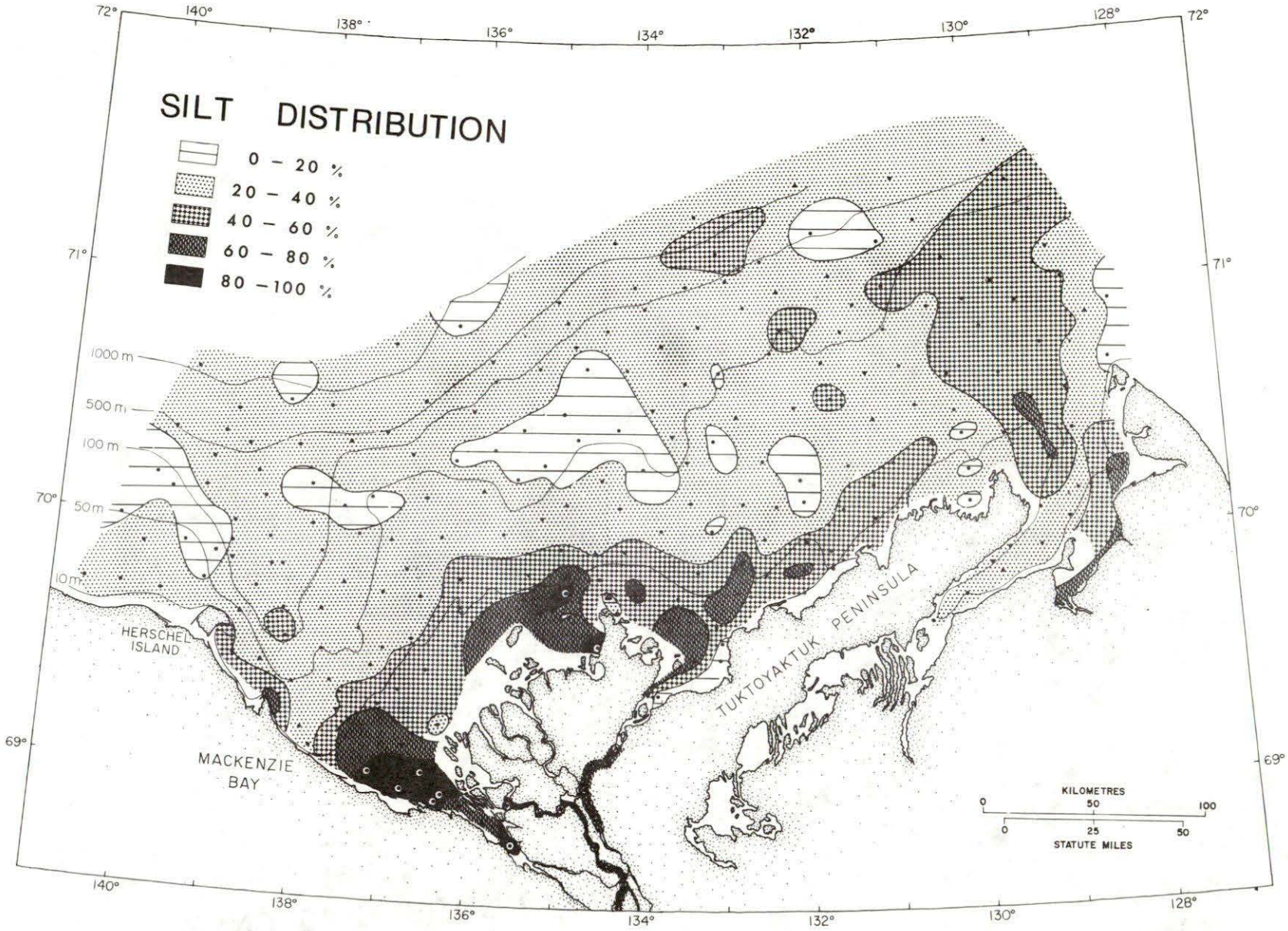

Figure 6. Distribution of silt showing heavy concentration in the delta area, and minor content offshore.

Figure 7. Satellite photograph of the sediment plume from the Mackenzie Delta, taken 26 July, 1973.

Figure 8. Satellite photograph of the sediment plume from the Mackenzie Delta, taken 1 September, 1973.

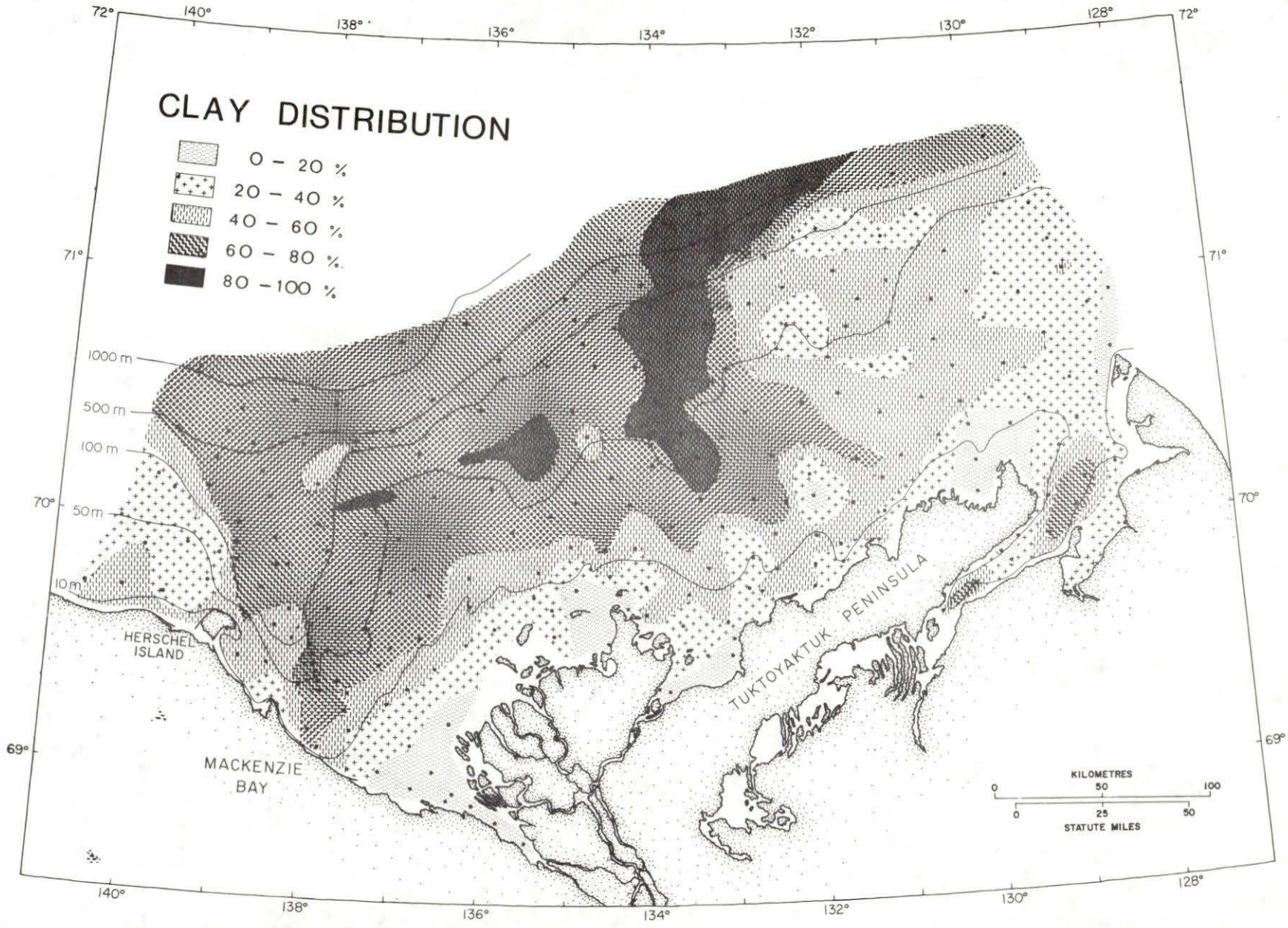

Figure 9. Distribution of clay showing minor amount in the delta areas and heavy concentration offshore.

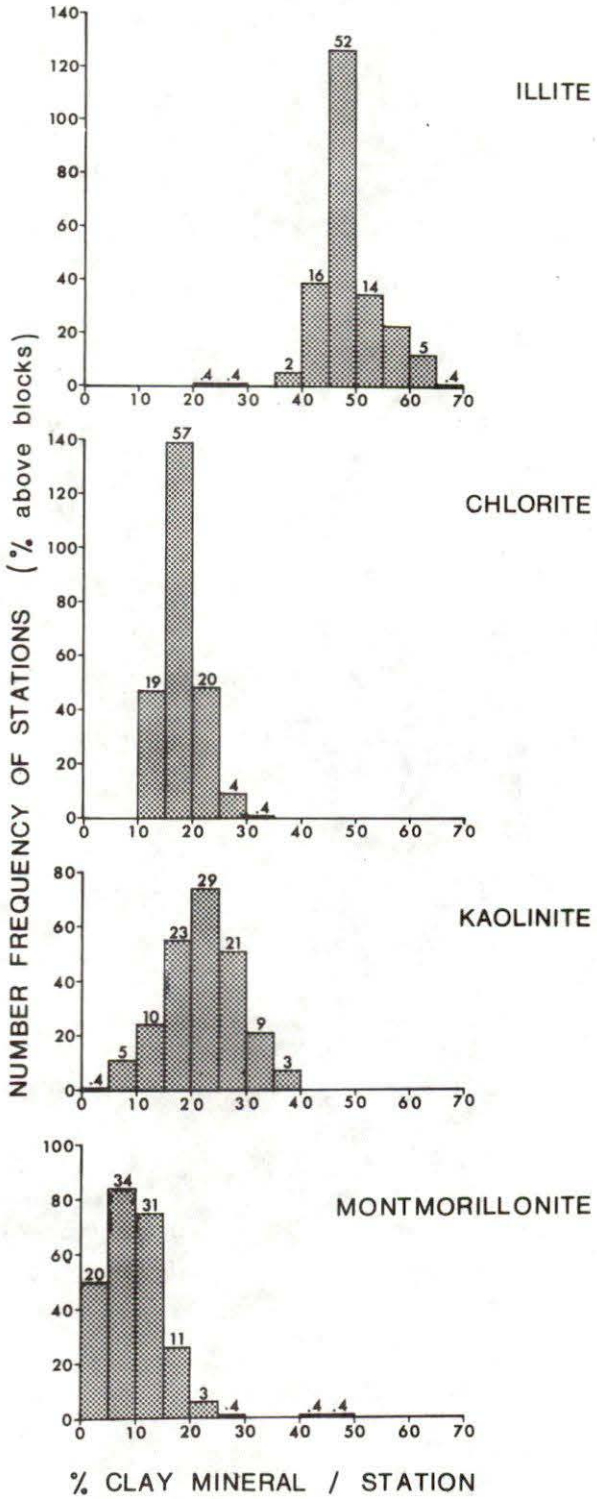

Figure 10. Bar diagram showing the frequency of stations and the distribution of the frequency of the clay minerals for those stations.

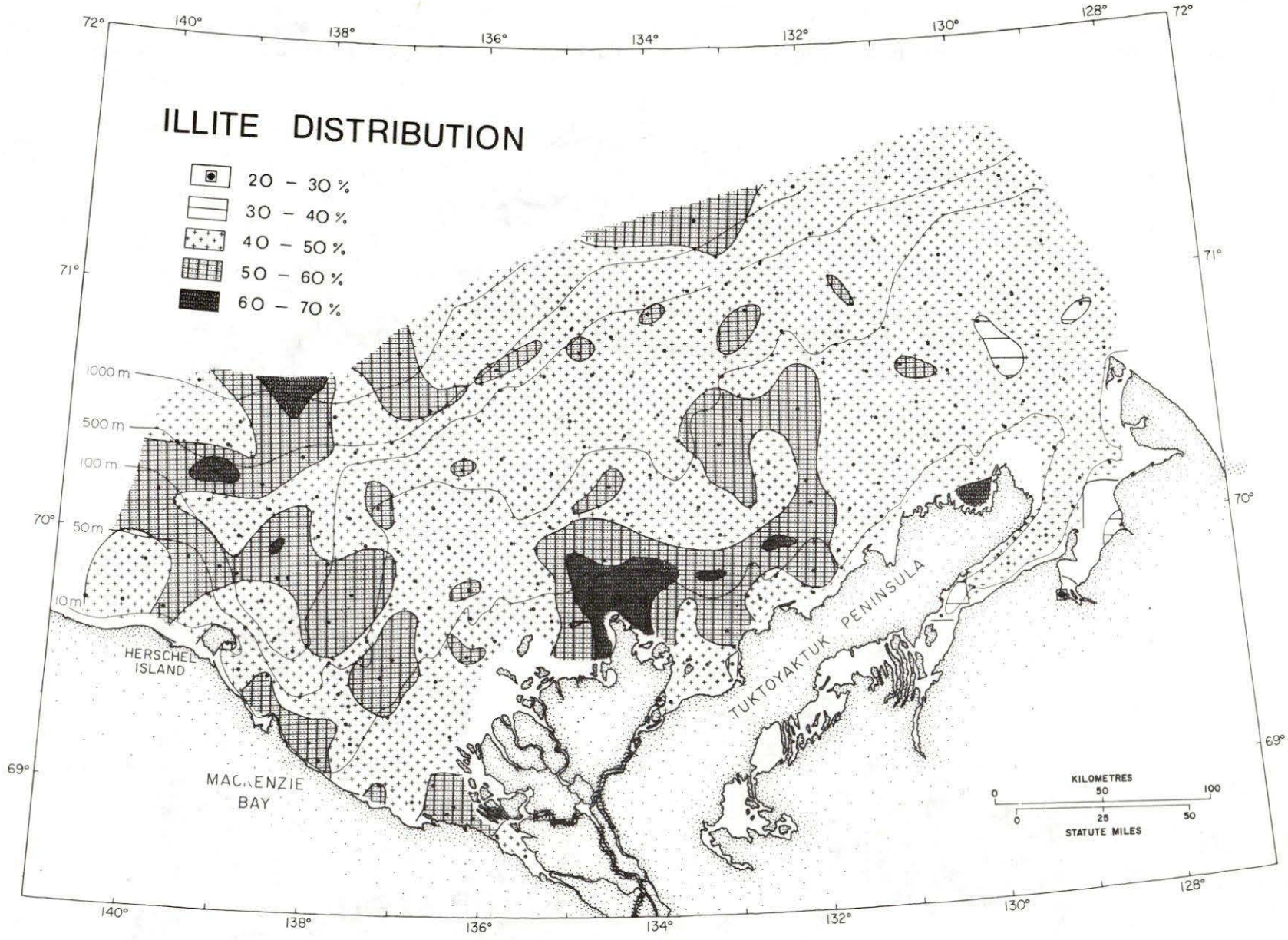

Figure 11. Distribution of illite showing fairly uniform but moderate concentrations over the shelf.

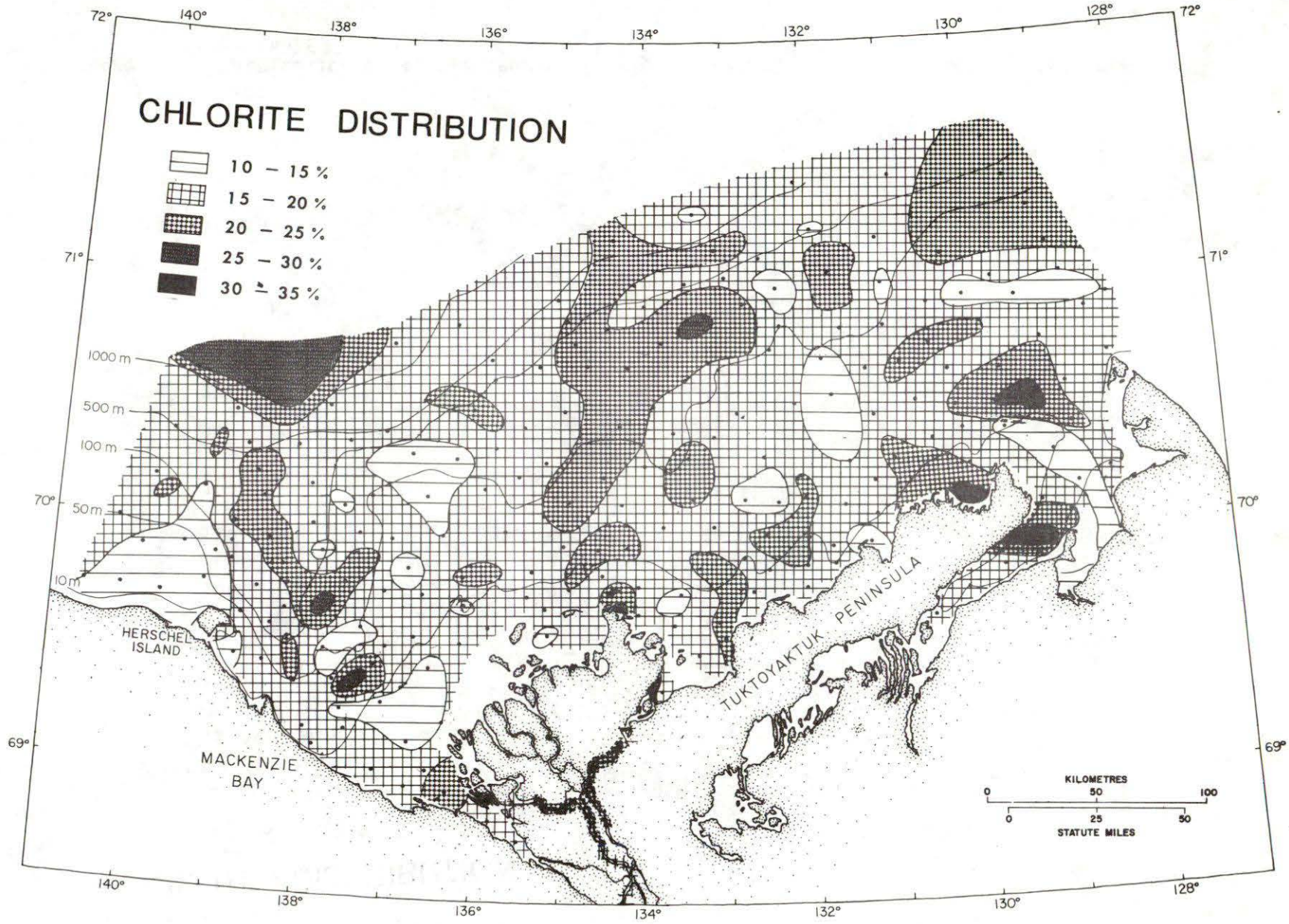

Figure 12. Distribution of chlorite showing low but somewhat uniform concentrations over the shelf.

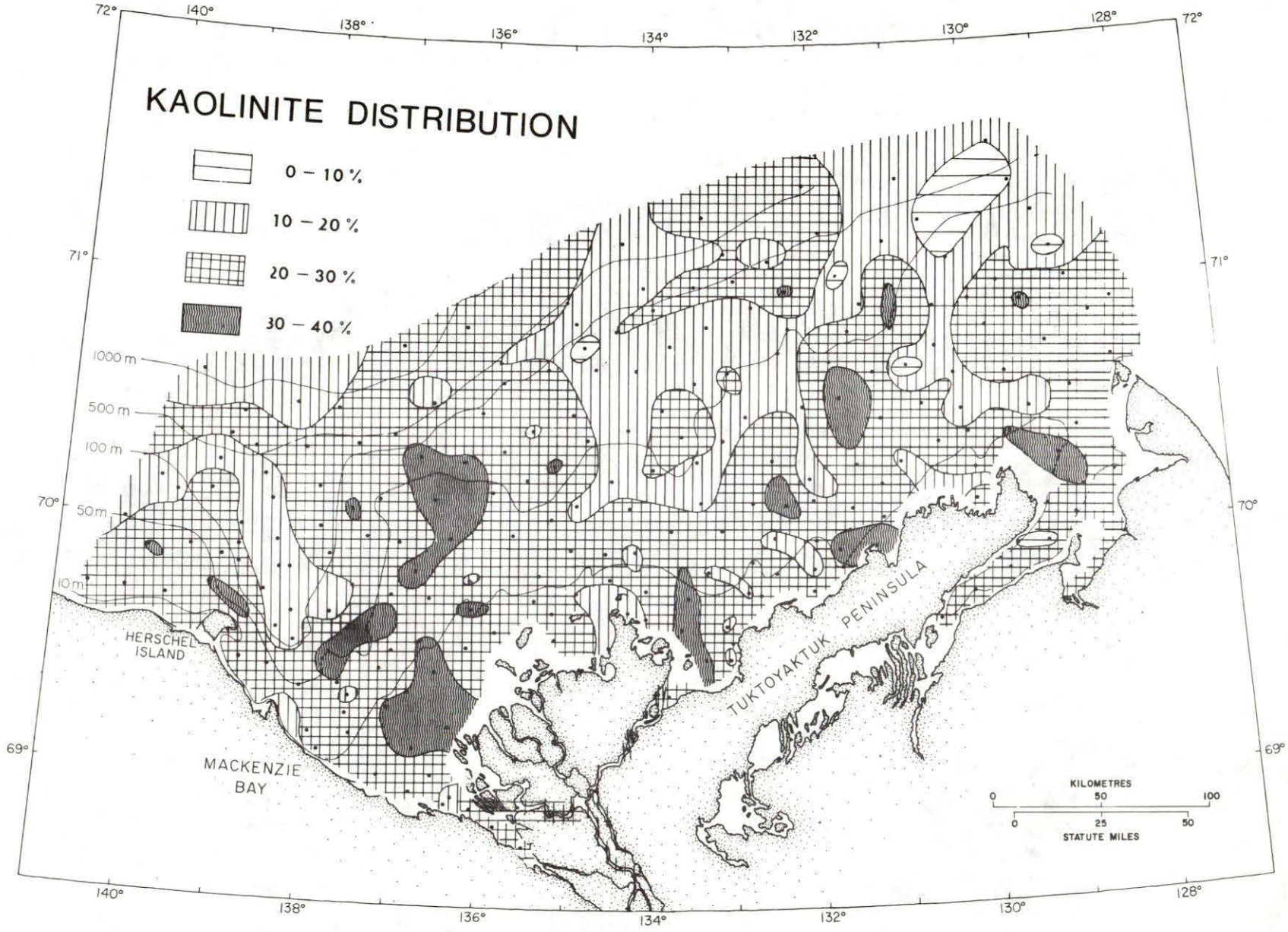

Figure 13. Distribution of kaolinite showing low but fairly uniform concentrations over the shelf.

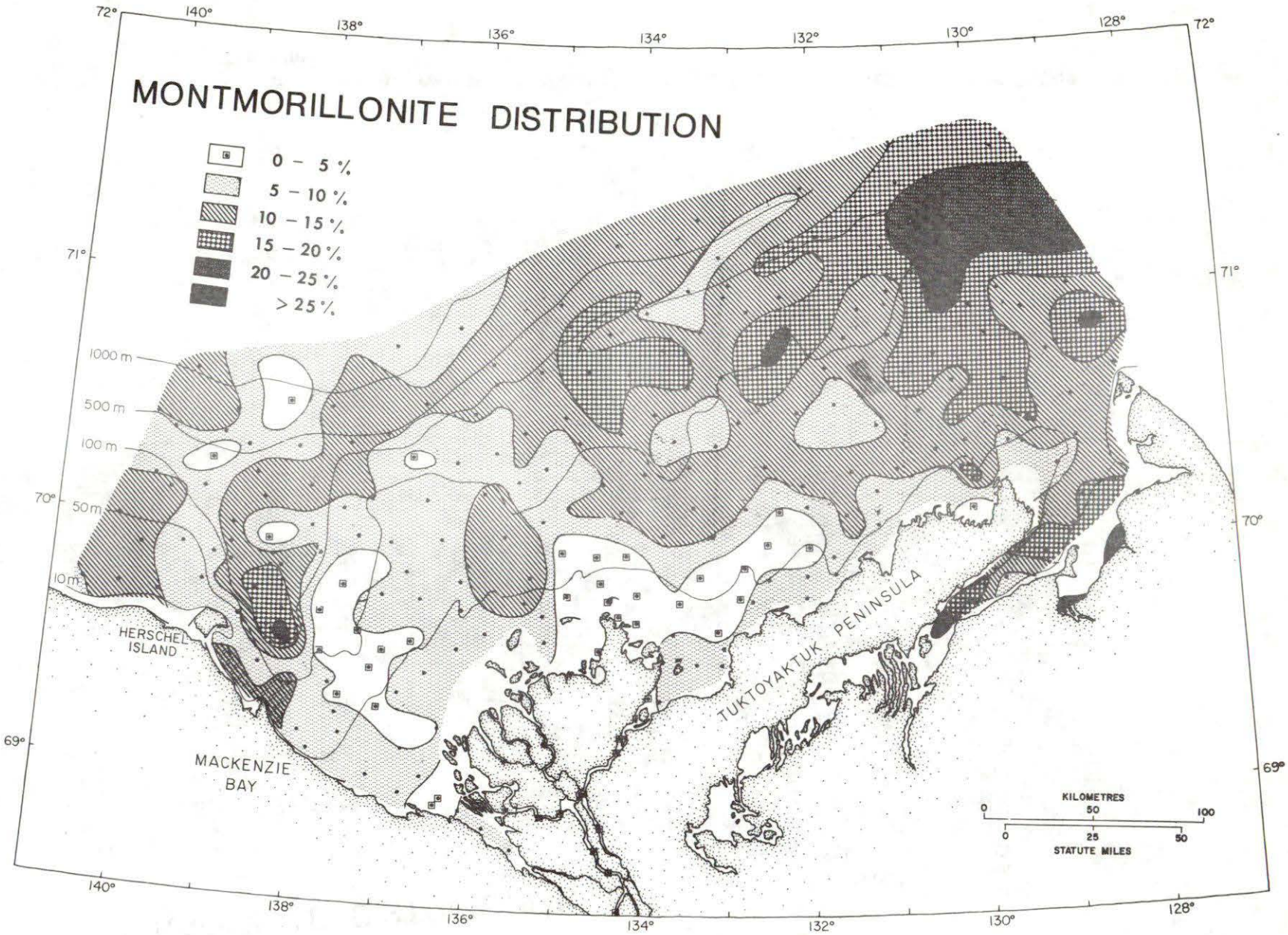

Figure 14. Distribution of montmorillonite showing very low but quite uniform concentrations over the shelf, with deficiencies in the delta and adjacent offshore.

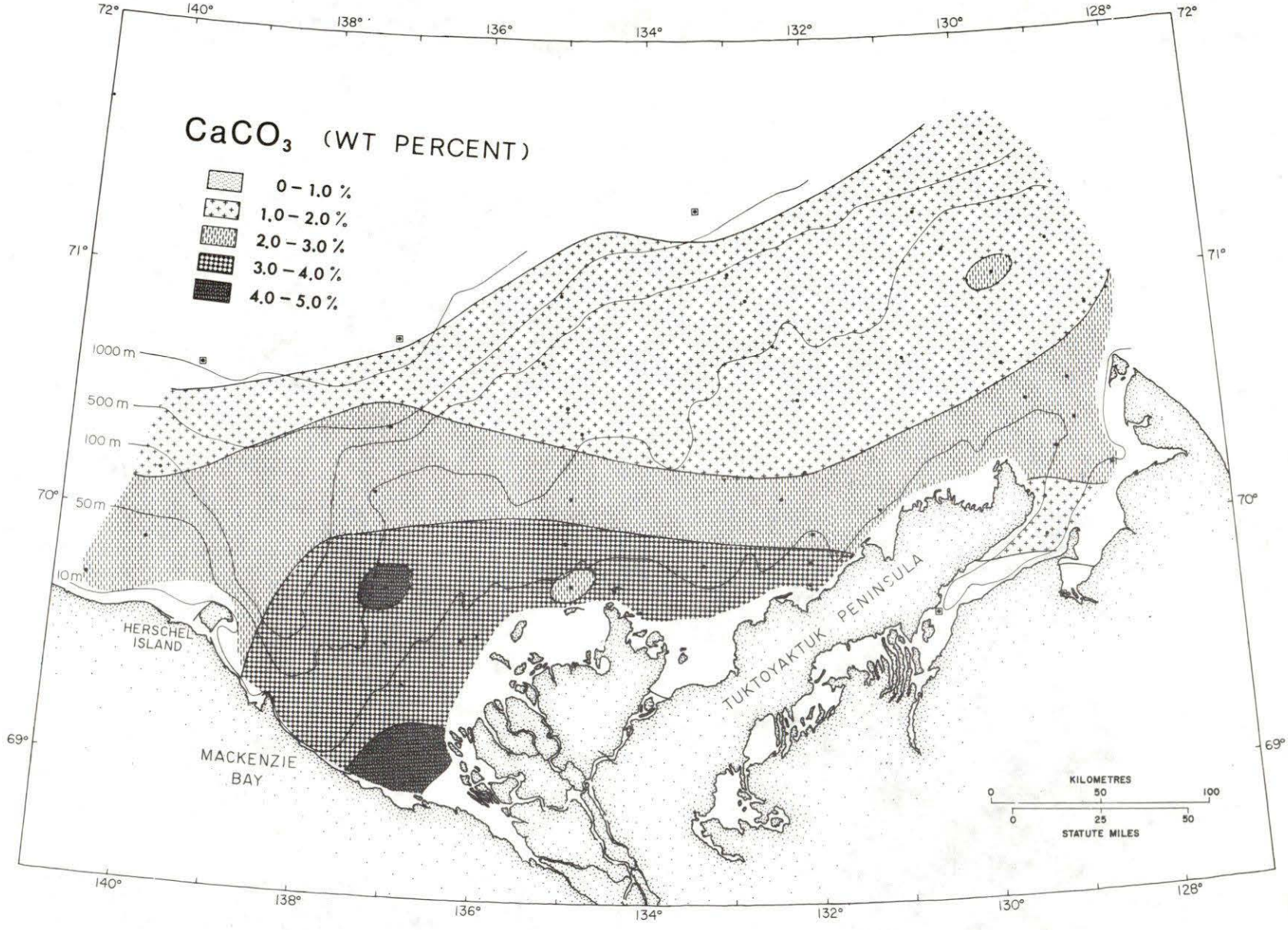

Figure 15. Distribution of carbonate (presumed $CaCO_3$) showing greatest concentration near shore, and progressive decrease seaward.

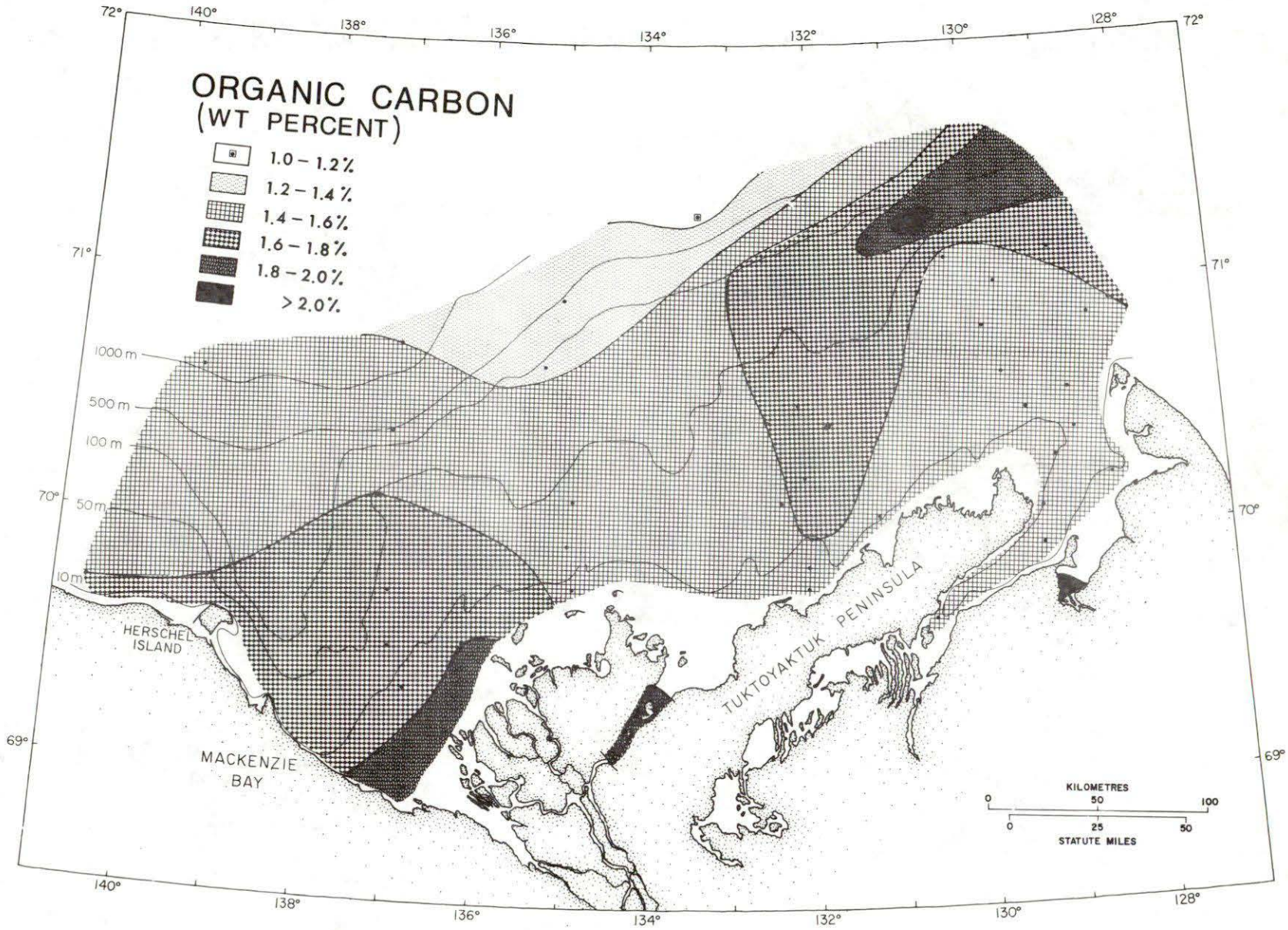

Figure 16. Distribution of organic carbon showing greatest concentrations in the delta area and northeastern part of the shelf, and generally decreasing in amounts seaward.

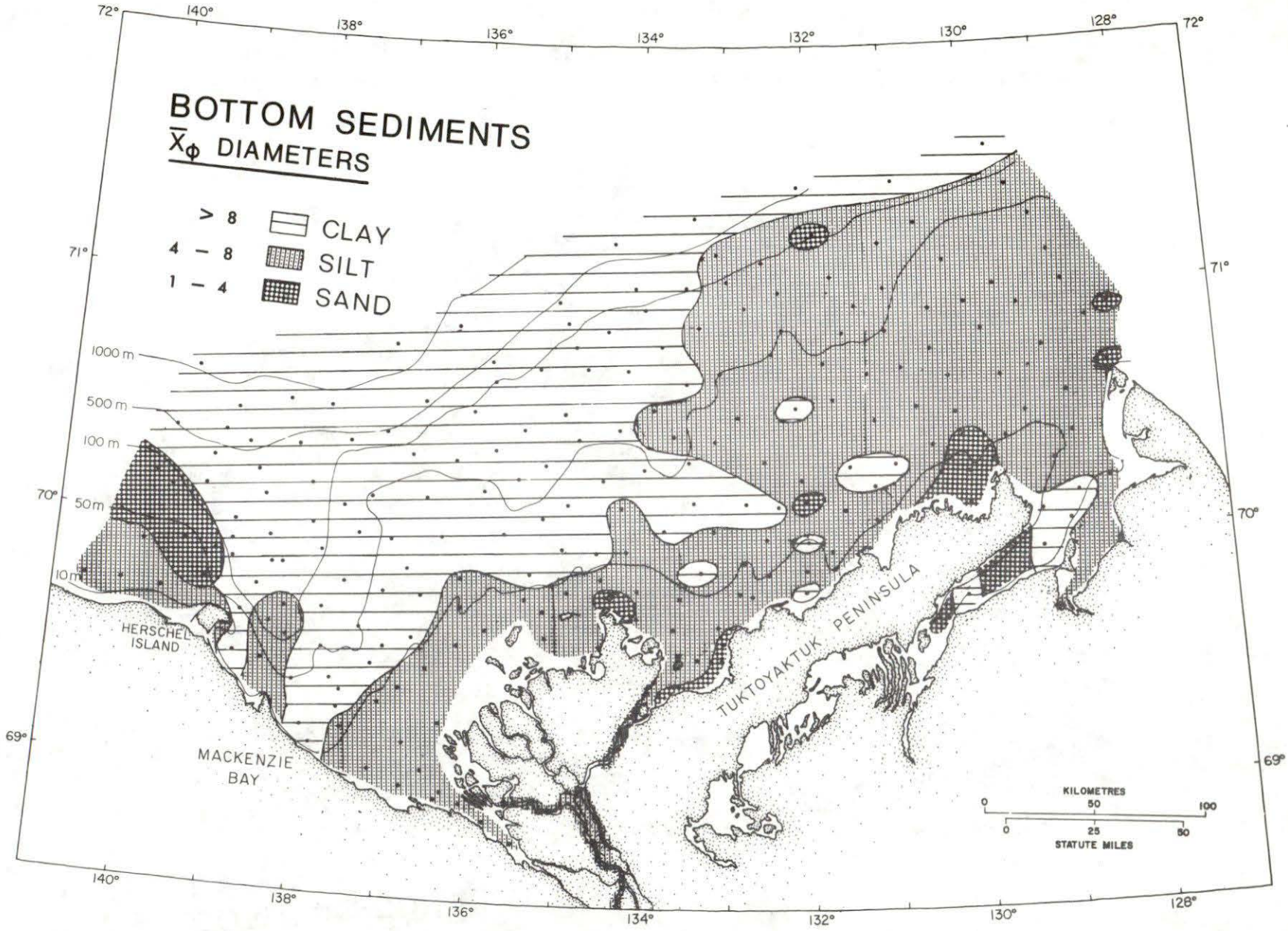

Figure 17. Map of types of bottom sediments based on phi mean diameters.

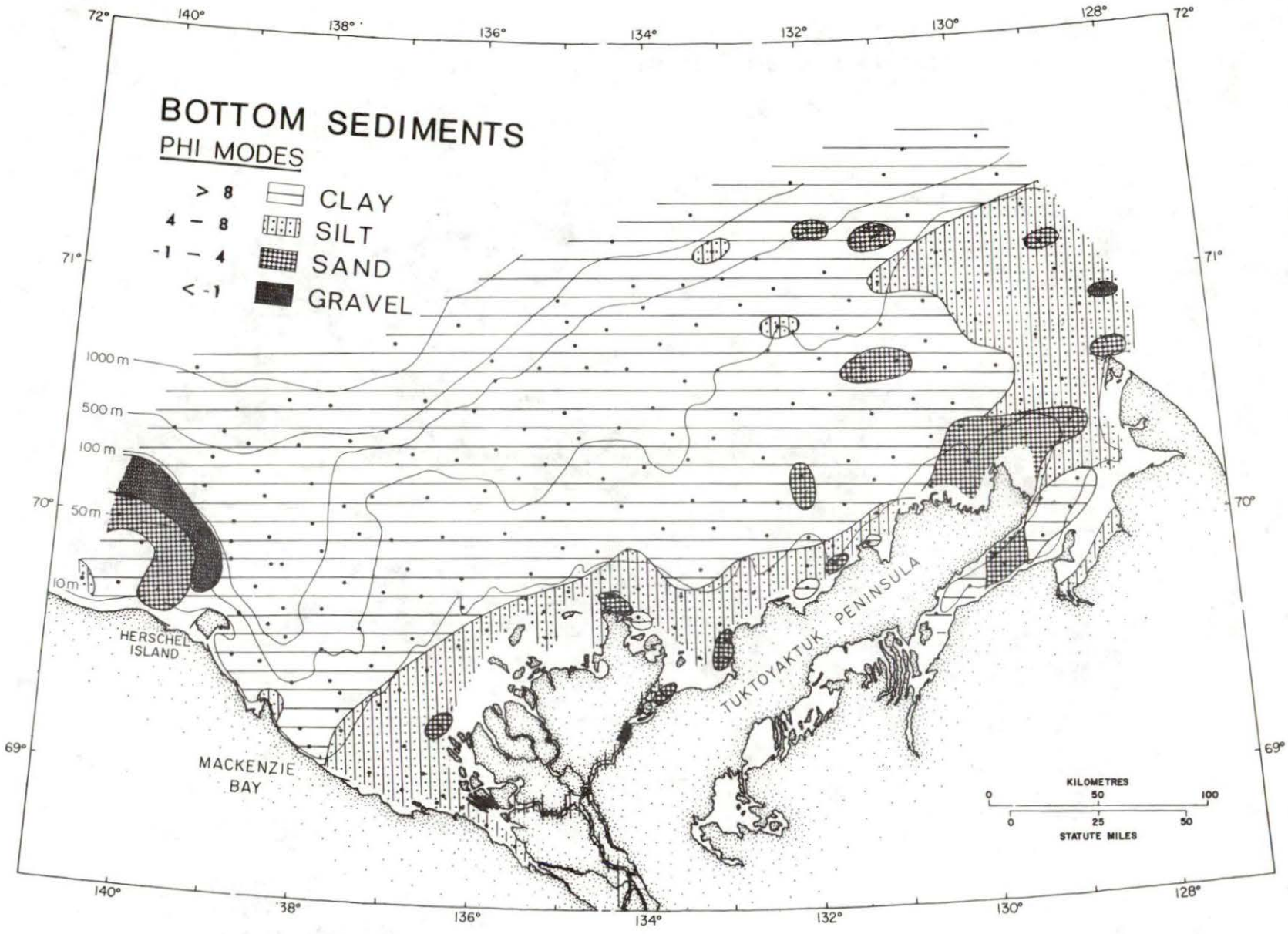

Figure 18. Map of types of bottom sediments based on phi modes. Note the appearance of the gravels in this presentation.

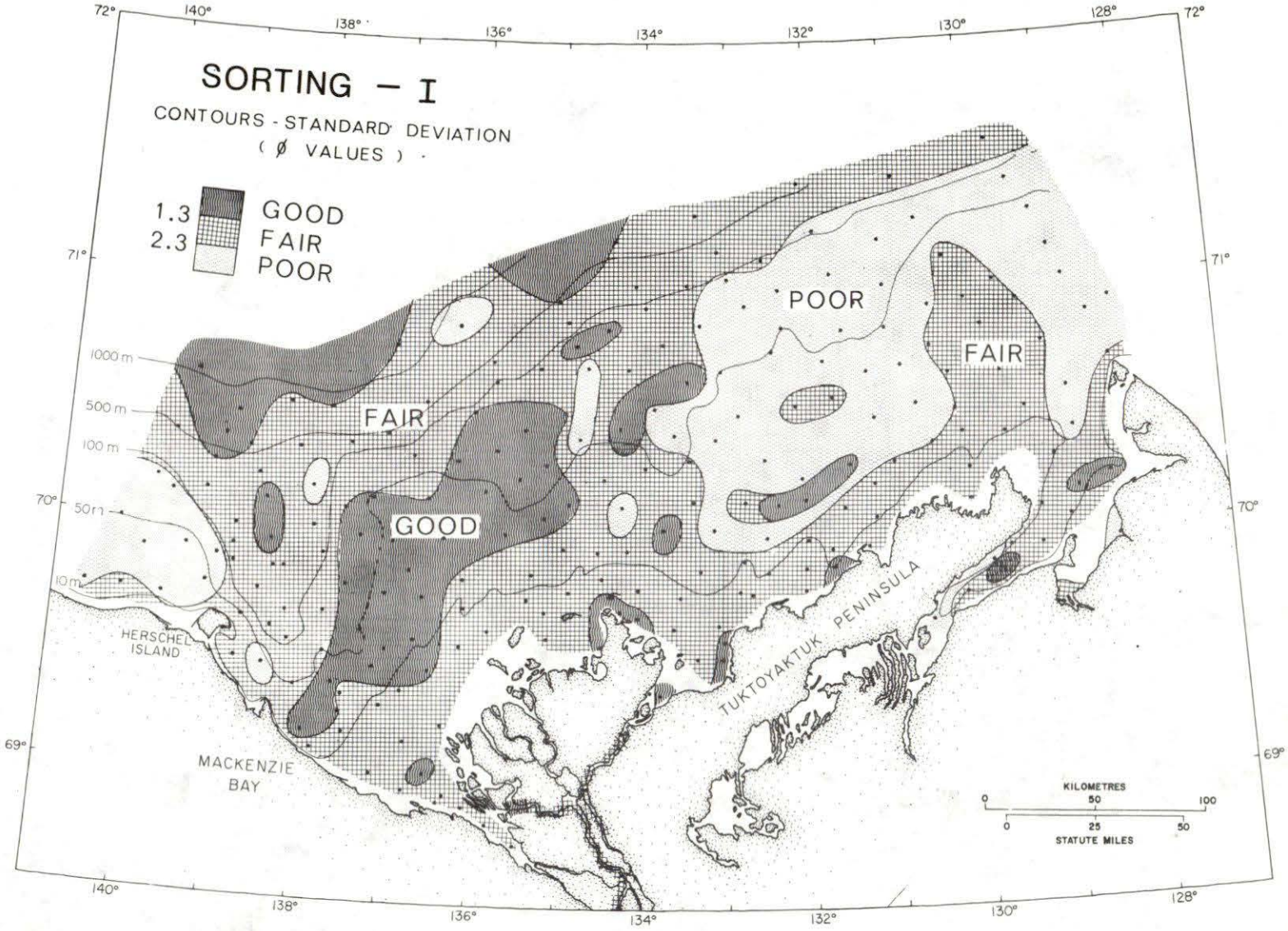

Figure 19. Sediment sorting based on phi standard deviation.

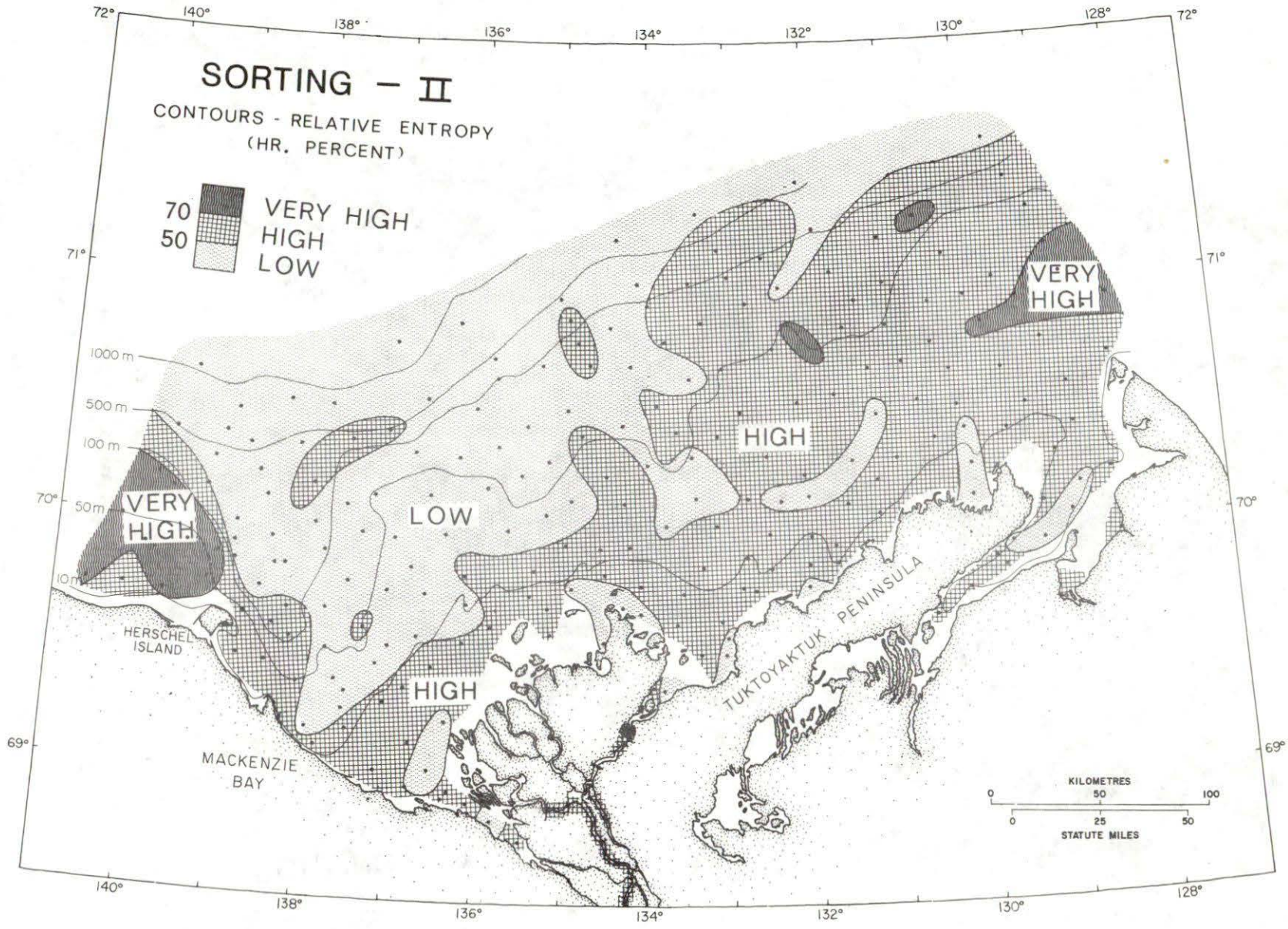

Figure 20. Sediment sorting based on relative entropy (Hr %).

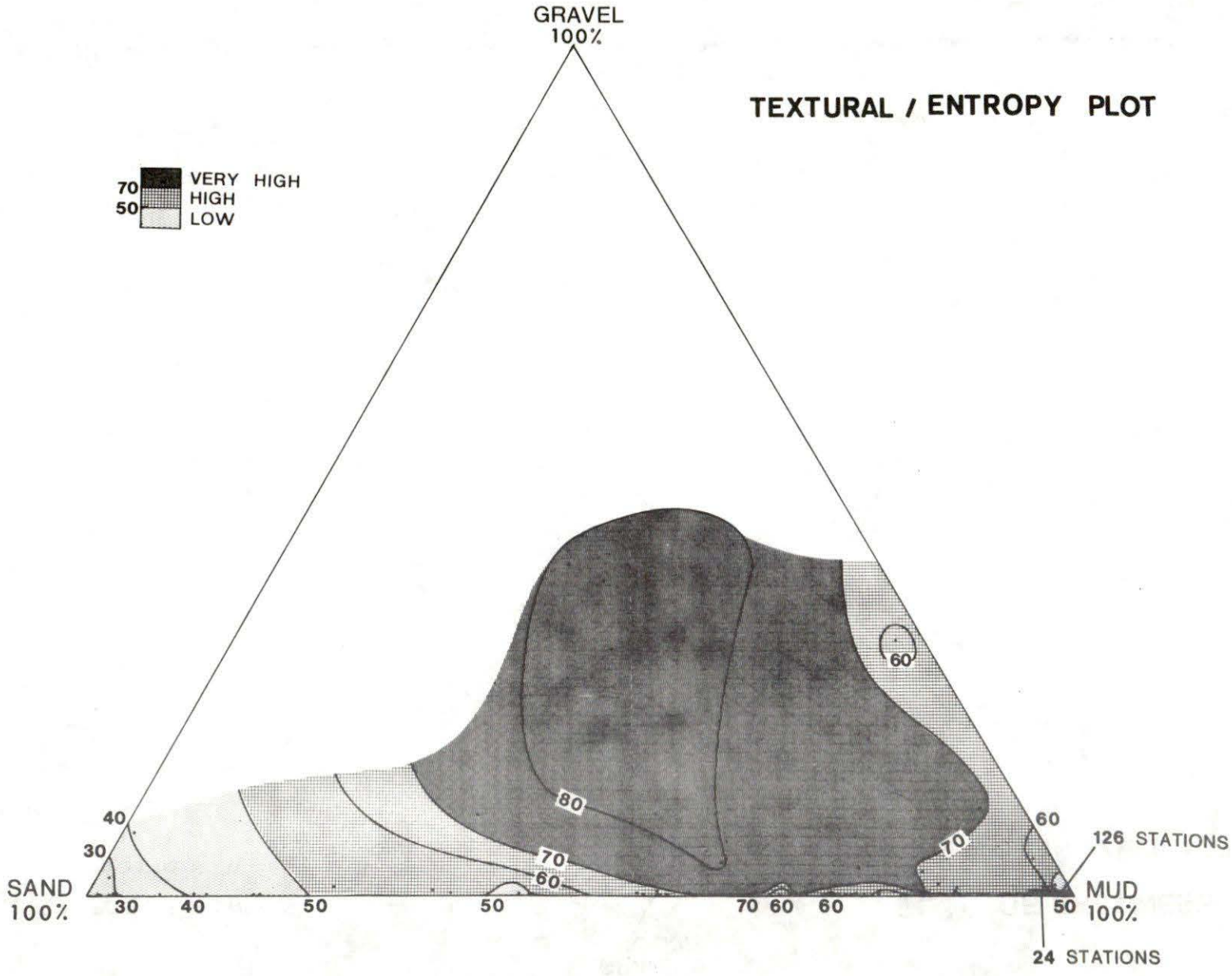

Figure 21. Ternary diagram of gross texture and relative entropy (Hr %).

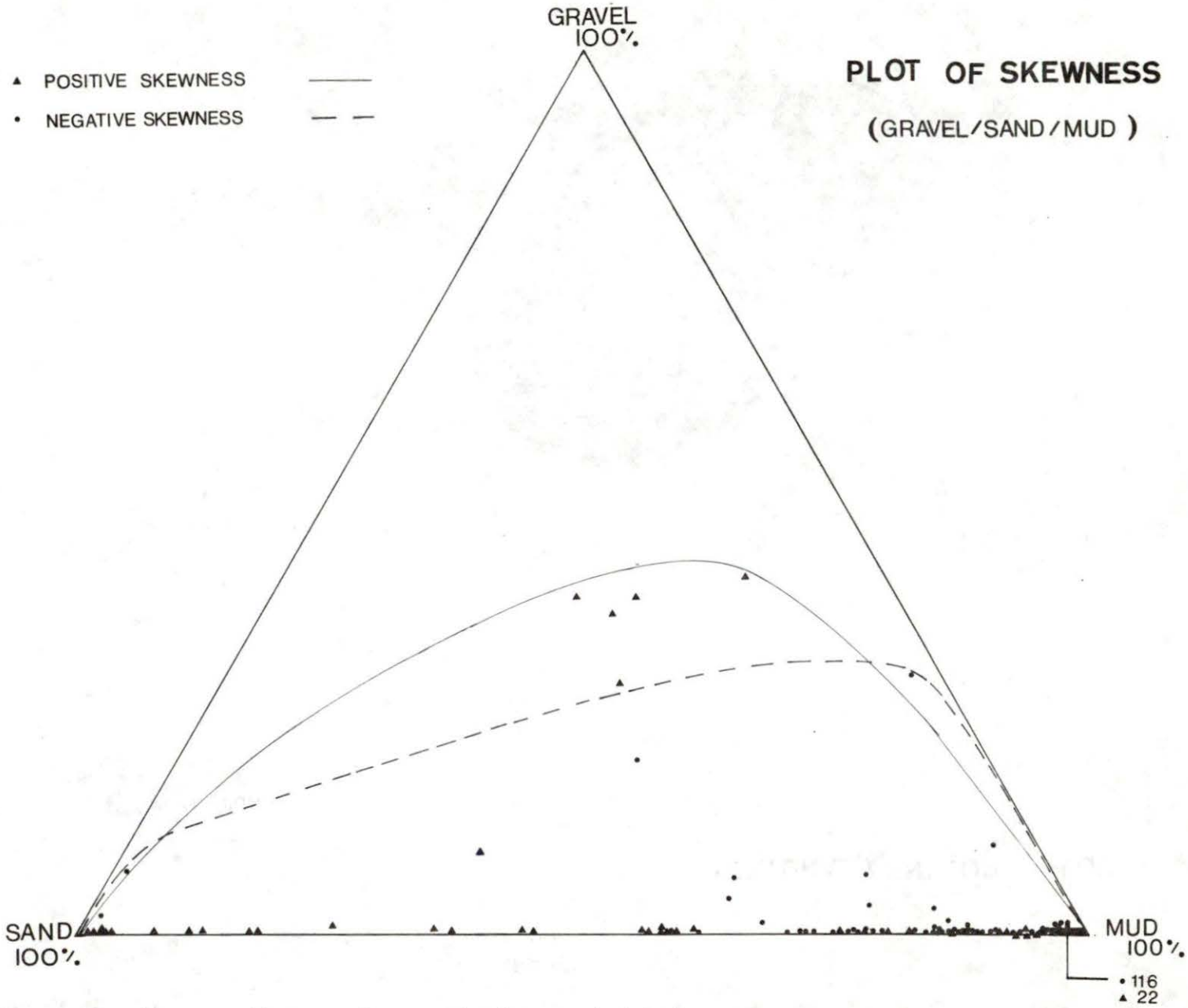

Figure 22. Ternary diagram of gross texture and phi skewness.

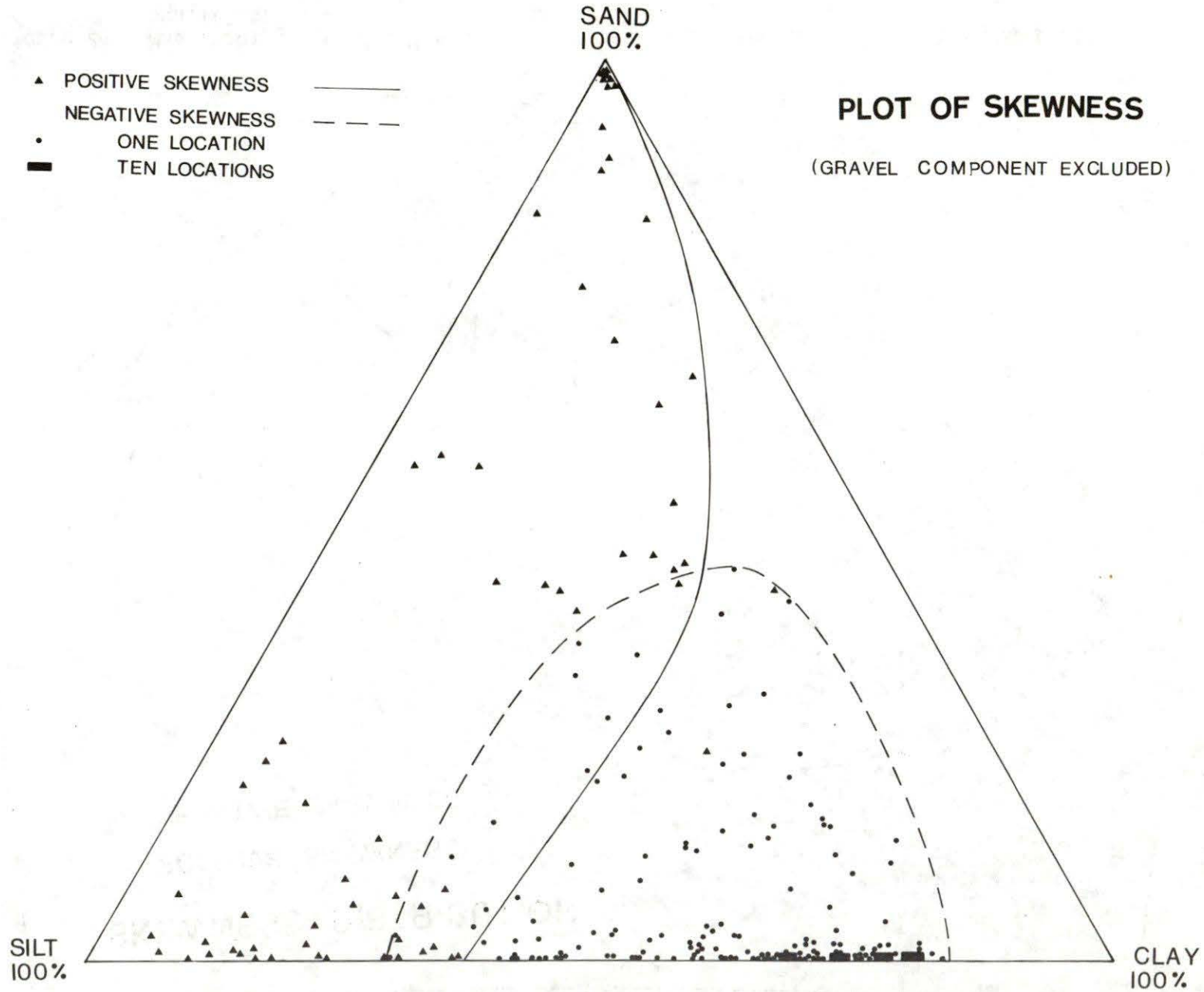

Figure 23. Ternary diagram of gross texture (gravel excluded) and phi skewness.

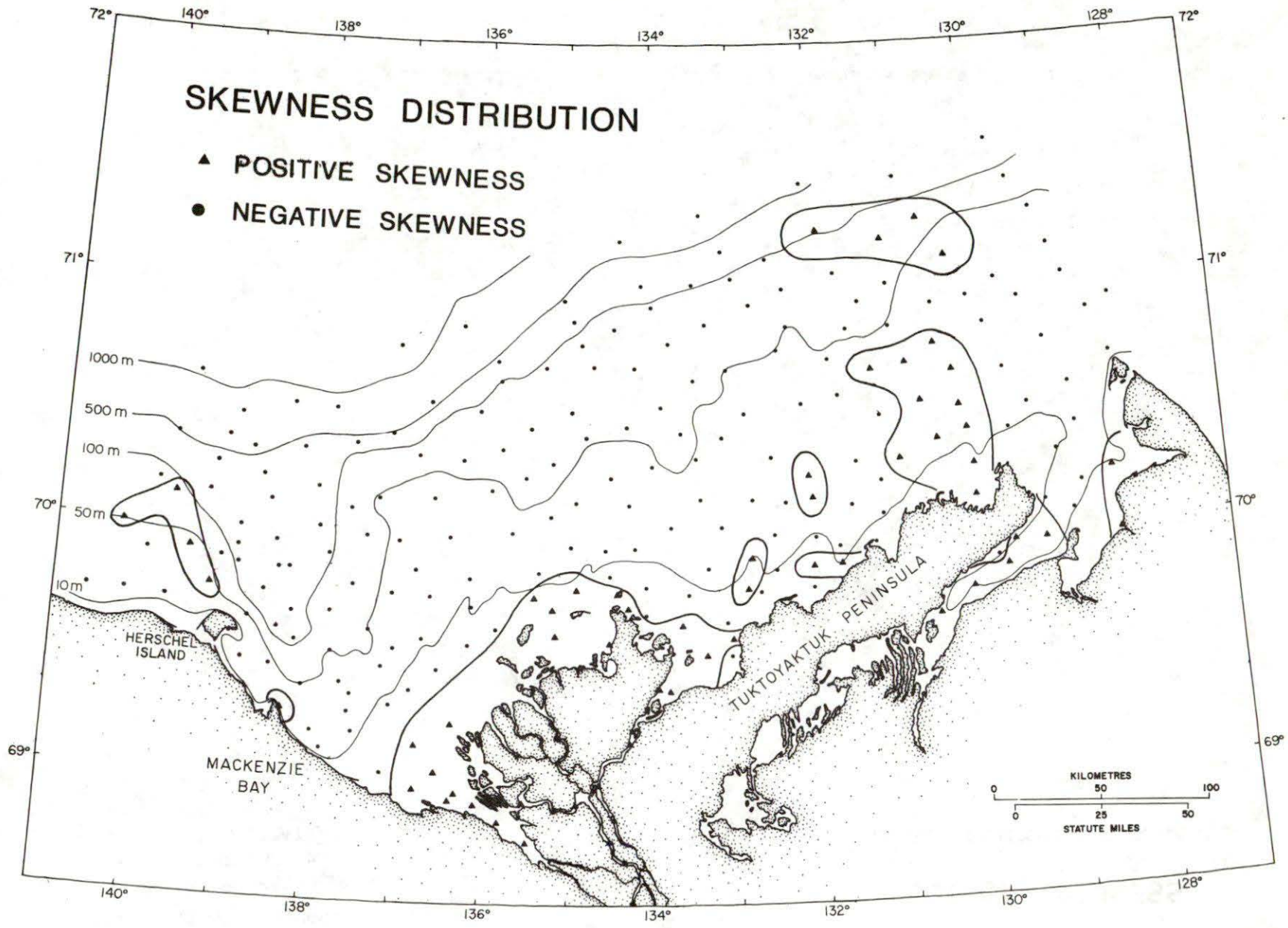

Figure 24. Map showing distribution of phi skewness according to positive and negative qualities.

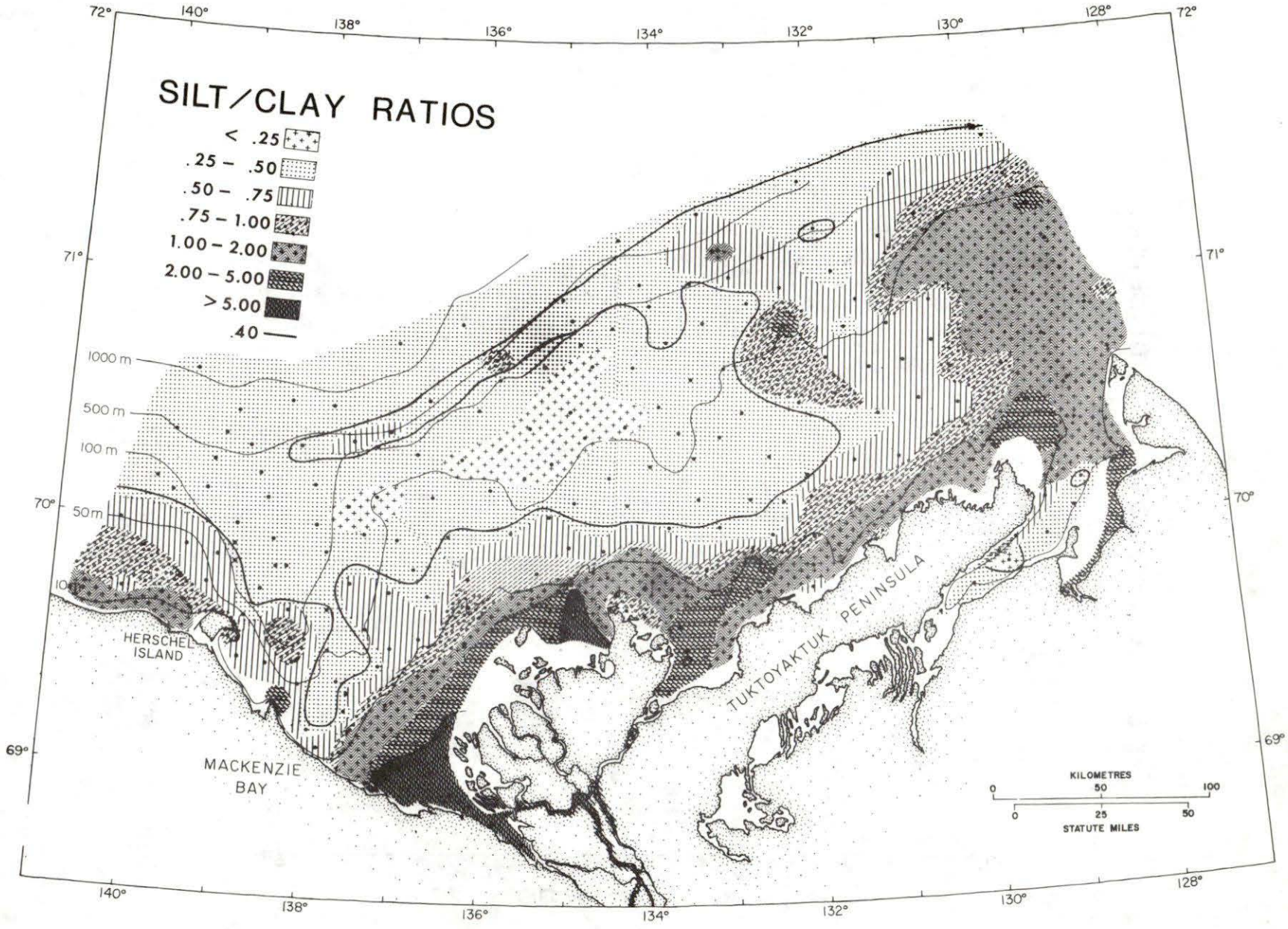

Figure 25. Map of silt/clay ratios.

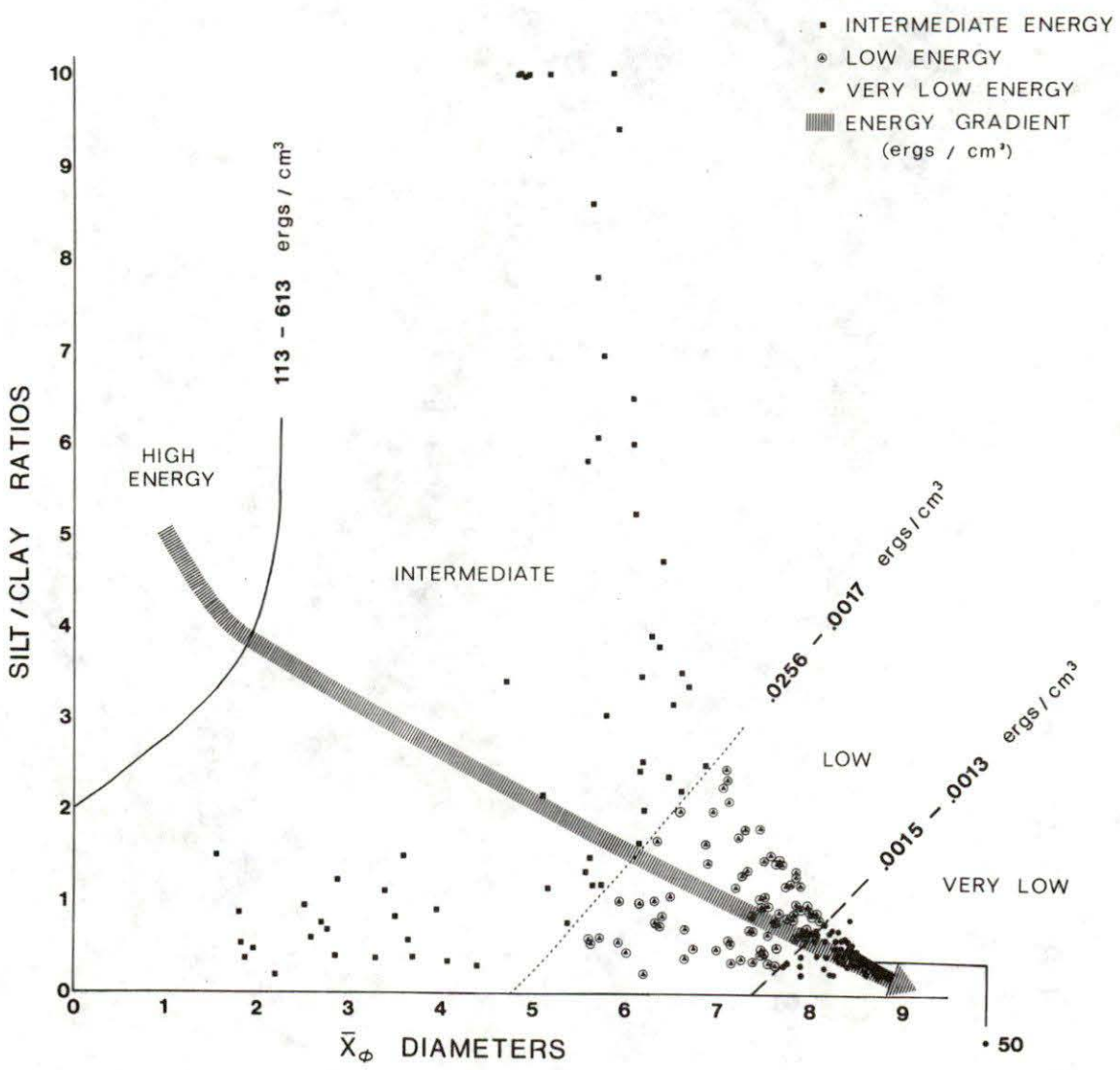

Figure 26. Graph showing silt/clay ratio versus phi mean diameter, and the relationship of energy volume to the sedimentational system.

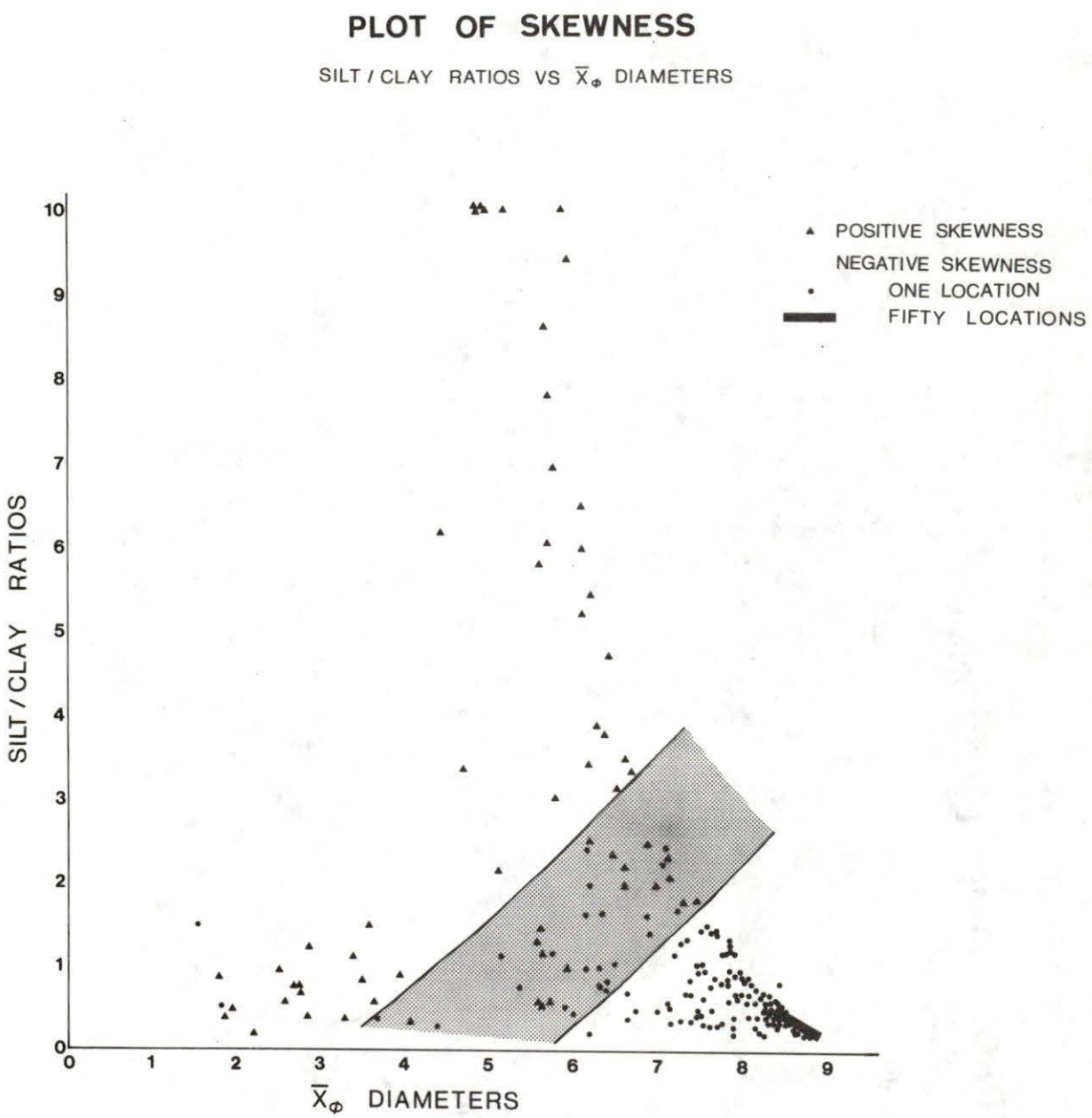

Figure 27. Graph showing silt/clay ratio versus mean diameter, and the relationship of phi skewness quality to the sedimentational system.

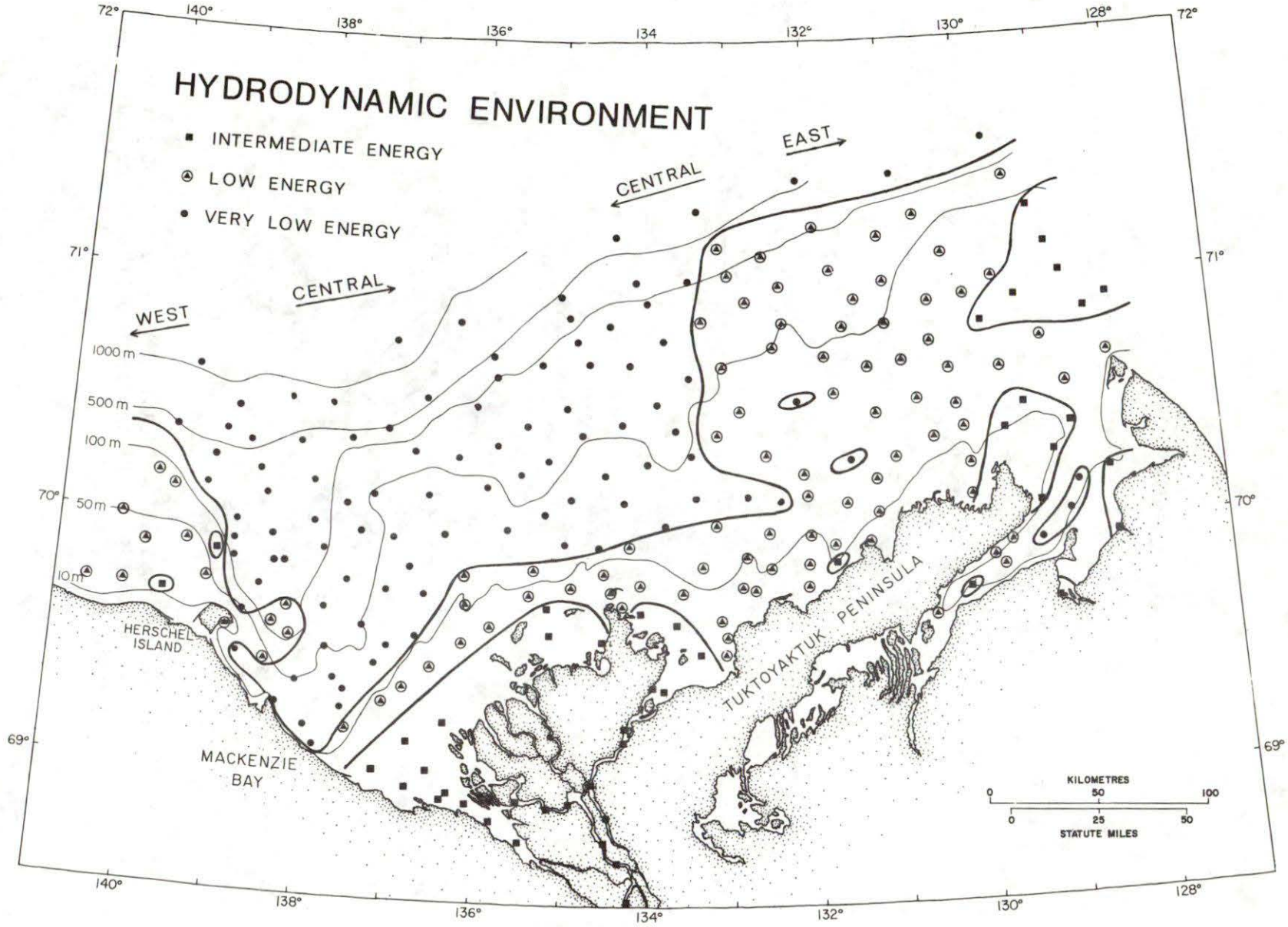

Figure 28. Map showing the distribution of the various hydrodynamic regimes.

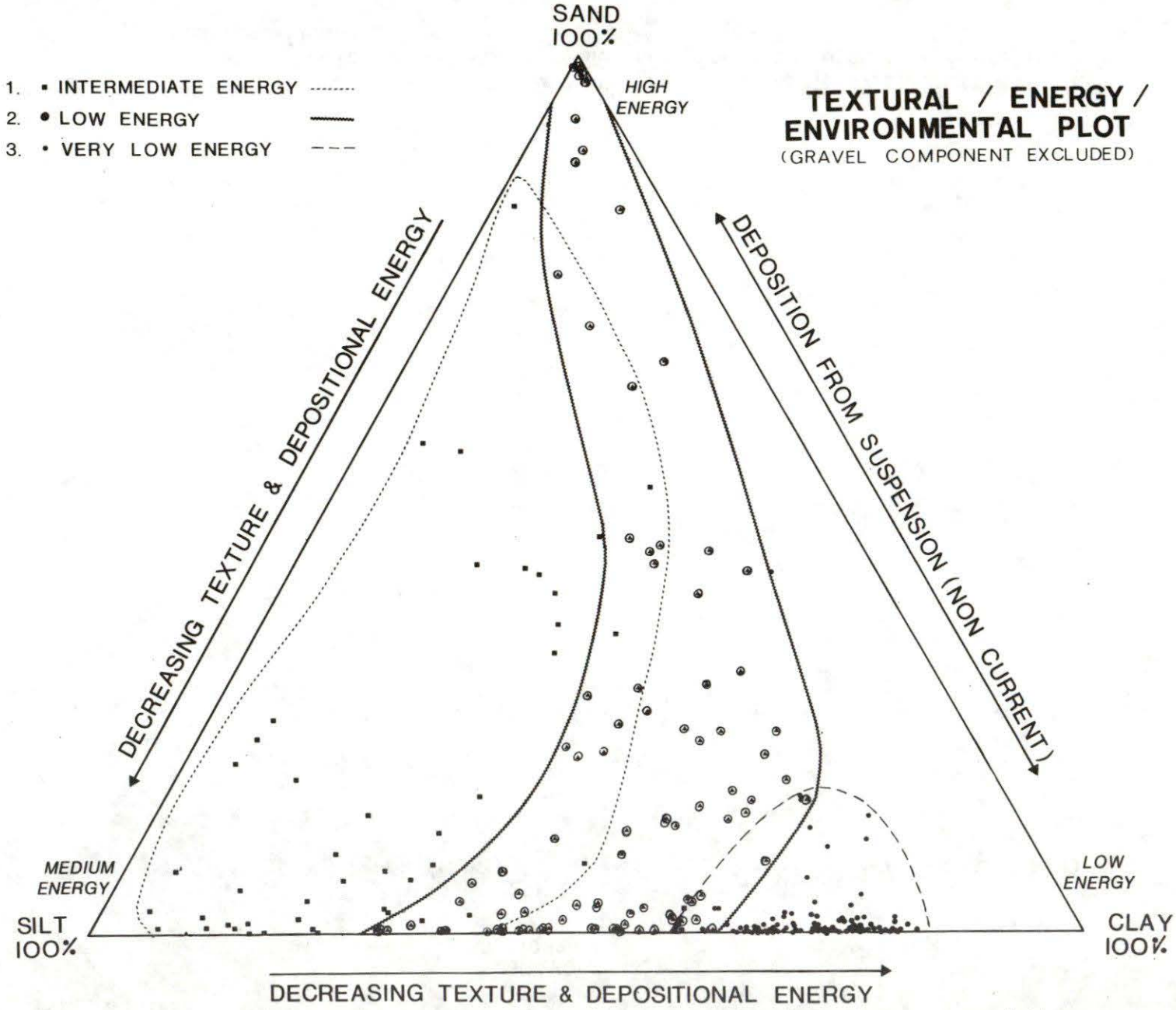

Figure 29. Ternary diagram of gross texture (gravel excluded, environments and the relative energy in the sedimentational system.

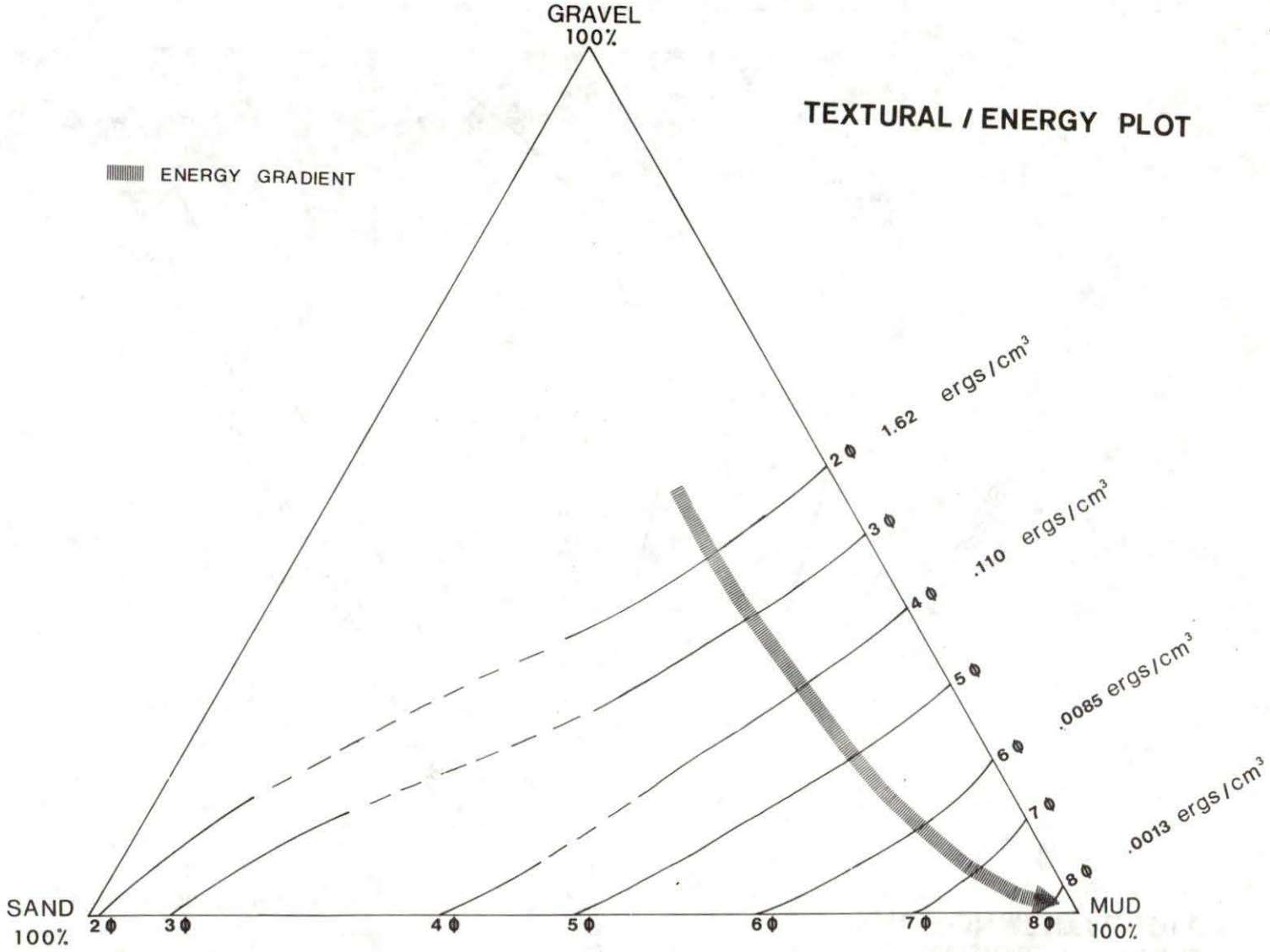

Figure 30. Ternary diagram of gross texture showing relationship of phi mean diameters for each sample (not shown) and the energy gradient occurring overall in sedimentational system.

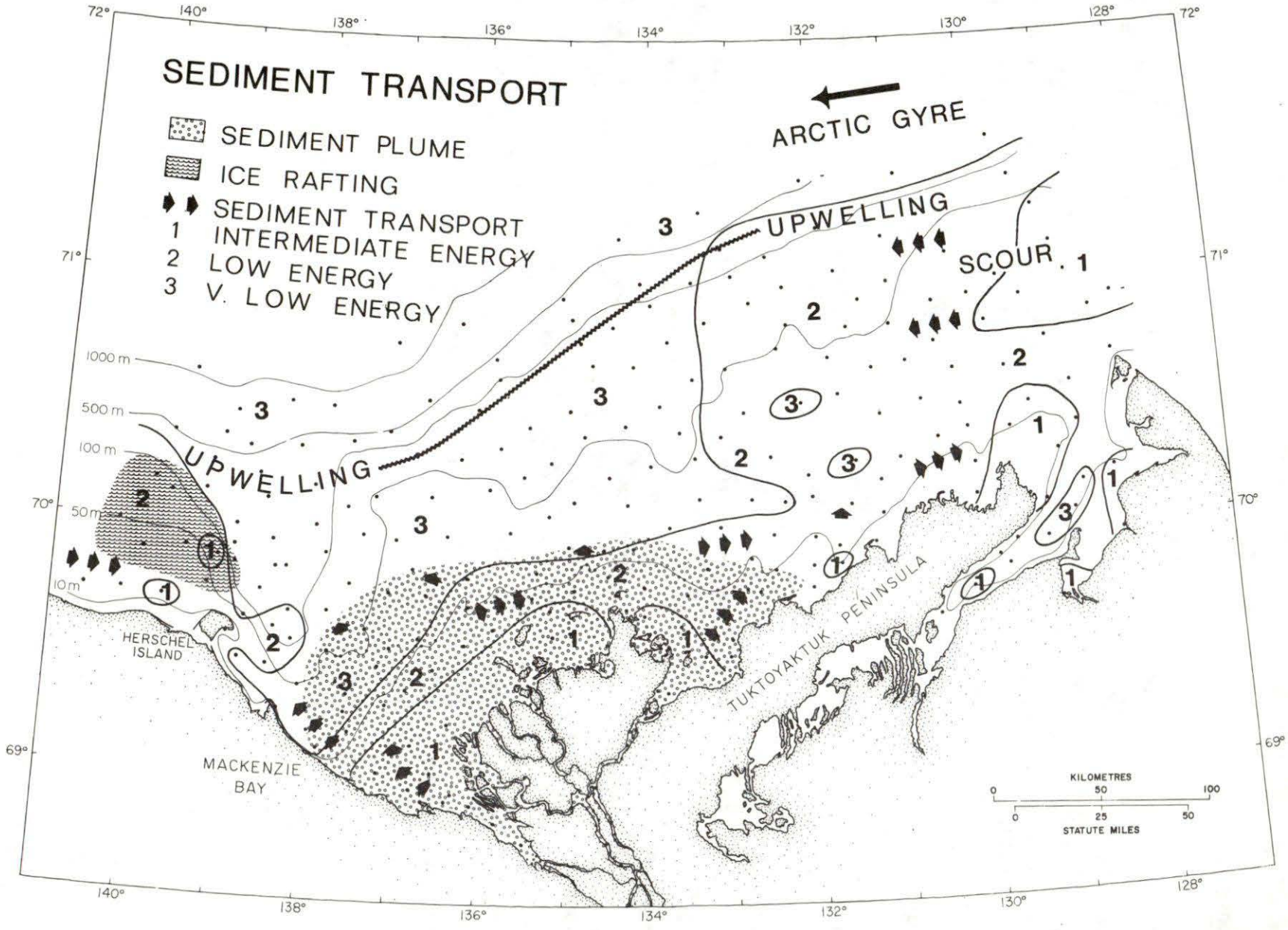

Figure 31. Model of sedimentary transport in the southern Beaufort Sea.

APPENDIX F - PROCEDURE ON X-RAY ANALYSES OF CLAY (R.N. Delabio)

Sample Preparation.

Clay samples were obtained in vials crushed to -200 mesh approximately. A portion of each sample (1-2 gms) was mixed with a sodium metaphosphate (5 g/litre sodium metaphosphate solution) in a 100 ml Nalgene centrifuge tube to the 10 cm. level. The residue from the fourth centrifuge run is the clay fraction used and small amounts were dispersed on glass slides and allowed to dry at room temperature. Three slides were made for each of the 244 samples, and air-dry slide, a glycerated slide and a heated slide at 550°C for 15 minutes. X-ray diffraction charts were obtained for all 3 slides with an XRD-GE. diffractometer using Cu radiation at 4SKV and 16MA. and a scan rate of 2 degrees 2θ per minute for the 2θ range 2½° to 35°.

X-ray Data

X-ray diffraction charts are recorded for each sample on an air-dry slide a glycerated slide (to determine presence of montmorillonite) and a slide heated at 550°C for 15 minutes (to determine presence of kaolinite).

Interpretation

The net intensities of the (001) reflections of chlorite, illite and kaolinite plus chlorite (002) are measured at 2θ values of 6.2 (001 chlorite), 8.1 (001 illite) and 12.4 (001 kaolinite + 002 chlorite) respectively on the charts of the air dry slides.

The net intensity of montmorillonite is measured at the 2θ value of 4.9 and is measured on the glycerated slides chart. If montmorillonite is present all values are measured from the glycerated chart.

In estimating the kaolinite (001) intensity, we assume that the chlorite (001) and (002) reflections are equal in intensity and subtract the net intensity of the chlorite (001) reflection from the net intensity of the combined kaolinite (001) plus chlorite (002) peak.

The abundances of the 4 mineral types are reported as ratios of the intensities of the (001) reflections.